AD-A111 163 AEROSPACE CORP SAN BERNARDINO CA TECHNOLOGY DIV F/G 20/4
THE BLUNT BODY PROBLEM IN AN EXPANDING, NONUNIFORM FLOW FIELD.(U)
JUL 70 P G CROWELL F04701-69-C-0059
UNCLASSIFIED TR-0059(S6816-76)-2 SAMSO-TR-70-302 NL

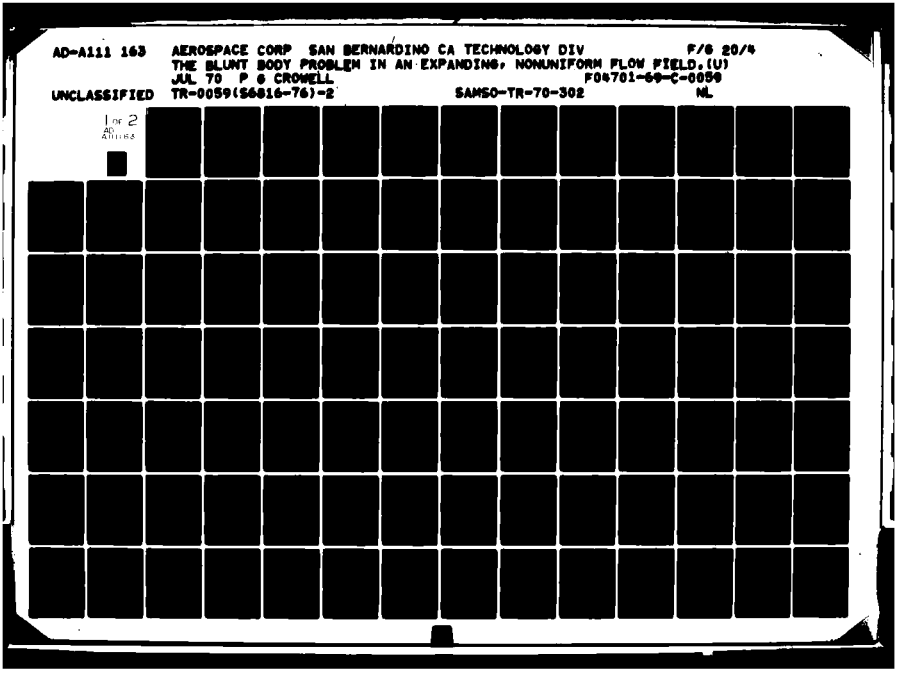

LEVEL II 1

THE AEROSPACE CORPORATION

LEVEL II

(1)

Air Force Report No.
SAMSO-TR-70-302

Aerospace Report No.
TR-0059(S6816-76)-2

THE BLUNT BODY PROBLEM IN AN EXPANDING, NONUNIFORM FLOW FIELD

by

P. G. Crowell

7Ø JUL Ø3

Technology Division
San Bernardino Operations
THE AEROSPACE CORPORATION
San Bernardino, California

Prepared for

SPACE AND MISSILE SYSTEMS ORGANIZATION
AIR FORCE SYSTEMS COMMAND
Air Force Unit Post Office
Los Angeles, California 90045

FOREWORD

This report by The Aerospace Corporation, San Bernardino Operations, has been prepared under Contract No. F04701-70-C-0059 as TR-0059(S6816-76)-2. The Air Force program monitor is Capt. Lawrence J. Hillebrand (SMYSE). The dates of research for this report include the period January through April 1970. This report was submitted by the authors June 1970.

The author gratefully acknowledges the assistance of Jerry C. South, (NASA - Langley) who supplied the original computer program used for this study and provided many helpful suggestions during the modification of the program. The author also wishes to acknowledge the efforts of Mickey Blackledge, (LMSC - Huntsville) who initiated the early phases of this work during the summer of 1969.

This document has been approved for public release and sale; its distribution is unlimited.

This technical report has been reviewed and is approved.

S. B. Batdorf, Director
Applied Mechanics and Physics Subdivision
Technology Division

L. J. Hillebrand, Capt. USAF
Project Officer
Thermal Protection Plan

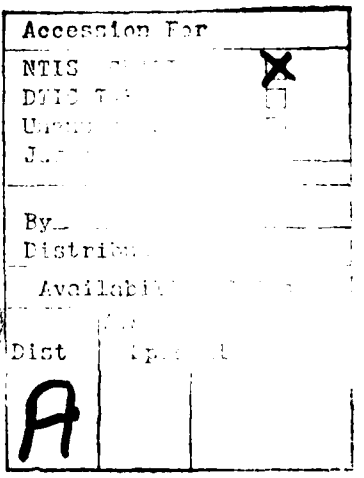

UNCLASSIFIED ABSTRACT

THE BLUNT BODY PROBLEM IN AN EXPANDING, NONUNIFORM FLOW FIELD
by P. G. Crowell

TR-0059(S6816-76)-2
7Ø SEP Ø7

The method of integral relations has been used to compute the inviscid flow over a blunt body immersed in a nonuniform, expanding flow field. Emphasis has been placed on defining the flow environment experienced by a nose tip model in the exhaust plume of an underexpanded arc jet or rocket engine. Accordingly, the integral method has been formulated for an arbitrary description of a free stream which possesses both axial and radial gradients in Mach No., flow angle, total pressure, and total enthalpy.

Computations are presented for two different descriptions of the free stream (spherical source flow and the exhaust plume from a contoured, Mach 2 nozzle) and two body shapes (sphere and circular disk). Results indicate a first order effect on all the blunt body characteristics.

The influence of the free stream derivatives of Mach No. and flow angle has been examined and found to exert only a second order effect upon the solutions, thereby allowing a considerably simplified description of the free stream. Moreover, it has been demonstrated that the influence of an expanding flow field upon a blunt body may be approximately characterized in terms of the flow angle gradient normal to the plume axis. Consequently, definition of the plume flow field is required only along its axis.

The possibility of sonic point movement off a sharp corner onto the face of a circular disk has been investigated and found to be entirely possible for a nonuniform free stream. To identify the magnitude of the free stream flow divergence required to move the sonic point off the corner, a set of solutions was obtained for an infinite circular disk in a spherical source flow.

Model size constraints, for the simulation of uniform flow pressure and heating distributions, have been identified for ablation testing in exhaust plumes. Furthermore, the region of a plume flow field immediately downstream of the Mach rhombus has been identified as the worst possible test location if simulation of a uniform flow environment is desired.

Requirements have been identified for additional cold flow experiments to define the capabilities and limitations of simulating uniform flow environments in underexpanded exhaust plumes. (Unclassified Report)

CONTENTS

FIGURES

FIGURES (Continued)

FIGURES (Continued)

TABLES

SECTION 1

INTRODUCTION

There are several fluid mechanics problems of current interest where it is necessary to compute the flow about a blunt nosed body in a nonuniform free stream. These problems may be considered to fall into two different categories, those where the free stream is essentially parallel and where the free stream is diverging. Nonuniform, parallel flow is encountered by a body when it is immersed in a constant pressure shear layer such as a wake or jet flow. A typical example of interest consists of deploying objects into the wake of a reentry vehicle.

When a body is immersed in an expanding flow field, such as a conical nozzle or exhaust plume, the free stream contains gradients in both the flow angle and gas properties. Several investigations have been made concerning the effects of a small amount of flow divergence upon the flow field properties of a body in a wind tunnel. Reference 1, for example, has used an inverse method with the method of characteristics, to compute the inviscid flow over spherical and elliptical bodies in a spherical source flow. Attention was restricted, however, to cases where the flow divergence was only a few degrees.

The interest in high performance reentry vehicles has led to considerable testing of ablative and transpiration nosetips in highly underexpanded free jets. A rapidly expanding free jet possesses large gradients in flow properties and flow angle, except in the Mach rhombus formed at the exit of a contoured nozzle. It is apparent, therefore, that in many ground test facilities, the flow over the nosetip will possess large gradients in flow properties in both the radial and axial directions. Depending upon the relative sizes of the nozzle exit diameter and model diameter and the distance of the model from the exit plane, free stream flow divergence angles of up to twenty degrees may be encountered.

In spite of the interest in such testing, there does not appear to be any systematic investigation of the effects of large free stream flow divergence angles upon the blunt body problem. Ref (2) used the method of integral relations coupled to a characteristics solution to compute the flow field for a sphere in a rocket exhaust, and Ref (3) has used a time dependent technique for a concave body in an exhaust plume. However, in each case, only one or two calculations were carried out for a specific body configuration and test geometry.

It is the purpose of this report to investigate the flow of a nonuniform, highly diverging free stream over a blunt nosed body. In particular, model size constraints will be identified for ablation testing in a free jet and the effect of nonuniform flow upon the simulated flight environment will be examined.

SECTION 2

DEFINITION OF FREE STREAM FLOW FIELD

As mentioned previously, the flow field is to be calculated over a blunt nosed body immersed in the exhaust plume of an underexpanded nozzle. Since the nozzle flow is supersonic, the method of characteristics has been used to compute the exhaust plume flow field for a contoured nozzle designed to produce a parallel Mach 2 flow at the exit (Ref 13). Mach No. and flow angle distributions and their gradients in the radial and axial directions are plotted in Figures 2 through 9. Figure 1 defines the geometry for the blunt body and the external flow field.

In addition to the free jet flow fields, computations have also been made for a spherical source flow. Mach No. and flow angle distributions for the spherical source flow may be described by the following expressions:

$$\frac{M}{M_o} = \left(\frac{\ell}{\ell_o}\right)^{\gamma-1} \quad ; \quad \text{Tan } \phi = \frac{r_o + \delta \text{Cos } \theta}{\ell_o - (\delta \text{Sin } \theta - Z)}$$

At any point on the shock wave;

$$\ell = \sqrt{\left(r_o + \delta \text{Cos}\theta\right)^2 + \left(\ell_o + Z - \delta \text{Sin}\theta\right)^2}$$

It is noted that the expression for the Mach No. variation assumes that the velocity is constant throughout the flow field, such that:

$$\frac{\rho}{\rho_o} = \left(\frac{V_o}{V}\right)\left(\frac{\ell_o}{\ell}\right)^2 = \left(\frac{\ell_o}{\ell}\right)^2$$

In the above expressions, the subscript o refers to source flow properties which would exist at the location of the body stagnation point if the body were not immersed in the flow field.

The calculation of the external flow field is uncoupled from the calculation over a body immersed in that flow field. Therefore, it is required that the body shock wave not influence the free stream in a region where the free stream definition is required for continuing the computation of the shock. This may be thought of in terms of a restriction on the free stream velocity and flow divergence angle, such that the component of the free stream velocity vector, normal to the shock wave, always remain supersonic. That is, it is required that:

$$M_\infty \, \mathrm{Sin}(\beta - \phi) > 1$$

It is possible, therefore, that there may exist some combination of body shapes and free stream flow conditions which will preclude uncoupling the body and free stream flow field calculations beyond some limiting distance downstream of the sonic point. In fact, there exists some limiting flow divergence angle such that the above restriction will be violated before the subsonic region of the flow field is closed. In this event, the two flow fields will be completely coupled and the computation will fail.

SECTION 3

METHOD OF INTEGRAL RELATIONS FOR A NONUNIFORM FREE STREAM

The method of integral relations (one strip approximation) has been used to make the computations in this report. It was decided not to use the inverse method of Ref 1 because of the difficulty of prescribing the shock shape for a nonuniform free stream, particularly where the external flow divergence angle is large enough to cause inflections in the shock shape. Furthermore, Inouye (Ref 1) has reported encountering numerical difficulties when the flow divergence increased beyond a few degrees. In addition, the inverse method cannot be used to handle a body with a sharp sonic corner. For these reasons, the direct method has been used.

In the development of the method of integral relations which follows, the fluid has been assumed to be a perfect gas where the ratio of specific heats is constant throughout the flow field. The free stream possesses both axial and radial gradients in Mach No., flow angle, total enthalpy, and total pressure. In the following discussion, a general outline is presented that emphasizes the differences between uniform and nonuniform flow. A detailed description is included in Appendix 1.

The continuity and normal momentum equations are written in body coordinates and integrated along a direction normal to the body surface out to the shock wave. Assuming that the resultant integrands are linear in the normal direction, n , and using the notation of South (Ref 4), we obtain:

$$\delta\tau_0\left(1 - M_0^2\right)\frac{du_0}{ds} = \left(\tau_1 u_1 - \tau_0 u_0\right)\frac{d\delta}{ds} - \frac{\delta \operatorname{Sin}\theta}{r_0}\left[\tau_0 u_0 + \tau_1 u_1\left(1 + K\delta\right)\right] - \frac{r_1}{r_0}\left[\delta\frac{d}{ds}\left(\tau_1 u_1\right) + 2\left(1 + K\delta\right)\tau_1 v_1\right] \tag{1}$$

$$\delta \frac{r_1}{r_0} \frac{d}{ds}\left(\rho_1 u_1 v_1\right) = \rho_1 u_1 v_1 (1 + K\delta)\left[\mathrm{Tan}(\beta-\theta) - \frac{\delta \mathrm{Sin}\theta}{r_0}\right]$$

$$+ K\delta\rho_0 u_0^2 - 2\frac{r_1}{r_0}(1+K\delta)\rho_1 v_1^2 + K\delta\left(\frac{r_1}{r_0}\right)\rho_1 u_1^2 \qquad (2)$$

$$+ \left(P_0 - P_1\right)\left(\frac{r_1}{r_0} + K\delta + 1\right)$$

From geometrical considerations (see Figure 1), the third equation is obtained:

$$\frac{d\delta}{ds} = (1 + K\delta)\,\mathrm{Tan}\,(\beta-\theta) \qquad (3)$$

It is noted that equations 1, 2, and 3 are valid for any description of the free stream. It is apparent that the free stream properties enter the differential equations through the use of the oblique shock relations to define the quantities behind the shock. Therefore, to evaluate the quantities behind the shock (subscript 1) the shock angle in the oblique shock equations is simply $\beta - \phi$ (see Figure 1). The only substantial effect of the nonuniform free stream upon the formulation is the presence of additional terms in the differential equations *(Ref 6)*. *These additional terms enter the equations when* the derivatives of $\rho_1 u_1 v_1$ and $\tau_1 u_1$ are evaluated. For example, consider $\rho_1 u_1 v_1$:

$$\frac{d}{ds}\left(\rho_1 u_1 v_1\right) = \rho_\infty V_\infty^2 \frac{d}{ds}\left(\frac{\rho_1 u_1 v_1}{\rho_\infty V_\infty^2}\right) + \frac{\rho_1 u_1 v_1}{\rho_\infty V_\infty^2}\frac{d}{ds}\left(\rho_\infty V_\infty^2\right)$$

$$\rho_\infty V_\infty^2 = \gamma P_\infty M_\infty^2 = \gamma M_\infty^2 P_{T_\infty}\left[1 + \frac{\gamma-1}{2} M_\infty^2\right]^{\frac{-\gamma}{\gamma-1}} \qquad (4)$$

$$F_1 \equiv \frac{\rho_1 u_1 v_1}{\rho_\infty V_\infty^2}$$

From the oblique shock relations, it is seen that: $F_1 = F_1\left(\beta,\ \theta,\ \phi,\ M_\infty\right)$

It is apparent, therefore, that differentiation of F_1 and $\rho_\infty V_\infty^2$ will yield derivatives of the flow angle, Mach No., and total pressure which would be zero for a uniform flow. Evaluation of $\frac{d}{ds}(t_1 u_1)$ will yield similar terms. The complete details are contained in Appendix 1.

The presence of these additional terms in the differential equations complicates the description of the free stream environment. If the external flow is described by analytic expressions for Mach No., flow angle, total pressure, and enthalpy, then these expressions may be differentiated to obtain the additional gradients. If, however, the free stream definition is obtained by either curve fitting or table look up and interpolation of a method of characteristics solution, the requirement for evaluating these additional terms involves a considerable effort. It will be of interest, therefore, to assess the effect of ignoring the derivatives of the free stream properties. This will be discussed further in Section 4.

As in the uniform flow case, Eq 1 and 2 yield indeterminate expressions for the initial derivatives of β and u_0. Application of L'hopitals rule yields the following expressions for a nonuniform external flow: (See Appendix 2.)

$$\delta\left(1 - \frac{\rho_\infty}{\rho_1}\right)\frac{d\beta}{ds} = \delta\frac{d\phi}{ds} + \frac{P_0 - P_1}{\rho_\infty V_\infty^2} - \frac{\rho_\infty}{\rho_1} \tag{5}$$

$$\frac{1}{V_\infty}\frac{du_0}{ds} = \frac{\rho_1(1 + K\delta)}{\rho_0\delta}\left(\frac{P_0 - P_1}{\rho_\infty V_\infty^2}\right) \tag{6}$$

It is quite interesting to note that the stagnation point velocity gradient has exactly the same form for either uniform or nonuniform flow. This is of considerable importance, since it implies that the stagnation point velocity gradient may still be obtained from a measurement of the shock standoff distance, even in a highly diverging flow field. Furthermore, although the method of integral relations does not accurately predict the

stagnation point velocity gradient (Ref 7), it may be obtained from the uniform flow correlation of Kaattari (Ref 8), even for a nonuniform flow. Kaattari's correlation requires the shock stand off distance, but this may be obtained accurately from the method of integral relations.

The initial derivative for the shock inclination angle, β, differs from the uniform flow result by the additional term for the derivative of the flow divergence angle, ϕ. Depending upon the magnitude of ϕ and its gradient, the external flow divergence may have a significant effect upon boundary layer edge properties and, thus, the heat transfer. This effect is due to the fact that entropy swallowing is dependent upon both the shock angle and its gradient normal to the flow field axis. It is possible, of course, that this effect may be overwhelmed by the presence of a large entropy gradient in the free stream (i.e., nonconstant total enthalpy and total pressure).

In order to evaluate the derivatives of the free stream properties with respect to the s direction, a transformation is required between the body centered coordinate system and the coordinate system of the external flow. The free stream properties shall be specified in either a cylindrical or spherical coordinate system. In all cases, circumferential symmetry is assumed. The gradient of any scalar property P may be written in cylindrical, spherical, or body centered coordinates as follows:

Cylindrical $$\vec{\nabla P} = \frac{\partial P}{\partial r}\,\vec{e_r} + \frac{\partial P}{\partial z}\,\vec{e_z}$$

Spherical $$\vec{\nabla P} = \frac{\partial P}{\partial \ell}\,\vec{e_\ell} + \frac{1}{\ell}\,\frac{\partial P}{\partial \phi}\,\vec{e_\phi}$$

Body $$\vec{\nabla P} = \frac{1}{1 + Kn}\,\frac{\partial P}{\partial s}\,\vec{e_s} + \frac{\partial P}{\partial n}\,\vec{e_n}$$

The dot products of the various unit vectors are as follows:

$$\vec{e_r} \cdot \vec{e_s} = \text{Sin}\,\theta \qquad \vec{e_z} \cdot \vec{e_s} = \text{Cos}\,\theta$$

$$\vec{e_\ell} \cdot \vec{e_s} = \text{Cos}\,(\theta - \phi) \qquad \vec{e_\phi} \cdot \vec{e_s} = \text{Sin}\,(\theta - \phi)$$

Taking the appropriate dot products between the gradients and the unit vectors, the transformations are obtained.

For a spherical external flow:

$$\frac{\partial P}{\partial s} = (1 + Kn)\ \mathrm{Cos}\ (\theta - \phi)\ \frac{\partial P}{\partial \ell} + \frac{(1 + Kn)}{\ell}\ \mathrm{Sin}\ (\theta - \phi)\ \frac{\partial P}{\partial \phi} \tag{7}$$

For a cylindrical external flow:

$$\frac{\partial P}{\partial s} = (1 + Kn)\ \mathrm{Sin}\ \theta\ \frac{\partial P}{\partial r} + (1 + Kn)\ \mathrm{Cos}\ \theta\ \frac{\partial P}{\partial z} \tag{8}$$

For a spherical source flow, the gradients in Mach No. and flow angle take on particularly simple forms because the thermodynamic state and flux properties are independent of ϕ and the flow angle is independent of ℓ.

$$\frac{\partial M_\infty}{\partial s} = (1 + Kn)\ \mathrm{Cos}\ (\theta - \phi)\ \frac{dM_\infty}{d\ell}$$

$$\frac{\partial \phi}{\partial s} = (1 + Kn)\ \frac{\mathrm{Sin}\ (\theta - \phi)}{\ell} \tag{9}$$

Eq 1-3, along with the boundary conditions (Eq 10) constitute a two point boundary value problem whose nature is unchanged by the fact that the external flow field is non-uniform. Therefore, as in the uniform flow case, the solution is obtained by iterating upon the initial value of the shock standoff distance until the correct sonic point behavior is achieved. A body whose sonic point is located at a sharp corner exhibits a singularity in the velocity gradient at that point and the correct behavior for the solution is simply that the sonic velocity be attained at the corner. For a body with sonic point located on a smooth contour, it is required that the velocity gradient remain finite as the sonic velocity is approached. For a comprehensive discussion of the behavior of the solution in the vicinity of the sonic point, Ref 10 may be consulted.

$$u_0(0) = 0 \qquad \beta(0) = \pi/2$$

$$u_0(s^*) = u_0^* \tag{10}$$

In light of the fact that the computational aspects of the problem are unchanged in the presence of a nonuniform free stream, it was decided to modify existing computer programs to account for nonuniformities in the external flow. The programs that were used in the study were written by Jerry C. South of NASA, Langley. The program to compute the flow field for bodies with sonic corners, in a uniform free stream, is documented in Ref 4. The second computer program, used to obtain the sonic saddle point convergence for smooth bodies, has been informally documented by South (Ref 5). Both programs used a fourth order Runge Kutta integration scheme with a variable step size.

SECTION 4

SPHERICAL SOURCE FLOW RESULTS

It is well known that the plume from an underexpanded nozzle may be simulated with reasonable accuracy by a spherical source flow located at the virtual origin of the plume flow field. Furthermore, in the case of a spherical source flow, the effect of the diverging free stream impinging upon a blunt body may be characterized by a single parameter, the ratio of the characteristic body length scale to the source distance from the body.

For these reasons, an extensive set of calculations has been carried out for a sphere and a circular disk immersed in a spherical source flow. The calculations covered a Mach No. range from 2.0 to 20.0 and values of the specific heat ratio of 1.2, 1.4 and 1.6667.

Before presenting the results of the calculations, a qualitative description of the effects of a diverging free stream upon the blunt body flow field is in order. The critical difference between a blunt body flow field with a parallel external flow and one with a diverging flow is that the shock angle, (i.e., $\beta - \phi$) decreases faster for the diverging flow, for the obvious reason that ϕ is non zero. Therefore, the pressure behind the shock, and thus also on the body surface, decreases faster than for the parallel flow case. This leads to an increase in the surface velocity gradient which causes a movement of the sonic point towards the stagnation point (except for a body whose sonic point is fixed at a sharp corner).

The behavior of the shock standoff distance may be inferred from one-dimensional streamtube continuity considerations. Since the sonic point location on the shock moves closer to the axis as the flow divergence increases, the free stream flow angle always remains relatively small up to the sonic point. Therefore, the mass flux passing through the shock at any radial distance from the axis is approximately the same for either the uniform or non-uniform flow, provided the free stream Mach numbers are

not significantly different. Since the mass flux per unit area between the shock wave and body surface is greater for the nonuniform flow, continuity of mass requires that the flow area (and thus the shock standoff distance) be smaller than for the corresponding uniform flow.

To summarize, the effect of a diverging free stream is to increase the stagnation point velocity gradient, decrease the surface pressure, move the sonic point closer to the axis, and decrease the shock standoff distance.

Typical results for the shock shape, pressure and heat flux distributions on a spherical body are presented in Figures 10 through 13. The laminar heat flux is Lee's cold wall distribution and the turbulent heating is Vaglio Laurin's formulation. It is apparent that for values of the source flow parameter $\frac{R}{\ell_0}$ of up to 0.5, the diverging free stream has a first order effect on all the blunt body properties. In Figures 14 and 15, the sonic point location and shock standoff distance are plotted for a range of Mach No. The shock standoff distance and stagnation point velocity gradient may vary by almost a factor of two over their uniform flow values. By taking the square root of the velocity gradient ratio in Figures 18 and 19, an estimate of the increase in the laminar stagnation point heat flux may be obtained. This indicates that for low supersonic Mach values, the stagnation point heating may be increased by thirty five percent over the corresponding uniform flow value. The sensitivity to Mach No. at low supersonic values, which is indicated in Figures 16 and 18 is due to the sensitivity of the normal shock density ratio to low supersonic values of the incident Mach No. Table 1 contains a summary of the solutions for a sphere in a spherical source flow.

Since the results of Ref 1 were obtained by an exact numerical solution of the inviscid equations, it is of interest to compare them with the results of the integral method of this report. The comparison of shock standoff distance, stagnation point velocity gradient, and pressure distribution is contained in Figures 20 through 22. The standoff distance and pressure distributions are in excellent agreement. The stagnation point velocity gradient is in error by about 18 percent, as expected (Ref 7). However, the values of the stagnation point velocity gradient normalized with the uniform flow value are in excellent agreement. It is felt, therefore, that the velocity gradient ratio may be accurately calculated by the integral method.

The use of Newtonian impact theory to compute pressure distributions on blunt bodies is a simple, yet accurate technique for uniform flows. Newtonian theory might also be expected to yield adequate predictions for bodies in an expanding flow field. Using the source density and flow angle along the body surface, the following expression is obtained for the pressure distribution on a sphere in a spherical source flow.

$$\frac{P}{P_{STAG}} = \frac{\mathrm{Sin}^2\phi \ \mathrm{Sin}^2(\theta-\phi)}{\mathrm{Cos}^2\theta}\left(\frac{\ell_0}{R}\right)^2 \quad , \ \mathrm{Tan}\ \phi = \frac{R}{\ell_0}\ \mathrm{Cos}\ \theta$$

The comparison of the pressure distributions is contained in Figure 23. It is seen that the Newtonian prediction is in reasonable agreement (within 10 percent) with the results of the integral method, except near the shoulder of the sphere. However, the integral method itself is inaccurate in this region. This is clearly evident from the uniform flow calculation where the integral method yields pressures which are somewhat higher than would be obtained from a characteristics calculation. Therefore, for small values of θ, the Newtonian result may be more accurate than the integral method.

As was mentioned earlier, one of the disadvantages of the integral method is that the free stream derivatives of Mach No. and flow angle must be specified as well as the Mach No. and flow angle themselves. Since the most significant aspect of the diverging free stream is its effect on the shock angle, it might be expected that these derivatives would exert only a second order effect on the solution. In order to ascertain the importance of these terms upon the solution, a set of solutions was obtained where the derivatives of free stream Mach No. and flow angle were ignored. The results for the shock standoff distance and stagnation point velocity gradient are presented in Figures 24 through 25. The values are normalized with the corresponding exact values. Results indicate that ignoring the free stream gradient terms underpredicts the stagnation point velocity gradient and overpredicts the shock standoff distance. The error increases with increasing values of the source flow parameter and is approximately ten to fifteen percent for $\frac{R}{\ell_0} = 0.5$. The effect on pressure distribution is of the same

order and is indicated by the dashed line in Figure 10. It is felt, therefore, that in situations where it is difficult to evaluate the free stream derivatives that they may be ignored without introducing large errors into the results.

In light of the substantial change in the sonic point location for a sphere in a diverging flow field (see Figure 14), it becomes pertinent to examine under what conditions the sonic point will move off a sharp corner onto the face of a blunt body. For a body surface with non zero curvature, the sonic point location is computed as previously discussed and truncating the body forward or aft of this point determines whether the sonic point is located at a corner or on a smooth contour.

The situation for a body with zero surface curvature, (i.e., a sharp cone or circular disk) is not quite so obvious. The contention that the sonic point must always remain at a sharp corner, for a body with zero surface curvature, is based on the argument that if the sonic point moves forward of the corner then the corner can no longer influence the subsonic flow field. In other words, there no longer exists any length scale to the problem. That this is physically reasonable is obvious for a uniform free stream.

However, for a nonuniform free stream, this argument is no longer valid since there are length scales associated with the gradients in the external flow. For a spherical source flow or an exhaust plume, the obvious length scale is the distance of the body from the source or nozzle exit plane. For a flow which is nonuniform but parallel, there exists some length scale associated with the Mach No. gradient.

In order to examine the behavior of a blunt body with a sonic corner, in an expanding flow field, a set of solutions has been generated for a circular disk in a spherical source flow. A typical set of results for shock shape, pressure, and heat flux distributions is contained in Figures 26 through 28. It is noted that the shock standoff distance at the sonic point is only weakly dependent on the nonuniform free stream. This is due to the fact that the mass flux and the mass flux per unit area through the "throat" are approximately the same for both uniform and nonuniform flow. This is a consequence of body geometry rather than external flow dictating the location of the sonic point. Therefore, the "throat" area and the standoff distance are virtually unaffected by the diverging free stream.

The results for the shock standoff distance and stagnation point velocity gradient and their sensitivity to Mach No. and specific heat ratio are contained in Figures 29 through 33. Table 2 contains a summary of the solutions for a circular disk in a spherical source flow.

It should be mentioned that the scaling between the shock standoff distance and the distance to the sonic point, which exists for bodies with zero curvature in a uniform flow, is no longer valid for nonuniform external flow. In Ref 10, it is pointed out that the shock standoff distance for a body with zero surface curvature is linearly proportional to the distance to the sonic point. Therefore, only one integration out to the sonic point is required to establish the proportionality constant. However, since there exists an additional length scale associated with the nonuniform free stream, the solutions must be obtained by iterating upon the shock standoff distance, just as for bodies with finite curvature.

It was mentioned earlier that Kaattari's correlation (Ref 8) for the stagnation point velocity gradient should be valid for nonuniform flows, since, at the axis, the differential equation for the velocity gradient has the same form irrespective of the nature of the external flow. This is seen to be the case in Figure 34, where the velocity gradient ratios for a sphere and circular disk are compared with the correlation.

As discussed above, it is desired to determine the value of the source flow parameter for which the sonic point will move off the corner of the circular disk and onto its face. When such movement occurs, as far as the subsonic portion of the flow field is concerned, the disk is infinite in extent. The problem, therefore, is that of an infinite circular disk in a spherical source flow with the source distance as the characteristic length. The sonic point convergence for this case is exactly the same as for any smooth body, namely, that the sonic point velocity gradient remain finite as the sonic velocity is approached.

The results for the infinite circular disk are contained in Figures 35 through 39. It is noted that since the disk is infinite in extent, the shock curvature is away from the body. For a finite disk whose sonic point has moved onto the face of the disk, the

shock will be concave in the vicinity of the stagnation point and convex as the corner is approached. Actually, an examination of the shock shapes in Figure 28 indicates that the shock is becoming concave in the vicinity of the stagnation point for values of the source flow parameter of 0.333. The sonic point location on the infinite circular disk is shown in Figure 35. Therefore, for values of the source flow parameter greater than the sonic distance for the infinite circular disk, the sonic point will move off the sharp corner. Table 3 contains the stagnation and sonic point properties for the solutions.

Although the inviscid flow equations admit solutions with the sonic point located ahead of the sharp corner on a circular disk, there is some question as to whether viscous effects will render the solution unstable. The available experimental data (Ref 11 and 12) for an underexpanded jet impinging upon a flat plate appear to be limited to surfaces which are infinite in extent, with respect to the exhaust plume. Additional experiments with a finite plate are required to answer the stability question.

SECTION 5

EXHAUST PLUME CALCULATIONS

In order to obtain some results which would be of quantitative use in defining the environment on a nose tip in an arc jet flow field, solutions have been generated for a sphere in the exhaust plume of a contoured nozzle. The nozzle was assumed to deliver a uniform, parallel, Mach 2 flow at its exit plane. Total enthalpy and pressure were assumed to be constant. The exhaust was assumed to be a perfect gas ($\gamma = 1.40$) with a ratio of chamber pressure to ambient pressure of 100.

The method of characteristics (Ref 13) was used to compute the exhaust plume flow field and the results are contained in Figures 2 through 9. In Figure 2, the physical size of the plume and the location of the boundary shock are shown. Since the flow is uniform and parallel in the nozzle exit plane, it will also be uniform inside a region bounded by the axis and the lead ray in the Prandtl Meyer fan emanating from the nozzle lip. This uniform flow region is indicated by the dashed line in Figure 2.

The characteristics solution was written on magnetic tape and used with a surface interpolation procedure to provide the definition of the free stream required for the blunt body solution. The surface interpolation scheme yielded a random error of one to two percent for all the flow properties. This error, in turn, caused a random error in the surface velocity gradient on the order of ten percent. In order to obtain well-behaved solutions, the following procedure was used. First, the shock wave location was approximately located by using the interpolated results for the free stream properties. Then the interpolated results were plotted and smoothed manually. The free stream variables were then fit with polynomial expressions and the solution was rerun.

Fortunately, the shock wave location was not sensitive to the error in the free stream properties, so this tedious procedure only had to be repeated once for each case. In any situation where it was desired to generate a large number of solutions, some automated procedure would have to be developed to smooth the interpolated values during the solution.

The computations for the plume flow field are in terms of two parameters, the distance of the sphere from the nozzle exit plane $\left(\frac{z}{r_e}\right)$ and the size of the sphere relative to the nozzle exit radius $\left(\frac{R}{r_e}\right)$. The corresponding uniform flow case occurs as the sphere radius shrinks to zero. A complete set of results is presented in Figures 40 through 42 for a sphere located one nozzle exit radius downstream of the nozzle. At this location, part of the sphere lies inside the Mach rhombus. Therefore, there is a discontinuity in the flow environment as the bow shock cuts across the Prandtl Meyer ray which bounds the Mach rhombus. This is reflected in the pressure distribution in Figure 40. It is apparent from the heat transfer and pressure that it is not possible to obtain uniform flow distributions for a sphere which is any larger than half the nozzle exit radius. If it is desired to test larger bodies and still obtain heat transfer and pressure distributions which are representative of those encountered for a uniform free stream, the body must be placed further downstream of the nozzle exit plane. Accordingly, a set of pressure distributions is presented in Figure 43 for a sphere which is four nozzle radii downstream. Results indicate that the sensitivity to body size is substantially less at larger distances from the nozzle. This is due to the decrease in flow angle with increasing distance from the nozzle, for the same radial distance from the axis.

Unfortunately, since the centerline Mach No. increases quite rapidly downstream of the nozzle exit, the total pressure loss across the bow shock becomes quite large. Therefore, if high stagnation pressure is required on the model, it will not be possible to test downstream of the Mach rhombus.

The stagnation point velocity gradient and shock standoff distance are presented in Figures 44 and 45. The greatest sensitivity to body size is seen to be immediately downstream of the Mach rhombus. This is precisely the location where the gradient in flow angle is most severe. (See Figures 3 and 6.) Therefore, the worst possible simulation of the flight environment (i.e., uniform flow) occurs immediately downstream of the Mach rhombus.

The results of the above calculations indicated that the Mach No. gradients and the flow angle gradient in the z direction exerted only a second order influence on the solution. For the range of body sizes considered $\left(\frac{R}{r_e} \approx 1\right)$, the flow angle gradient normal to the axis was the dominating factor. Examination of Figures 5 and 6 indicate that the flow angle is nearly linear in r out to the location of the plume barrel shock. Furthermore, in the vicinity of the flow field axis, the influence of the nonuniform free stream is exerted only through the normal component of the flow angle gradient $\left(\text{i.e., for a nonuniform external flow, the stagnation point Eq (5) and (6) contain only the additional term, } \frac{d\phi}{ds}\right)$.

The above considerations suggest that the influence of the nonuniform free stream might be characterized by a single parameter, the value of $\frac{\partial \phi}{\partial r}$ on the flow field axis. For a body inside the Mach rhombus, the appropriate value would be $\frac{\partial \phi}{\partial r}$ evaluated at the interface between uniform and nonuniform flow. In order to test this hypothesis, several solutions were generated for constant Mach No., $\frac{\partial \phi}{\partial z} \equiv 0$, and a constant value of $\frac{\partial \phi}{\partial r}$. The approximate solution is indicated by the triangles in Figure 43. The error in the pressure distribution is approximately 10 to 15 percent. (For smaller values of $\frac{R}{r_e}$, the error would decrease.) The error in the shock standoff distance and stagnation point velocity gradient was about five percent.

It appears, therefore, that the description of the plume flow field may be greatly simplified with only a small sacrifice in the accuracy of the blunt body solution. Thus, instead of specifying the entire plume flow field, only the values along the plume axis are required. Since the plume axis is a streamline, the flow angle

gradient may be expressed in terms of the Mach No. gradient along the axis. That is, for an axisymmetric, inviscid, irrotational flow field, the following expression is valid on the flow field axis:

$$\frac{\partial \phi}{\partial r} = \frac{M^2 - 1}{2M\left(1 + \frac{\gamma - 1}{2} M^2\right)} \frac{\partial M}{\partial z} \quad .$$

In summary, if it is assumed that the effect of the nonuniform free stream may be characterized solely by the value of $\frac{\partial \phi}{\partial r}$ on the plume axis, then the description of the plume flow field is reduced to specifying the Mach No. and its gradient on the axis.

SECTION 6

SUMMARY AND CONCLUSIONS

It has been shown that a nonuniform, expanding flow field can significantly affect all the characteristics of a blunt body immersed in that flow field. In particular, solutions have been generated for a sphere and circular disk in flows where the free stream divergence is of the same order as may be encountered in underexpanded arc jets or rocket engines.

In light of the similarity between spherical source flows and underexpanded exhaust plumes, an extensive set of calculations has been carried out over a range of body sizes to source distances. It is felt that by suitably locating the "effective" origin of the flow, these solutions may be used to provide reasonable estimates of the blunt body characteristics for arbitrary nozzle geometries and operating conditions. Since the Mach gradient for the spherical source flows is quite weak, reasonable simulation should be expected only for exhaust plumes where the flow angle gradient is the dominating factor.

It has been demonstrated that there exists the possibility of the sonic point moving off a sharp corner onto the face of a blunt body, even for bodies with zero surface curvature. The results of the calculations for an infinite circular disk may be used to assess the probability of this occurring.

The description of the nonuniform free stream may itself pose considerable difficulties, particularly if it is a rotational inviscid flow or a viscous flow. Even the irrotational exhaust plume requires a numerical solution to the equations of motion. When the definition of the external flow is in terms of a tabular array in two space variables, considerable effort may be required to evaluate all the derivatives of the free stream properties. Furthermore, the blunt body solutions proved to be quite sensitive to small errors in interpolating for the free stream properties. Therefore, the effect upon the blunt body solutions, of various simplifications for the free stream

description, has been examined. Solutions were generated for a sphere, where the Mach No. and flow angle variation were correctly accounted for but the derivatives of Mach No. and flow angle were ignored. The results indicated that these derivatives could be ignored without introducing large errors. The simplification of the free stream definition was carried a step further for a few of the exhaust plume calculations, where only the radial variation of flow angle was accounted for. Again, the error introduced by this approximation was relatively small.

In order to obtain high stagnation pressures on the model, most ablation tests are conducted at low supersonic Mach No. Usually the nozzle is contoured to produce a region of uniform flow downstream of the exit plane. Since the Mach rhombus is limited in size, it imposes a size constraint on the test model if uniform flow is desired. In order to examine the effect of body size on the simulated flight environment, computations were performed for a sphere in a Mach 2 exhaust plume. It has been shown that the maximum body size, for uniform flow simulation in the Mach rhombus, is about one half the nozzle exit radius. In order to obtain a uniform flow pressure distribution on a body which is equal in size to the nozzle exit radius, it is necessary to test four nozzle radii downstream of the exit plane. The region immediately downstream of the Mach rhombus has been identified as the worst possible test location for the simulation of uniform flow.

Due to the difficulty and expense of obtaining data in high temperature flows, there does not exist any comprehensive set of measurements with which the present calculations can be compared. Furthermore, in spite of the large amount of impingement testing in exhaust plumes, there also does not appear to be any cold flow data which are applicable to the present problem. This points up the need for additional experimental work to define the capabilities and limitations of testing in underexpanded exhaust plumes.

REFERENCES

1. Inouye, Mamoru, "Numerical Solutions for Blunt Axisymmetric Bodies in a Supersonic Spherical Source Flow," NASA TN D-3383, April 1966.

2. Blackledge, M. L., "Lockheed Test Program and Flowfield Studies," Minutes of the Working Group Meeting on Testing in the Malta Pit 4 Rocket Engine Exhaust, The Aerospace Corp., TOR-1101(S2516-311-7, Edited by S. L. Channon, Feb. 1967.

3. Bastianon, R. A., "Computation of Supersonic, Non Uniform Flow Over a Blunt Body Using Finite Difference Techniques," LMSC, Proceedings of the Rocket Plume Phenomena Specialists Meeting - Volume II, The Aerospace Corp., TOR-0200(S4960-10)-1 (Confidential), October 1968.

4. South, Jr., Jerry C., "Calculation of Axisymmetric Supersonic Flow Past Blunt Bodies with Sonic Corners, Including a Program Description and Listi NASA TN D-4563, May 1968.

5. South, Jr., J. C., Private Communication, January 27, 1970.

6. South, Jr., J. C., Private Communication, November 19, 1969.

7. Kuby, W. C., "Use of the Method of Integral Relations for the Determination of the Convective Heat Flux to a Re-Entry Body," AIAA Journal, May 1966, pp 947-949.

8. Kaattari, George, "A Method for Predicting Shock Shapes and Pressure Distributions for a Wide Variety of Blunt Bodies at Zero Angle-of-Attack," NASA TN D-4539, April 1968.

9. Kaattari, George, "Predicted Shock Envelopes About Two Types of Vehicles Large Angles-of-Attack," NASA TN D-860, 1961.

10. Xerikos, J., and Anderson, W.A., "A Critical Study of the Direct Blunt Bo Integral Method," Douglas Report SM-42603, December 28, 1962.

11. Vick, Allen R., and Andrews, Jr., Earl H., "An Investigation of Highly Underexpanded Exhaust Plumes Impinging Upon a Perpendicular Flat Surface, NASA TN D-3269, Feb. 1966.

REFERENCES (Continued)

12. Stitt, Leonard E., "Interaction of Highly Underexpanded Jets with Simulated Lunar Surfaces," NASA TN D-1095, 1961.

13. Prozan, R. J., "Development of a Method of Characteristics Solution for Supersonic Flow of an Ideal, Frozen or Equilibrium Gas Mixtures," LMSC HREC A 782535-A, April 1966.

14. Traugott, Stephen C., "An Approximate Solution of the Direct Supersonic Blunt Body Problem for Arbitrary Axisymmetric Shapes," Journal of the Aerospace Sciences, May 1960, 11 361-370.

15. Chu, S. T., "Extension of BELOTSERKOVSKII's Direct Method to Reacting Gas in Thermodynamic Equilibrium," Aerospace SSD-TDR-64-81, May 18, 1964.

16. Crowell, P. G., "The Effect of a Large Total Enthalpy Spike Upon the Flow Field Characteristics of the Wright-Patterson 50 Megawatt RENT Facility," Aerospace IOC 69-3952-121, November 14, 1969.

17. Crowell, P. G., "Flow Field Characteristics of the Wright-Patterson 50 Megawatt Arc Jet," Aerospace IOC 69-3952C-100, September 8, 1969.

18. Patterson, Jerold L., and Lewis, Arthur B., "An Investigation of Nonuniform Hypersonic Free-Stream Flows About Blunt Axisymmetric Bodies," AFFDL-TR-69-57, November 1969.

APPENDIX 1

INTEGRAL RELATIONS FOR A NONUNIFORM FREE STREAM

It is the purpose of this section to develop the method of integral relations for a nonuniform free stream.

The three basic equations are listed in Section 3 as Eq 1-3. The dependent variables are the shock standoff distance, δ , the surface velocity, u_0 , and the shock inclination angle, β. The independent variable is distance measured along the body surface, s .

The oblique shock relations are required to evaluate the properties behind the shock. These may be written as follows:

$$\frac{\rho_1}{\rho_\infty} = \frac{(\gamma + 1)\, M_\infty^2\, \mathrm{Sin}^2\,(\beta-\phi)}{(\gamma-1)\, M_\infty^2\, \mathrm{Sin}^2\,(\beta-\phi) + 2}$$

$$\frac{P_1}{\rho_\infty V_\infty^2} = \frac{2\gamma M_\infty^2\, \mathrm{Sin}^2\,(\beta-\phi) - (\gamma - 1)}{\gamma(\gamma + 1)\, M_\infty^2}$$

$$\frac{u_1}{V_\infty} = \frac{\rho_\infty}{\rho_1}\, \mathrm{Sin}\,(\beta-\phi)\, \mathrm{Sin}\,(\beta-\theta) + \mathrm{Cos}\,(\beta-\phi)\, \mathrm{Cos}\,(\beta-\theta)$$

$$\frac{v_1}{V_\infty} = \mathrm{Cos}\,(\beta-\phi)\, \mathrm{Sin}\,(\beta-\theta) - \frac{\rho_\infty}{\rho_1}\, \mathrm{Sin}\,(\beta-\phi)\, \mathrm{Cos}\,(\beta-\theta)$$

Refer to Figure 1 for sign conventions and geometry.

In order to evaluate the derivatives of the shock properties with respect to s, the partial derivatives of the properties behind the shock must be obtained.

For notational convenience, let $F_1 \equiv \dfrac{\rho_1 u_1 v_1}{\rho_\infty V_\infty^2}$

$$F_2 \equiv \frac{u_1}{V_\infty} \quad , \quad F_3 \equiv \frac{P_1}{\rho_\infty V_\infty^2} \quad , \quad F_4 \equiv \frac{\rho_1}{\rho_\infty}$$

$$\frac{\partial F_1}{\partial \theta} = -\frac{\rho_1}{\rho_\infty}\left[\left(\frac{u_1}{V_\infty}\right)^2 - \left(\frac{v_1}{V_\infty}\right)^2\right] \tag{1-1}$$

$$\frac{\partial F_1}{\partial \beta} = \frac{-\rho_1 u_1}{\rho_\infty V_\infty}\left[\left(\frac{\rho_\infty}{\rho_1}\right)\mathrm{Cos}\,(\beta-\phi)\,\mathrm{Cos}\,(\beta-\theta) - \frac{u_1}{V_\infty} + \mathrm{Sin}\,(\beta-\theta)\,\mathrm{Sin}\,(\beta-\phi)\right]$$
$$+ \frac{\rho_1 v_1}{\rho_\infty V_\infty}\left[\frac{\rho_\infty}{\rho_1}\,\mathrm{Sin}\,(\beta-\theta)\,\mathrm{Cos}\,(\beta-\phi) - \frac{v_1}{V_\infty} - \mathrm{Sin}\,(\beta-\phi)\,\mathrm{Cos}\,(\beta-\theta)\right] - F_5 \tag{1-2}$$

$$F_5 \equiv \frac{4\,\mathrm{Cos}\,(\beta-\phi)}{(\gamma+1)\,M_\infty^2\,\mathrm{Sin}^3(\beta-\phi)}\left(\frac{\rho_1}{\rho_\infty}\right)^2\left[\frac{v_1}{V_\infty}\,\mathrm{Cos}\,(\beta-\theta)\,\mathrm{Cos}\,(\beta-\phi)\right.$$
$$\left. + \frac{u_1}{V_\infty}\left(\frac{\rho_\infty}{\rho_1}\right)\mathrm{Sin}\,(\beta-\phi)\,\mathrm{Cos}\,(\beta-\theta)\right]$$

$$\frac{\partial F_1}{\partial \phi} = \frac{u_1}{V_\infty}\left[\mathrm{Cos}\,(\beta-\phi)\,\mathrm{Cos}\,(\beta-\theta) + \frac{\rho_1}{\rho_\infty}\,\mathrm{Sin}\,(\beta-\phi)\,\mathrm{Sin}\,(\beta-\theta)\right] +$$
$$+ \frac{v_1}{V_\infty}\left[\frac{\rho_1}{\rho_\infty}\,\mathrm{Sin}\,(\beta-\phi)\,\mathrm{Cos}\,(\beta-\theta) - \mathrm{Cos}\,(\beta-\phi)\,\mathrm{Sin}\,(\beta-\theta)\right] - F_5 \tag{1-3}$$

$$\frac{\partial F_1}{\partial M_\infty} = \frac{4}{(\gamma+1)\,M_\infty^3\,\mathrm{Sin}^2\,(\beta-\phi)}\left(\frac{\rho_1}{\rho_\infty}\right)^2\left[\frac{v_1}{V_\infty}\,\mathrm{Cos}\,(\beta-\theta)\,\mathrm{Cos}\,(\beta-\phi)\right.$$
$$\left. + \frac{u_1}{V_\infty}\left(\frac{\rho_\infty}{\rho_1}\right)\,\mathrm{Sin}\,(\beta-\phi)\,\mathrm{Cos}\,(\beta-\theta)\right] \tag{1-4}$$

$$\frac{\partial F_2}{\partial \beta} = \frac{\rho_\infty}{\rho_1} \left[\text{Cos}\,(\beta-\phi)\,\text{Sin}\,(\beta-\theta) + \text{Sin}\,(\beta-\phi)\,\text{Cos}\,(\beta-\theta) \right] +$$

(1-5)

$$- \text{Sin}\,(\beta-\phi)\,\text{Cos}\,(\beta-\theta) - \text{Cos}\,(\beta-\phi)\,\text{Sin}\,(\beta-\theta) - \frac{4\,\text{Cos}(\beta-\phi)\,\text{Sin}\,(\beta-\theta)}{(\gamma+1)\,M_\infty^2\,\text{Sin}^2\,(\beta-\phi)}$$

$$\frac{\partial F_2}{\partial \phi} = \text{Sin}\,(\beta-\phi)\,\text{Cos}\,(\beta-\theta) - \frac{\rho_\infty}{\rho_1}\,\text{Cos}\,(\beta-\phi)\,\text{Sin}\,(\beta-\theta)$$

(1-6)

$$+ \frac{4\,\text{Cos}\,(\beta-\phi)\,\text{Sin}\,(\beta-\theta)}{(\gamma+1)\,M_\infty^2\,\text{Sin}^2\,(\beta-\phi)}$$

$$\frac{\partial F_2}{\partial \theta} = \frac{v_1}{V_\infty} \tag{1-7}$$

$$\frac{\partial F_2}{\partial M_\infty} = - \frac{4\,\text{Sin}\,(\beta-\theta)}{(\gamma+1)\,M_\infty^3\,\text{Sin}\,(\beta-\phi)} \tag{1-8}$$

$$\frac{\partial F_3}{\partial \beta} = \frac{4\gamma\,\text{Sin}\,(\beta-\phi)\,\text{Cos}\,(\beta-\phi)}{\gamma(\gamma+1)} \tag{1-9}$$

$$\frac{\partial F_3}{\partial \phi} = - \frac{\partial F_3}{\partial \beta} \tag{1-10}$$

$$\frac{\partial F_3}{\partial M_\infty} = \frac{2\,(\gamma-1)}{\gamma(\gamma+1)\,M_\infty^3} \tag{1-11}$$

$$\frac{\partial F_4}{\partial \beta} = \frac{4 \cos(\beta-\phi)}{(\gamma+1)\, M_\infty^2 \sin^3(\beta-\phi)} \left(\frac{\rho_1}{\rho_\infty}\right)^2 \tag{1-12}$$

$$\frac{\partial F_4}{\partial \phi} = -\frac{\partial F_4}{\partial \beta} \tag{1-13}$$

$$\frac{\partial F_4}{\partial M_\infty} = \frac{4}{(\gamma+1)\, M_\infty^3 \sin^2(\beta-\phi)} \left(\frac{\rho_1}{\rho_\infty}\right)^2 \tag{1-14}$$

The total derivatives with respect to s may be evaluated using the chain rule for differentiation:

$$\frac{d}{ds}\left(\frac{\rho_1 u_1 v_1}{\rho_\infty V_\infty^2}\right) = \frac{\partial F_1}{\partial \beta}\frac{d\beta}{ds} + \frac{\partial F_1}{\partial \phi}\frac{d\phi}{ds} + \frac{\partial F_1}{\partial \theta}\frac{d\theta}{ds} + \frac{\partial F_1}{\partial M_\infty}\frac{dM_\infty}{ds} \tag{1-15}$$

$$\frac{d}{ds}\left(\frac{u_1}{V_\infty}\right) = \frac{\partial F_2}{\partial \beta}\frac{d\beta}{ds} + \frac{\partial F_2}{\partial \phi}\frac{d\phi}{ds} + \frac{\partial F_2}{\partial \theta}\frac{d\theta}{ds} + \frac{\partial F_2}{\partial M_\infty}\frac{dM_\infty}{ds} \tag{1-16}$$

$$\frac{d}{ds}\left(\frac{P_1}{\rho_\infty V_\infty^2}\right) = \frac{\partial F_3}{\partial \beta}\frac{d\beta}{ds} + \frac{\partial F_3}{\partial \phi}\frac{d\phi}{ds} + \frac{\partial F_3}{\partial M_\infty}\frac{dM_\infty}{ds} \tag{1-17}$$

$$\frac{d}{ds}\left(\frac{\rho_1}{\rho_\infty}\right) = \frac{\partial F_4}{\partial \beta}\frac{d\beta}{ds} + \frac{\partial F_4}{\partial \phi}\frac{d\phi}{ds} + \frac{\partial F_4}{\partial M_\infty}\frac{dM_\infty}{ds} \tag{1-18}$$

The derivatives for $\rho_1 u_1 v_1$ and $\tau_1 u_1$ may now be computed:

$$\frac{d}{ds}\left(\rho_1 u_1 v_1\right) = \rho_\infty V_\infty^2 \frac{dF_1}{ds} + F_1 \frac{d}{ds}\left(\rho_\infty V_\infty^2\right) \tag{1-19}$$

$$\frac{dP_1}{ds} = \rho_\infty V_\infty^2 \frac{dF_3}{ds} + F_3 \frac{d}{ds}\left(\rho_\infty V_\infty^2\right) \tag{1-20}$$

$$\frac{d\rho_1}{ds} = \rho_\infty \frac{dF_4}{ds} + F_4 \frac{d\rho_\infty}{ds} \tag{1-21}$$

$$\frac{du_1}{ds} = V_\infty \frac{dF_2}{ds} + F_2 \frac{dV_\infty}{ds} \tag{1-22}$$

$$\frac{d}{ds}\left(\tau_1 u_1\right) = \tau_1 \frac{du_1}{ds} + u_1 \left[\frac{\rho_1 \tau_1}{(\gamma-1)P_1} \frac{d}{ds}\left(\frac{P_1}{\rho_1}\right)\right] \tag{1-23}$$

$$= \tau_1 \frac{du_1}{ds} + \frac{u_1 \tau_1}{(\gamma-1)} \left[\frac{1}{P_1} \frac{dP_1}{ds} - \frac{1}{\rho_1} \frac{d\rho_1}{ds}\right]$$

The only remaining derivatives to evaluate are those involving the free stream density, velocity and dynamic pressure:

$$\rho_\infty V_\infty^2 = \gamma P_\infty M_\infty^2 , \qquad P_\infty = P_{T_\infty}\left[1 + \frac{\gamma-1}{2} M_\infty^2\right]^{\frac{-\gamma}{\gamma-1}}$$

$$\frac{V_\infty}{V_{max}} = \sqrt{\frac{(\gamma-1)M_\infty^2}{2 + (\gamma-1)M_\infty^2}} , \qquad V_{max} \equiv \sqrt{2 H_{T_\infty}}$$

$$\frac{\rho_\infty}{\rho_{T_\infty}} = \left[1 + \frac{\gamma-1}{2} M_\infty^2\right]^{\frac{-1}{\gamma-1}} , \qquad \rho_{T_\infty} = \frac{\gamma P_{T_\infty}}{(\gamma-1) H_{T_\infty}}$$

$$\frac{d}{ds}\left(\frac{V_\infty}{V_{max}}\right) = \frac{2M_\infty (\gamma-1)}{\left[2 + (\gamma-1)M_\infty^2\right]^2} \left(\frac{V_\infty}{V_{max}}\right)^{-1} \frac{dM_\infty}{ds}$$

$$\frac{d}{ds}\left(\frac{\rho_\infty}{\rho_{T_\infty}}\right) = -M_\infty\left[1+\frac{\gamma-1}{2}\,M_\infty^2\right]^{\frac{-\gamma}{\gamma-1}}\,\frac{dM_\infty}{ds}$$

$$\frac{d\,V_{max}}{ds} = \frac{1}{V_{max}}\,\frac{dH_{T_\infty}}{ds}$$

$$\frac{d\,\rho_{T_\infty}}{ds} = \frac{\gamma}{\gamma-1}\left[\frac{1}{H_{T_\infty}}\,\frac{dP_{T_\infty}}{ds} - \frac{P_{T_\infty}}{H_{T_\infty}^2}\,\frac{dH_{T_\infty}}{ds}\right]$$

$$\frac{dV_\infty}{ds} = V_{max}\,\frac{d}{ds}\left(\frac{V_\infty}{V_{max}}\right) + \frac{V_\infty}{V_{max}}\,\frac{d}{ds}\left(V_{max}\right)$$

$$\frac{d\,\rho_\infty}{ds} = \rho_{T_\infty}\,\frac{d}{ds}\left(\frac{\rho_\infty}{\rho_{T_\infty}}\right) + \frac{\rho_\infty}{\rho_{T_\infty}}\,\frac{d}{ds}\left(\rho_{T_\infty}\right)$$

$$\frac{d}{ds}\left(\rho_\infty V_\infty^2\right) = \gamma P_\infty M_\infty\,\frac{dM_\infty}{ds}\left[2-\frac{2\gamma M_\infty^2}{2+(\gamma-1)M_\infty^2}\right] +$$

$$\gamma M_\infty^2\left[1+\frac{\gamma-1}{2}\,M_\infty^2\right]^{\frac{-\gamma}{\gamma-1}}\,\frac{dP_{T_\infty}}{ds}$$

Thus, given the free stream Mach No., flow angle, total pressure and total enthalpy, and their gradients, all the above expressions may be computed. It is noted that if the total pressure and enthalpy are constant, then the free stream thermodynamic state properties may be normalized with their respective total values. If that is the case, then only the Mach No. and flow angle are needed to completely define the free stream flow field.

APPENDIX 2

STAGNATION POINT BEHAVIOR OF THE DIFFERENTIAL EQUATIONS

As mentioned earlier, Eq 1 and 2 are indeterminate at the stagnation point. To evaluate the initial derivatives for β and u_0, L'hopitals rule may be applied to the equations.

At the stagnation point, the initial values may be expressed as follows:

$$\phi = 0,\ \beta = \frac{\pi}{2},\ u_0 = 0,\ \theta = \frac{\pi}{2},\ \tau_1 = \rho_1(0),\ \tau_0 = \rho_0(0),\ u_1 = 0$$

The following limits are easily obtained:

$$\lim_{s \to 0} \frac{u_0}{r_0} = \frac{du_0}{ds}$$

$$\lim_{s \to 0} \frac{r_1}{r_0} = 1 - K\delta$$

$$\lim_{s \to 0} \frac{v_1}{V_\infty} = -\frac{\rho_\infty}{\rho_1}$$

From the results of Appendix 1, we get:

$$\lim_{s \to 0} \frac{\partial F_1}{\partial \beta} = 1 - \frac{\rho_\infty}{\rho_1}$$

$$\lim_{s \to 0} \frac{\partial F_1}{\partial \phi} = -1$$

$$\lim_{s \to 0} \frac{\partial F_1}{\partial \theta} = \frac{\rho_\infty}{\rho_1}$$

$$\lim_{s \to 0} \frac{\partial F_1}{\partial M_\infty} = 0$$

Substitution of these expressions into Eq 2 yields the following:

$$\delta\left(1 - \frac{\rho_\infty}{\rho_1}\right)\frac{d\beta}{ds} \quad \delta\frac{d\phi}{ds} \cdot \frac{P_0 - P_1}{\rho_\infty V_\infty^2} + \frac{v_1}{V_\infty} \tag{2-1}$$

Again, from Appendix 1, we get

$$\lim_{s \to 0} \quad \frac{d}{ds}\left(\frac{u_1}{V_\infty}\right) - \left(\frac{\rho_\infty}{\rho_1} - 1\right)\frac{d\beta}{ds} + \frac{d\phi}{ds} + \frac{v_1}{V_\infty}\frac{d\theta}{ds}$$

Substitution of this expression and Eq 2-1 into Eq 1 yields the following expression for the stagnation point velocity:

$$\frac{1}{V_\infty}\frac{du_0}{ds} = \frac{\rho_1(1 + K\delta)}{\delta\rho_0}\left(\frac{P_0 - P_1}{\rho_\infty V_\infty^2}\right) \tag{2-2}$$

It is interesting to note that $\frac{d\phi}{ds}$ cancels out upon substitution of eq. 2-1 into Eq 1. Therefore, the stagnation point velocity gradient has the same form for either uniform or non uniform external flow.

LIST OF SYMBOLS

s - Distance measured along body surface.

n - Distance measured normal to body surface.

δ - Shock standoff distance - measured normal to body surface.

R - Radius of sphere or circular disk.

θ - Body surface angle.

β - Shock angle measured to the body axis.

ϕ - Flow inclination angle between free stream velocity vector and flow field axis.

r - Distance measured normal to flow field or body axis.

z - Distance measured parallel to flow field or body axis.

u - Velocity component parallel to body surface.

v - Velocity component normal to body surface.

P - Static pressure.

ρ - Static density.

γ - Ratio of specific heats.

ℓ_o - Distance measured from a spherical source to the stagnation point of a body in the source flow field.

M - Mach number.

K - Local curvature of body surface.

τ - $\left(\frac{P}{\rho\,\phi}\right)^{\frac{1}{\gamma-1}}$, $\phi \equiv \frac{P_1(0)}{\rho_1^{\gamma}(0)}$

V_{max} - Maximum thermodynamic limiting velocity of the free stream.

r_e - Nozzle exit radius

H_T - Total enthalpy

P_T - Total pressure

SUBSCRIPTS:

∞ - Free stream flow conditions.

0 - Body surface conditions or conditions at the stagnation point location of a body in a spherical source flow.

1 - Conditions immediately behind the shock wave.

u - Uniform flow conditions.

SUPERSCRIPTS:

* - Sonic point conditions - either on the body surface or on the bow shock.

- - Refers to solutions for which the free stream derivatives of mach and flow angle were ignored. that is;

$$\frac{d\phi}{ds} \equiv 0 \text{ and } \frac{dM_n}{ds} \equiv 0.$$

Table 1

SUMMARY OF SOLUTIONS FOR A SPHERE IN A SPHERICAL SOURCE FLOW

			STAGNATION POINT PARAMETERS		SONIC POINT COORDINATES		
					BODY	SHOCK WAVE	
γ	M_0	$\frac{R}{r_0}$	$\frac{R}{\sqrt{\frac{dv_\theta}{d\theta}}}_{max}$	$\frac{\delta}{R}$	θ^*	θ^*	ϕ^*
1.66	2.0	0	0.3473	0.2950	43.1	44.4	0.651
		0.10	0.4059	0.2482	46.1	54.4	0.551
		0.20	0.4[illegible]	0.2115	52.0	57.[illegible]	0.293
		0.25	0.4[illegible]	0.1[illegible]	54.7	59.5	0.270
		0.3333	0.5[illegible]44	0.1[illegible]	58.0	63.[illegible]	0.241
		0.50	0.6[illegible]	0.1[illegible]	64.6	68.6	0.210
1.80	5.0	0	0.5742	0.1001	50.7	65.8	0.121
		0.10	0.6[illegible]4	0.[illegible]	54.[illegible]	68.4	0.[illegible]
		0.20	0.7[illegible]	0.0[illegible]	[illegible].9	70.4	0.0950
		0.25	0.7[illegible]	0.0[illegible]	[illegible].2	71.3	0.0900
		0.3333	0.7[illegible]	0.0[illegible]	[illegible].1	72.5	0.0814
		0.50	0.9[illegible]3	0.0[illegible]	64.5	74.6	0.0728
1.80	10.0	0	0.6[illegible]72	0.0[illegible]	52.1	69.0	0.0925
		0.10	0.7[illegible]	0.0[illegible]	56.9	72.2	0.0840
		0.20	0.[illegible]	0.0[illegible]	[illegible].6	73.8	0.0797
		0.25	0.8[illegible]	0.0[illegible]	[illegible].8	74.6	0.0771
		0.3333	0.[illegible]	0.0[illegible]	[illegible].4	74.7	0.0731
		0.50	1.0[illegible]	0.0[illegible]	[illegible].6	76.5	0.0588
1.80	20.0	0	0.[illegible]	0.0[illegible]	53.5	69.4	0.0900
		0.10	0.[illegible]	0.0[illegible]	58.3	71.9	0.0[illegible]
		0.20	0.[illegible]	0.0[illegible]	[illegible].4	73.4	0.0[illegible]
		0.25	0.8[illegible]	0.0[illegible]	[illegible].8	74.2	0.0[illegible]
		0.3333	0.9[illegible]	0.0[illegible]	[illegible].7	75.0	0.0[illegible]
		0.50	1.0[illegible]	0.0454[illegible]	[illegible].6	76.9	0.0529
1.40	2.0	0	0.4[illegible]	0.2615	41.1	38.3	0.597
		0.10	0.5[illegible]	0.2[illegible]	47.[illegible]	49.0	0.[illegible]
		0.20	0.5[illegible]	0.[illegible]	[illegible]	55.1	0.[illegible]44
		0.25	0.6[illegible]	0.23[illegible]	[illegible].[illegible]	57.2	0.[illegible]
		0.3333	0.[illegible]	0.[illegible]	[illegible].[illegible]	60.2	0.[illegible]
		0.50	0.7[illegible]	0.2[illegible]	[illegible]	[illegible].7	0.[illegible]
1.40	5.0	0	0.44[illegible]	0.1[illegible]	48.[illegible]	56.[illegible]	0.[illegible]4
		0.10	0.5[illegible]	0.1[illegible]	52.[illegible]	60.5	0.[illegible]7
		0.20	0.6[illegible]	0.12[illegible]	[illegible].[illegible]	63.[illegible]	0.[illegible]
		0.25	0.6[illegible]	0.1[illegible]	[illegible].[illegible]	64.[illegible]	0.140
		0.3333	0.7[illegible]	0.1054	[illegible].[illegible]	[illegible].2	0.127
		0.50	1.05[illegible]	0.0867	[illegible].4	[illegible].9	0.109
1.40	10.0	0	0.6911	0.1352	49.1	61.9	0.142
		0.10	0.7292	0.1152	53.[illegible]	64.9	0.121
		0.20	0.8062	0.1051	57.0	66.5	0.[illegible]
		0.25	0.8[illegible]	0.0[illegible]	58.[illegible]	67.4	0.[illegible]
		0.3333	0.9[illegible]	0.09[illegible]	62.5	68.8	0.[illegible]
		0.50	1.1235	0.0791	64.0	72.2	0.0939
1.40	20.0	0	0.7082	0.1294	49.4	62.5	0.155
		0.10	0.7918	0.1[illegible]	53.7	65.4	0.[illegible]
		0.20	0.8[illegible]	0.10[illegible]	57.[illegible]	67.[illegible]	0.[illegible]
		0.25	0.9254	0.0[illegible]	58.[illegible]	68.[illegible]	0.[illegible]
		0.3333	1.0006	0.0[illegible]	60.[illegible]	70.[illegible]	0.1048
		0.50	1.1428	0.0762	64.0	72.6	0.0908
1.6667	2.0	0	0.4[illegible]	0.4[illegible]	34.9	29.1	0.441
		0.10	0.5833	0.3[illegible]	43.5	45.[illegible]	0.514
		0.20	0.6769	0.2[illegible]	50.0	53.[illegible]	0.[illegible]
		0.25	0.7192	0.2740	51.8	55.8	0.366
		0.3333	0.7[illegible]	0.2452	54.5	59.3	0.320
		0.50	0.9232	0.2035	58.7	64.0	0.259
1.6667	5.0	0	0.6772	0.2[illegible]	46.0	52.3	0.291
		0.10	0.7756	0.1972	50.7	57.[illegible]	0.[illegible]
		0.20	0.8715	0.1[illegible]	54.6	60.8	0.[illegible]
		0.25	0.9197	0.1586	56.1	62.3	0.[illegible]
		0.3333	0.9[illegible]	0.1445	58.4	64.4	0.[illegible]
		0.50	1.1610	0.1229	62.2	67.6	0.151
1.6667	10.0	0	0.7136	0.2038	46.8	54.7	0.254
		0.10	0.8143	0.1743	51.5	59.0	0.214
		0.20	0.9126	0.1527	55.3	62.3	0.187
		0.25	0.9612	0.1438	56.7	63.6	0.176
		0.3333	1.0418	0.1313	59.1	65.5	0.160
		0.50	1.2006	0.1120	62.7	68.6	0.136
1.6667	20.0	0	0.[illegible]	0.1941	47.0	55.3	0.245
		0.10	0.[illegible]	0.1[illegible]	51.8	59.5	0.[illegible]
		0.20	0.9[illegible]	0.1[illegible]	55.5	62.6	0.191
		0.25	0.[illegible]	0.1[illegible]	[illegible].0	[illegible].0	0.[illegible]
		0.3333	1.0[illegible]	0.1[illegible]	[illegible].6	[illegible].9	0.[illegible]
		0.50	1.21[illegible]	0.1[illegible]	[illegible].1	[illegible].8	0.[illegible]

Table 2

SUMMARY OF SOLUTIONS FOR A CIRCULAR DISK IN A SPHERICAL SOURCE FLOW

			STAGNATION POINT PARAMETERS		SHOCK WAVE SONIC POINT COORDINATES	
γ	M_0	$\frac{R}{r_0}$	$\nabla \frac{R}{u_{max}} \frac{du_0}{da}$	$\frac{\delta}{R}$	$\frac{S^*}{R}$	$\frac{\delta^*}{R}$
1.20	3.0	0	0.1241	0.5088	0.960	0.304
		0.05	0.1337	0.4774	0.962	0.286
		0.10	0.1434	0.4460	0.965	0.268
		0.20	0.1626	0.3830	0.970	0.231
		0.25	0.1844	0.3450	0.979	0.211
		0.3333	0.2134	0.2993	0.986	0.209
1.20	5.0	0	0.1309	0.3969	0.968	0.277
		0.05	0.1417	0.3685	0.970	0.257
		0.10	0.1540	0.3399	0.972	0.238
		0.20	0.1830	0.2830	0.976	0.241
		0.25	0.2020	0.2547	0.981	0.241
		0.3333	0.2372	0.2121	0.986	0.250
1.20	10.0	0	0.1381	0.3491	0.967	0.243
		0.05	0.1502	0.3231	0.969	0.227
		0.10	0.1634	0.2971	0.969	0.209
		0.20	0.1927	0.2457	0.981	0.217
		0.25	0.2124	0.2199	0.987	0.220
		0.3333	0.2503	0.1838	0.990	0.184
1.20	20.0	0	0.1441	0.3360	0.967	0.233
		0.05	0.1567	0.3095	0.969	0.215
		0.10	0.1705	0.2831	0.971	0.196
		0.20	0.1952	0.2312	0.976	0.204
		0.25	0.2210	0.2044	0.982	0.205
		0.3333	0.2636	0.1760	0.989	0.187
1.40	3.0	0	0.1327	0.4872	0.957	0.413
		0.05	0.1435	0.4564	0.959	0.402
		0.10	0.1553	0.4255	0.962	0.390
		0.20	0.1810	0.3638	0.968	0.366
		0.25	0.1959	0.3330	0.973	0.350
		0.3333	0.2340	0.2844	0.979	0.340
1.40	5.0	0	0.1714	0.3810	0.961	0.373
		0.05	0.1848	0.3543	0.963	0.358
		0.10	0.1994	0.3276	0.965	0.343
		0.20	0.2321	0.2741	0.972	0.317
		0.25	-	-	-	-
		0.3333	0.2960	0.2074	0.979	0.290
1.40	10.0	0	0.1751	0.4703	0.955	0.395
		0.05	0.1889	0.4459	0.957	0.381
		0.10	0.2045	0.4029	0.960	0.367
		0.20	0.2420	0.3440	0.966	0.339
		0.25	0.2645	0.3111	0.971	0.324
		0.3333	0.3025	0.2594	0.979	0.310
1.40	20.0	0	0.1766	0.4588	0.955	0.386
		0.05	0.1949	0.4329	0.957	0.372
		0.10	0.2077	0.4070	0.959	0.358
		0.20	0.2418	0.3552	0.964	0.331
		0.25	0.2666	0.3294	0.971	0.317
		0.3333	0.3101	0.2965	0.977	0.303
1.667	3.0	0	0.1482	0.7197	0.944	0.504
		0.05	0.2010	0.6826	0.951	0.478
		0.10	0.2210	0.6457	0.961	0.474
		0.20	0.2601	0.5721	0.975	0.447
		0.25	0.2850	0.4484	0.977	0.422
		0.3333	0.3255	0.4264	0.977	0.409
1.667	5.0	0	0.2011	0.6218	0.963	0.447
		0.05	0.2193	0.5900	0.971	0.424
		0.10	0.2410	0.5579	0.969	0.402
		0.20	0.2718	0.4595	0.969	0.358
		0.25	0.2984	0.4230	0.980	0.336
		0.3333	0.3412	0.3688	0.987	0.319
1.667	10.0	0	0.2037	0.5874	0.972	0.415
		0.05	0.2215	0.5567	0.980	0.394
		0.10	0.2392	0.5054	0.987	0.379
		0.20	0.2711	0.4410	0.993	0.353
		0.25	0.2975	0.4101	0.994	0.338
		0.3333	0.3386	0.3585	0.994	0.324
1.667	20.0	0	0.2063	0.5745	0.974	0.40
		0.05	0.2243	0.5435	0.984	0.38
		0.10	0.2421	0.4924	0.988	0.37
		0.20	0.2741	0.4291	0.994	0.34
		0.25	0.3005	0.3982	0.994	0.32
		0.3333	0.3441	0.3466	0.994	0.31

Table 3

SUMMARY OF SOLUTIONS FOR AN INFINITE CIRCULAR DISK IN A SPHERICAL SOURCE FLOW

		STAGNATION POINT PARAMETERS		SONIC POINT COORDINATES		
				BODY	SHOCK WAVE	
γ	M_0	$\frac{\delta}{r_0}$	$\frac{r_0}{V_{max}}\frac{du_o}{ds}$	$\frac{s^*}{r_0}$	$\frac{s^*}{r_0}$	$\frac{\delta^*}{r_0}$
1.20	2.0	0.1706	0.4745	0.868	0.558	0.220
	3.0	0.1141	0.5606	0.759	0.472	0.141
	5.0	0.0801	0.6555	0.671	0.390	0.096
	10.0	0.0646	0.7224	0.626	0.348	0.076
	20.0	0.0606	0.7436	0.614	0.336	0.071
1.4	2.0	0.1910	0.6301	0.865	0.575	0.242
	3.0	0.1410	0.7123	0.760	0.530	0.176
	5.0	0.1119	0.7880	0.688	0.481	0.137
	10.0	0.0991	0.8326	0.654	0.455	0.120
	20.0	0.0958	0.8454	0.644	0.447	0.116
1.6667	2.0	0.2131	0.7584	0.880	0.583	0.263
	3.0	0.1681	0.8294	0.781	0.578	0.210
	5.0	0.1428	0.8877	0.722	0.559	0.179
	10.0	0.1318	0.9188	0.693	0.544	0.164
	20.0	0.1291	0.9274	0.687	0.539	0.161

Table 4

SUMMARY OF SOLUTIONS FOR A SPHERE IN A MACH 2 EXHAUST PLUME $\gamma = 1.40$

		STAGNATION POINT PARAMETERS		SONIC POINT COORDINATES		
				BODY	SHOCK WAVE	
$\frac{Z}{r_e}$	$\frac{R}{r_e}$	$\frac{\delta}{R}$	$\frac{R}{V_{max}}\frac{du_0}{ds}$	θ^*	$\frac{\delta^*}{R}$	θ^*
1.0	0.0	0.362	0.435	41.1	0.593	38.3
	0.50	0.353	0.443	44.5	0.471	48.5
	1.0	0.290	0.515	55.6	0.299	62.6
	1.5	0.238	0.601			
1.50	0.50	0.286	0.520			
	1.00	0.225	0.629			
2.0	0.0	0.268	0.500	44.2	0.382	47.5
	0.50	0.181	0.703	55.9	0.251	58.4
	1.00	0.144	0.860			
3.0	0	0.197	0.579			
	0.50	0.157	0.704			
	1.0	0.128	0.847			
	2.0	0.092	1.141			
4.0	0	0.175	0.613	47.7	0.220	57.3
	0.5	0.144	0.724	53.3	0.180	62.2
	1.0	0.123	0.838	58.4	0.154	65.3
	2.0	0.091	1.095	65.2	0.114	70.7

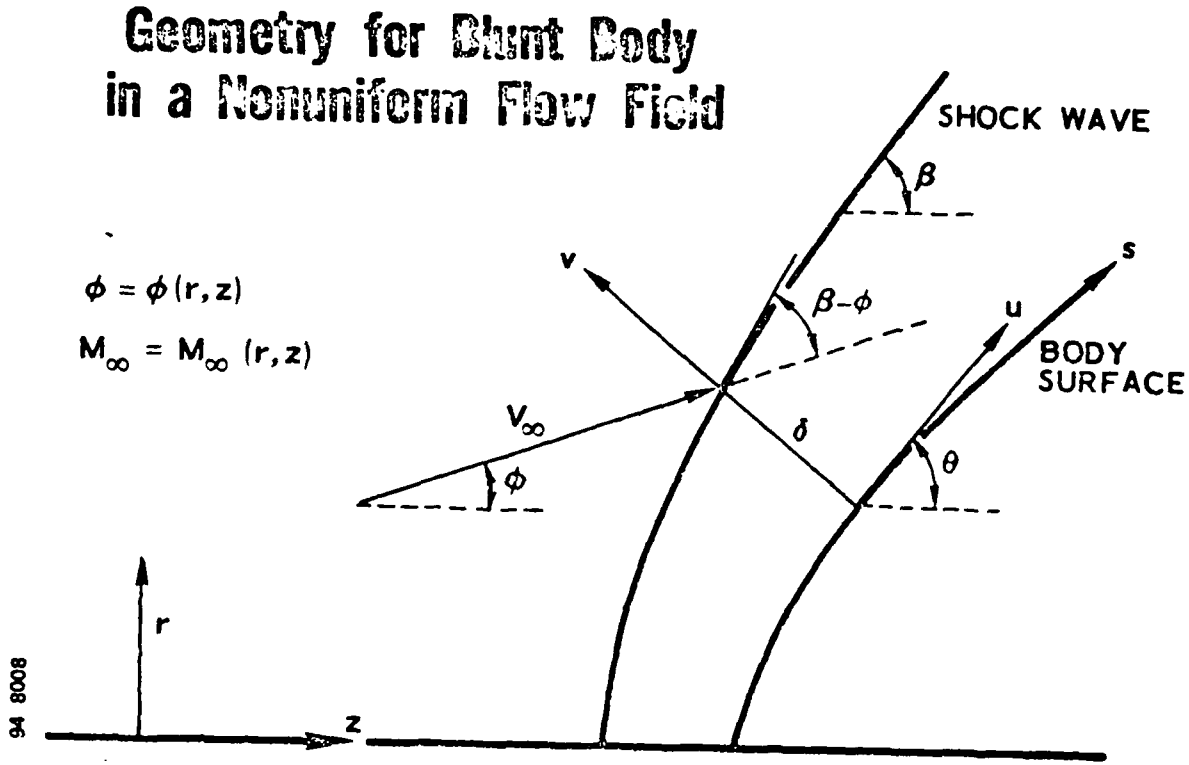

Figure 1. Geometry for Blunt Body in a Nonuniform Flow Field

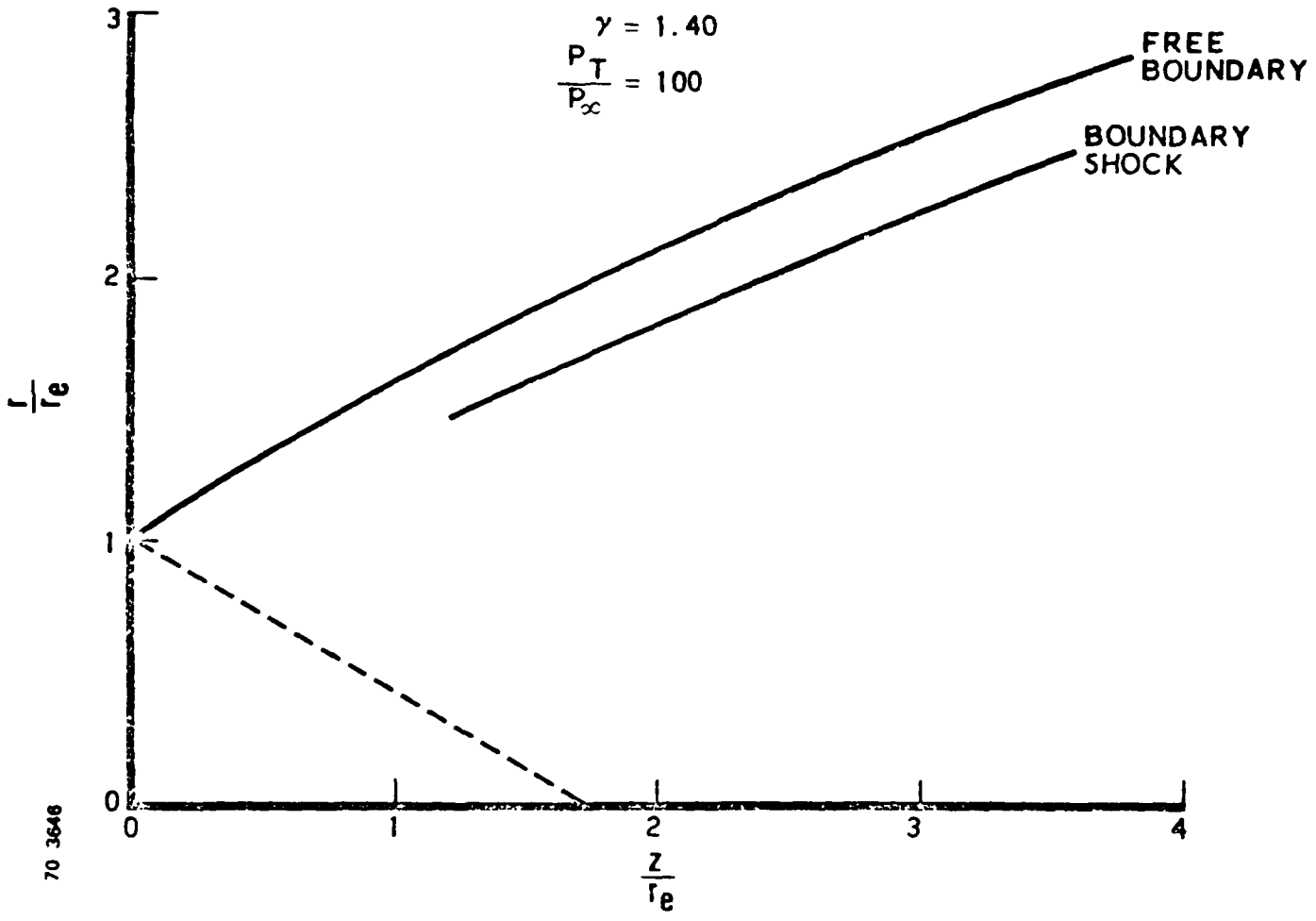

Figure 2. Flow Field Exhaust Plume for a Mach 2 Contoured Nozzle

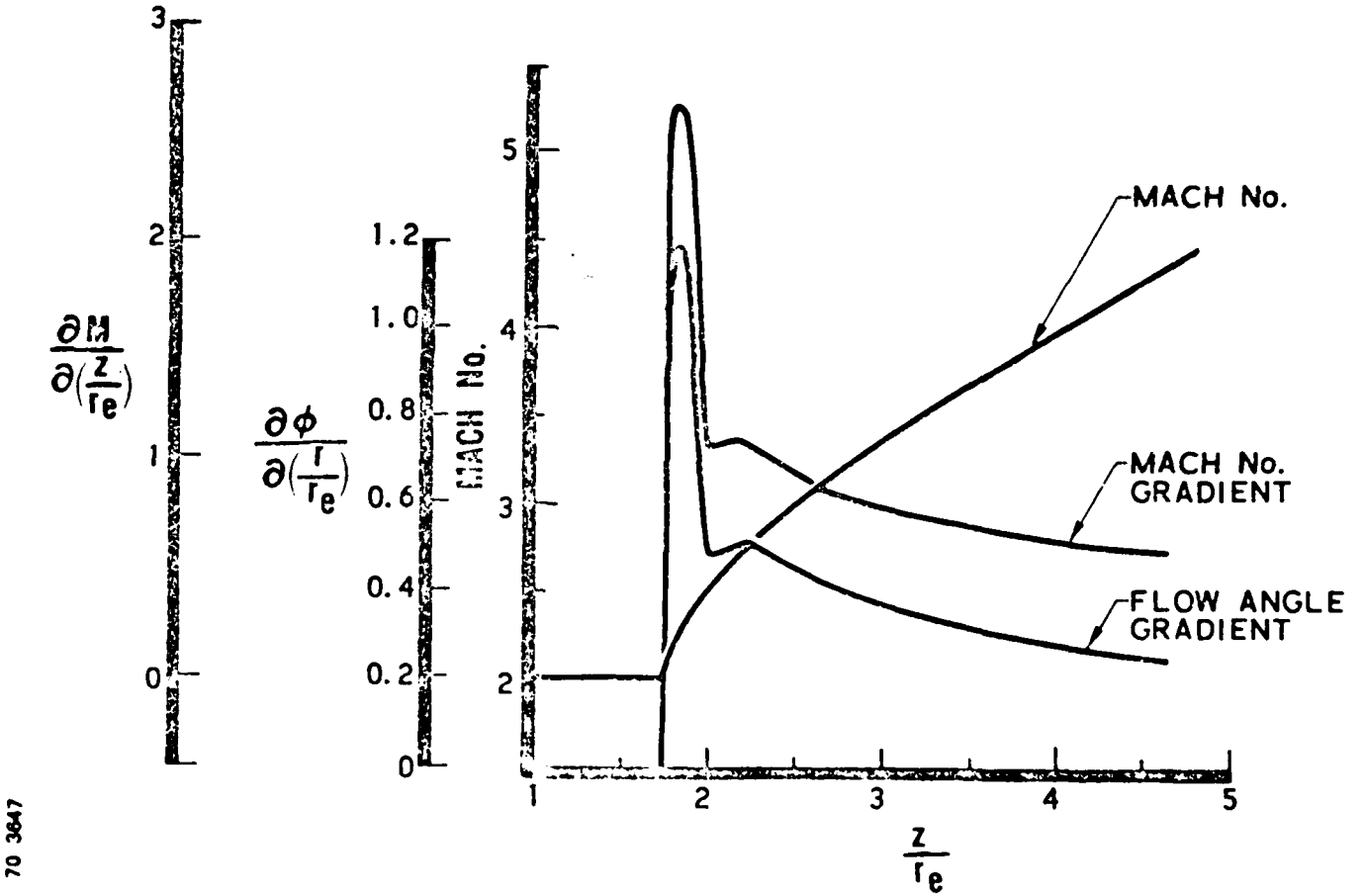

Figure 3. Centerline Properties for the Exhaust Plume

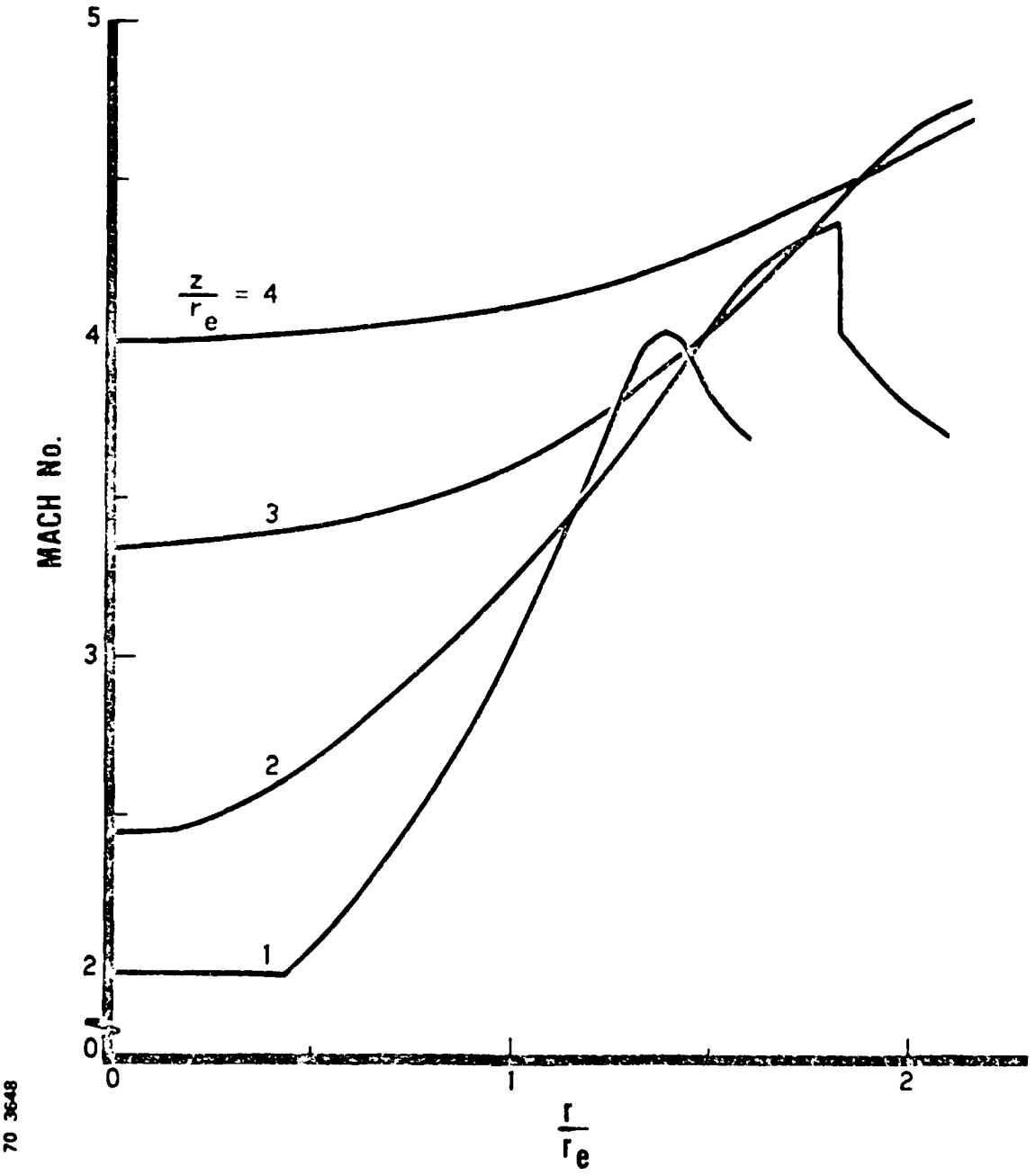

Figure 4. Mach No. Profiles for the Contoured Nozzle Exhaust Plume

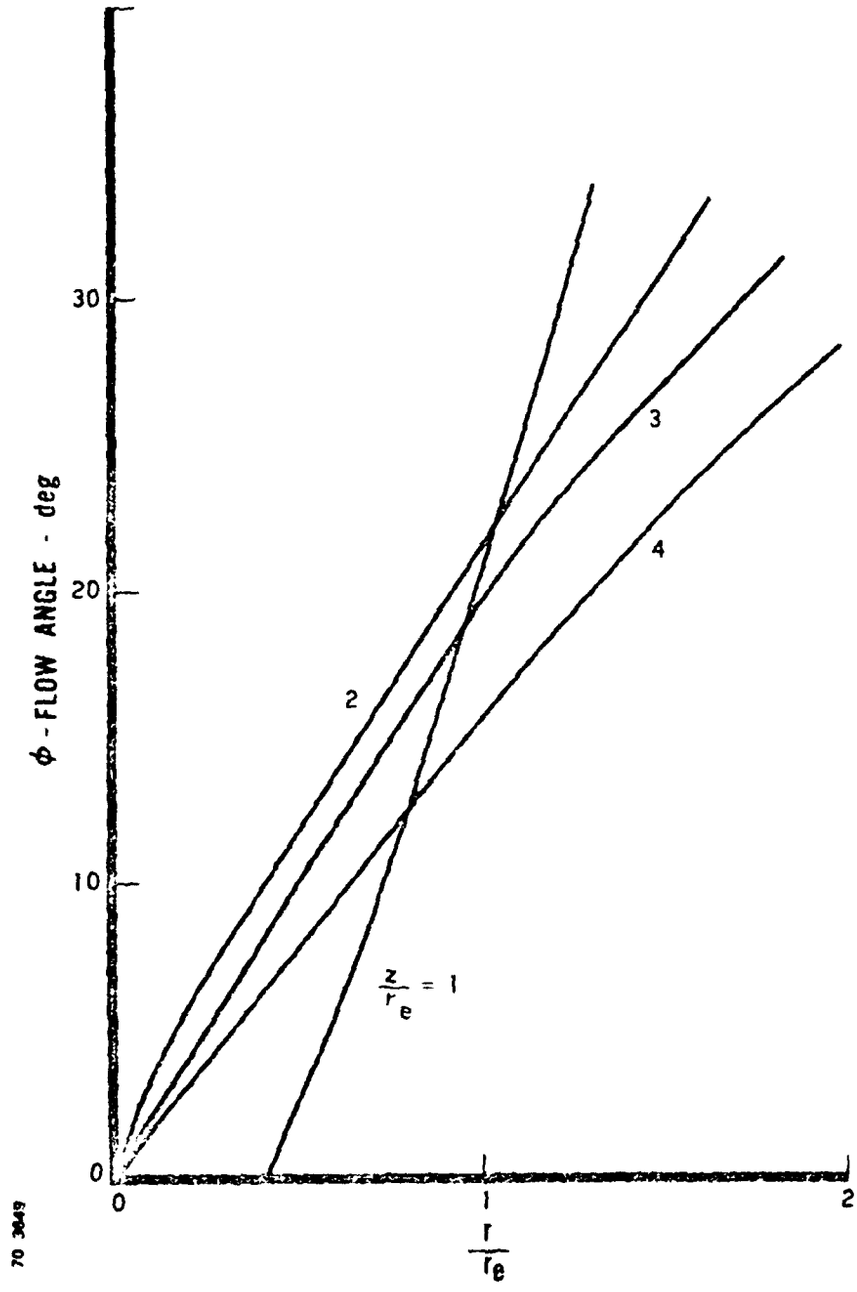

Figure 5. Flow Angle Distributions for the Contoured Nozzle Exhaust Plume

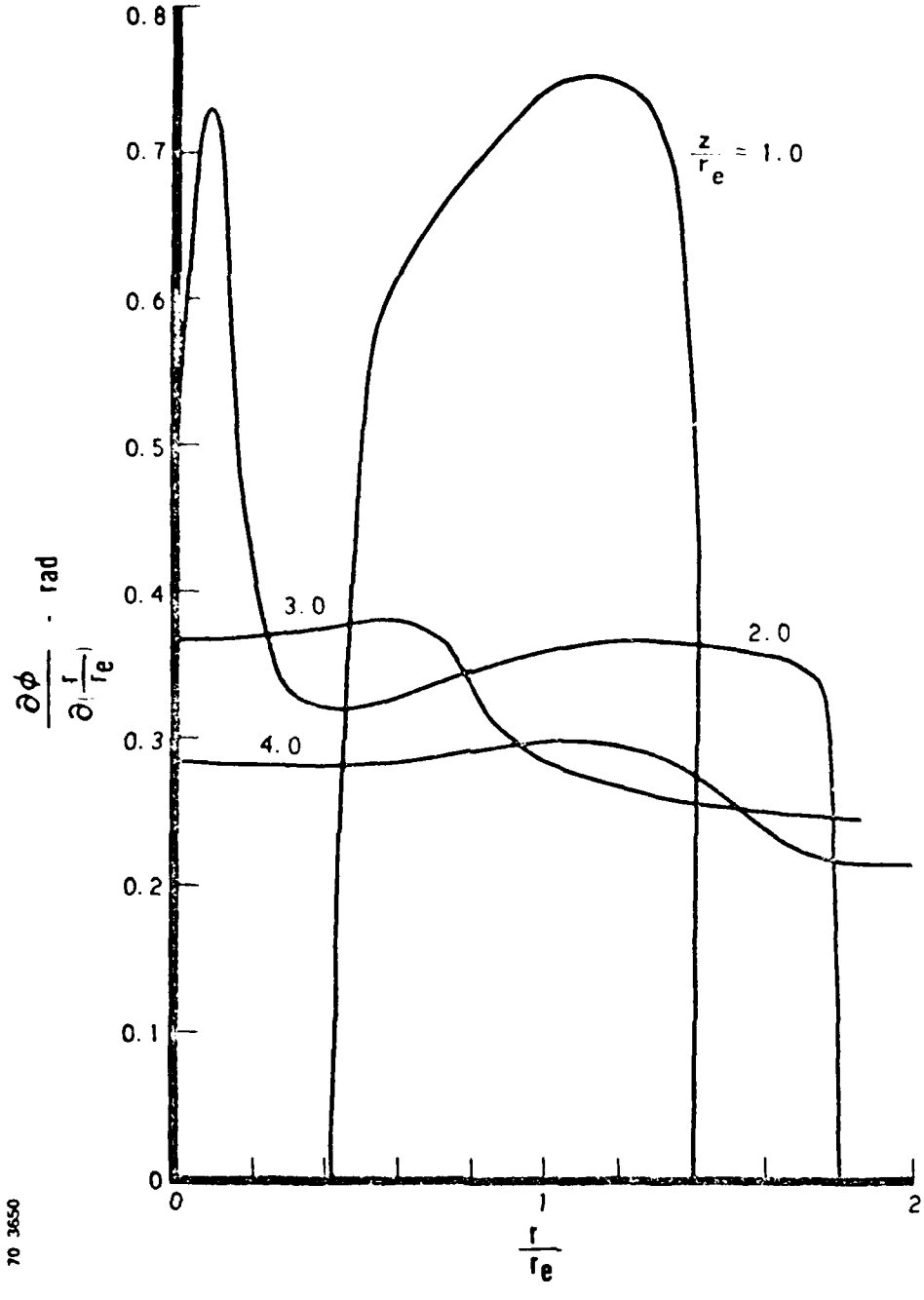

Figure 6. Flow Angle Gradient Normal to the Plume Axis

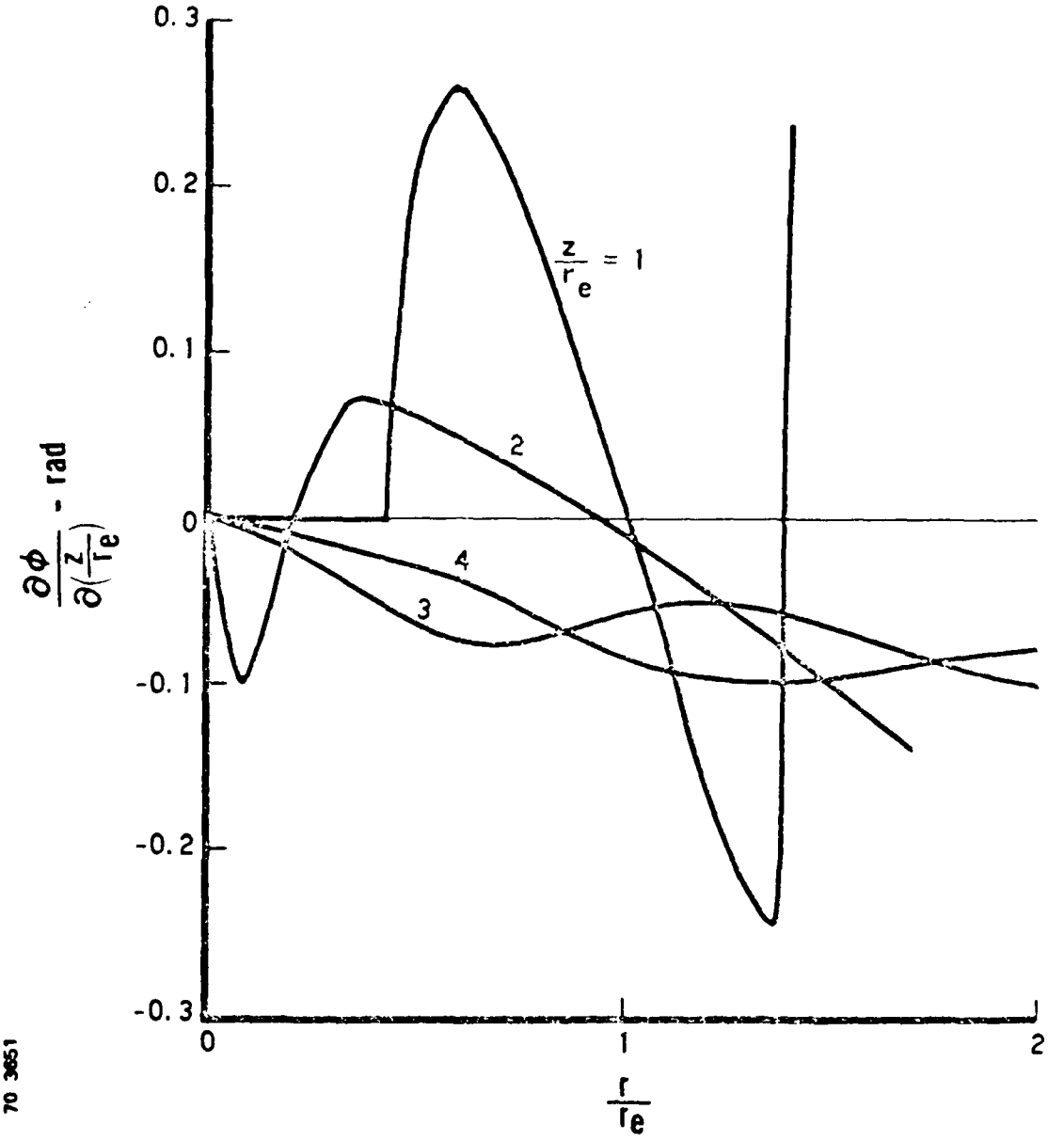

Figure 7. Flow Angle Gradient Parallel to the Plume Axis

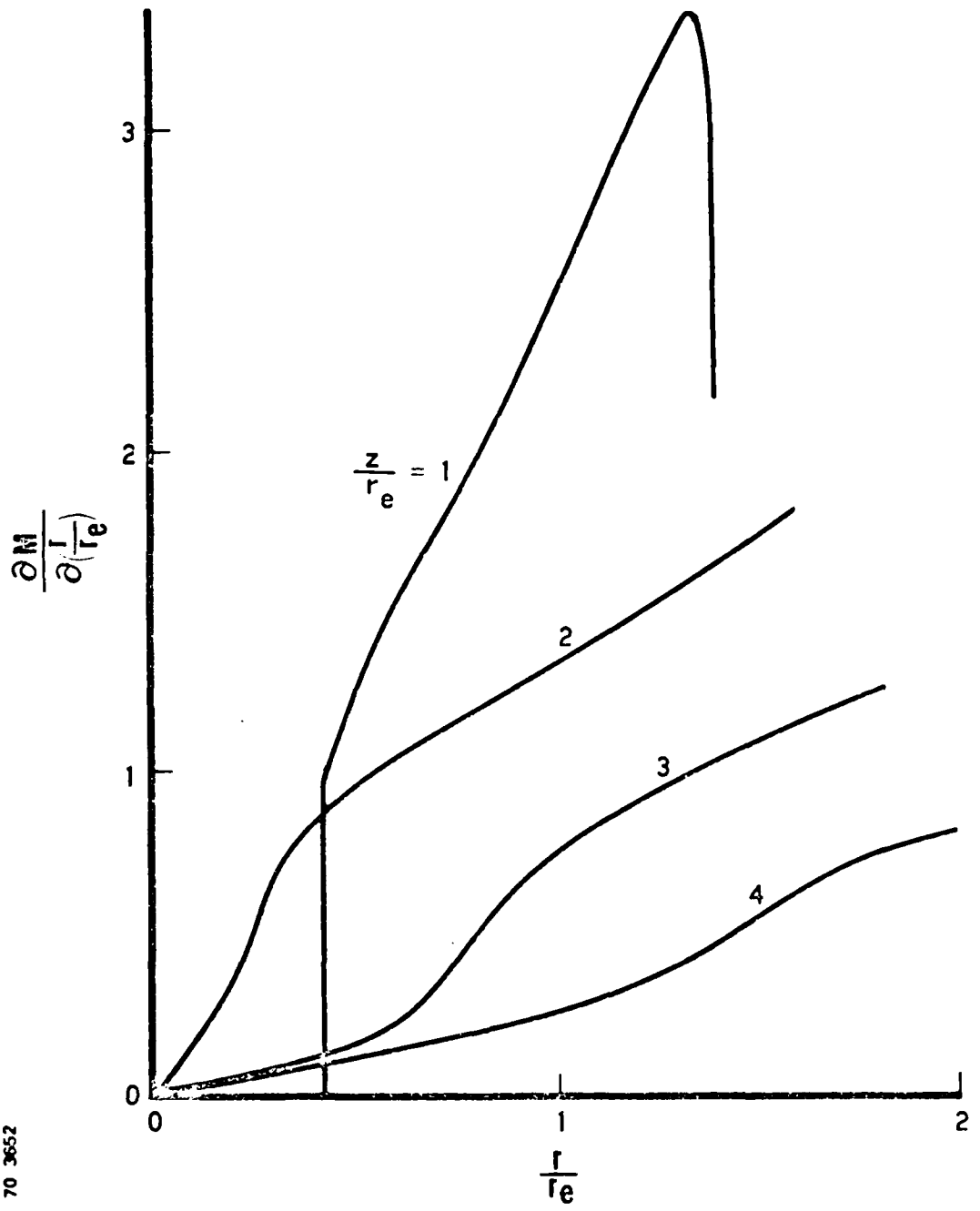

Figure 8. Mach No. Gradient Normal to the Plume Axis

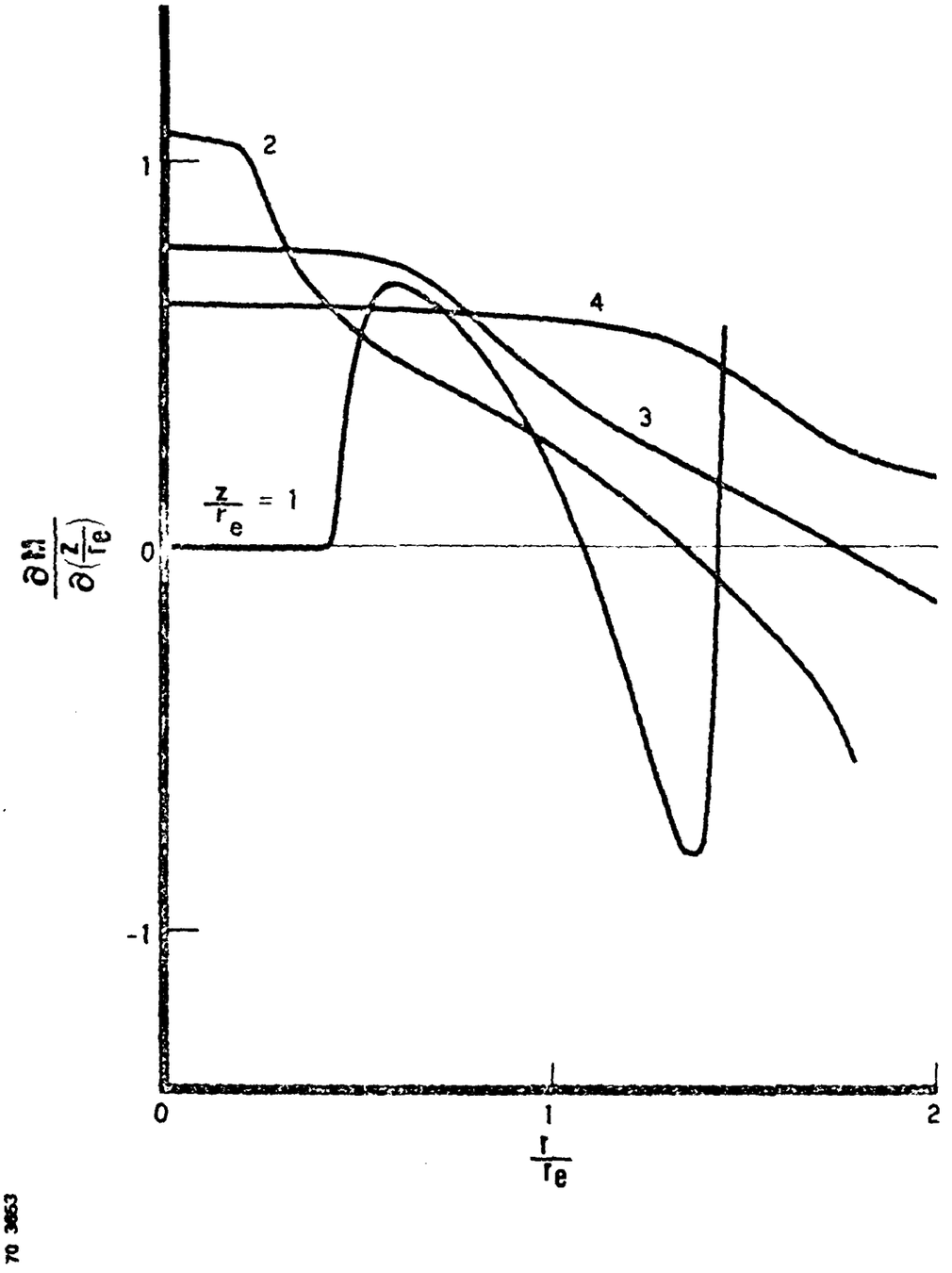

Figure 9. Mach No. Gradient Parallel to the Plume Axis

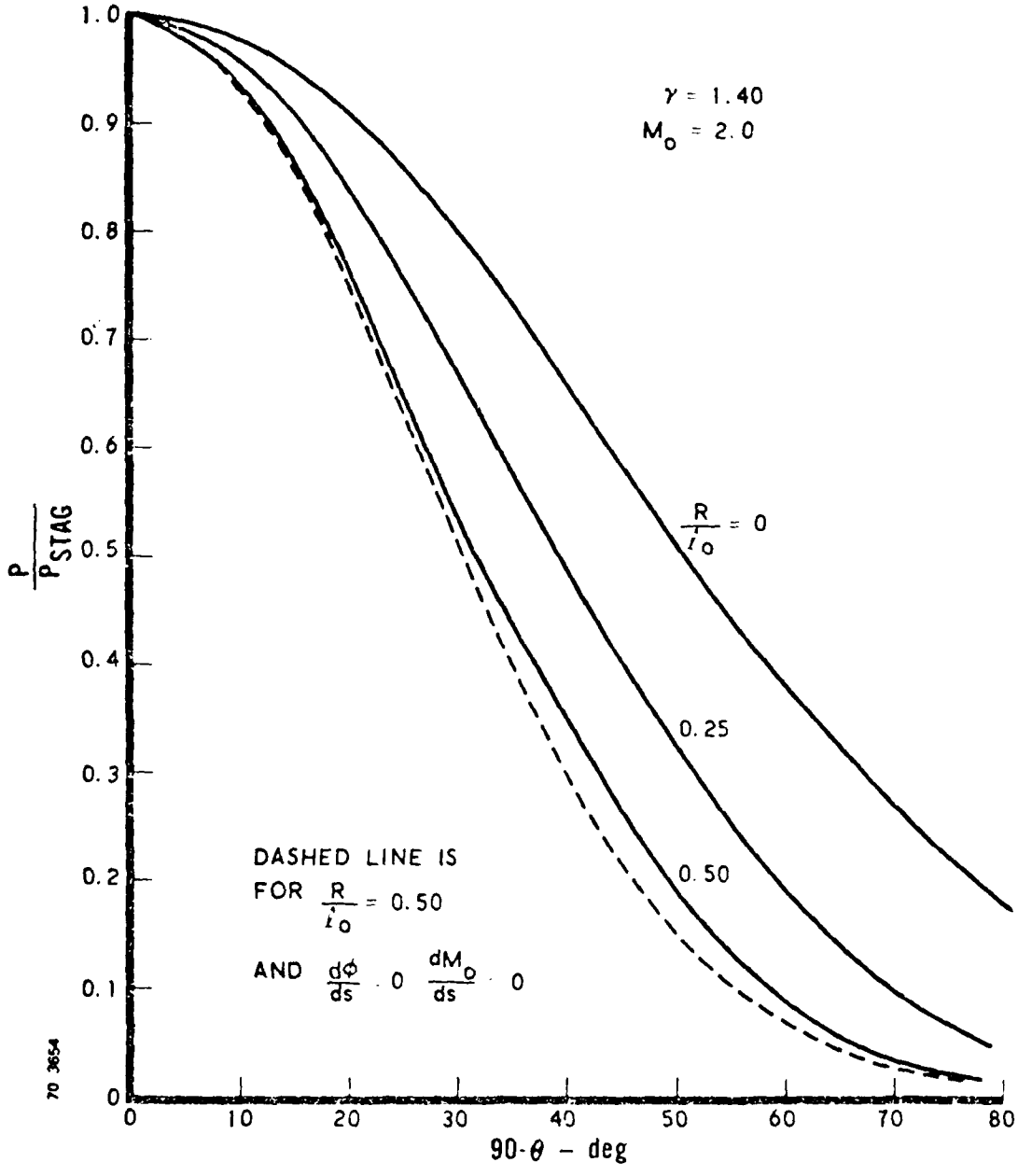

Figure 10. Pressure Distribution on a Spherical Nose in a Spherical Source Flow

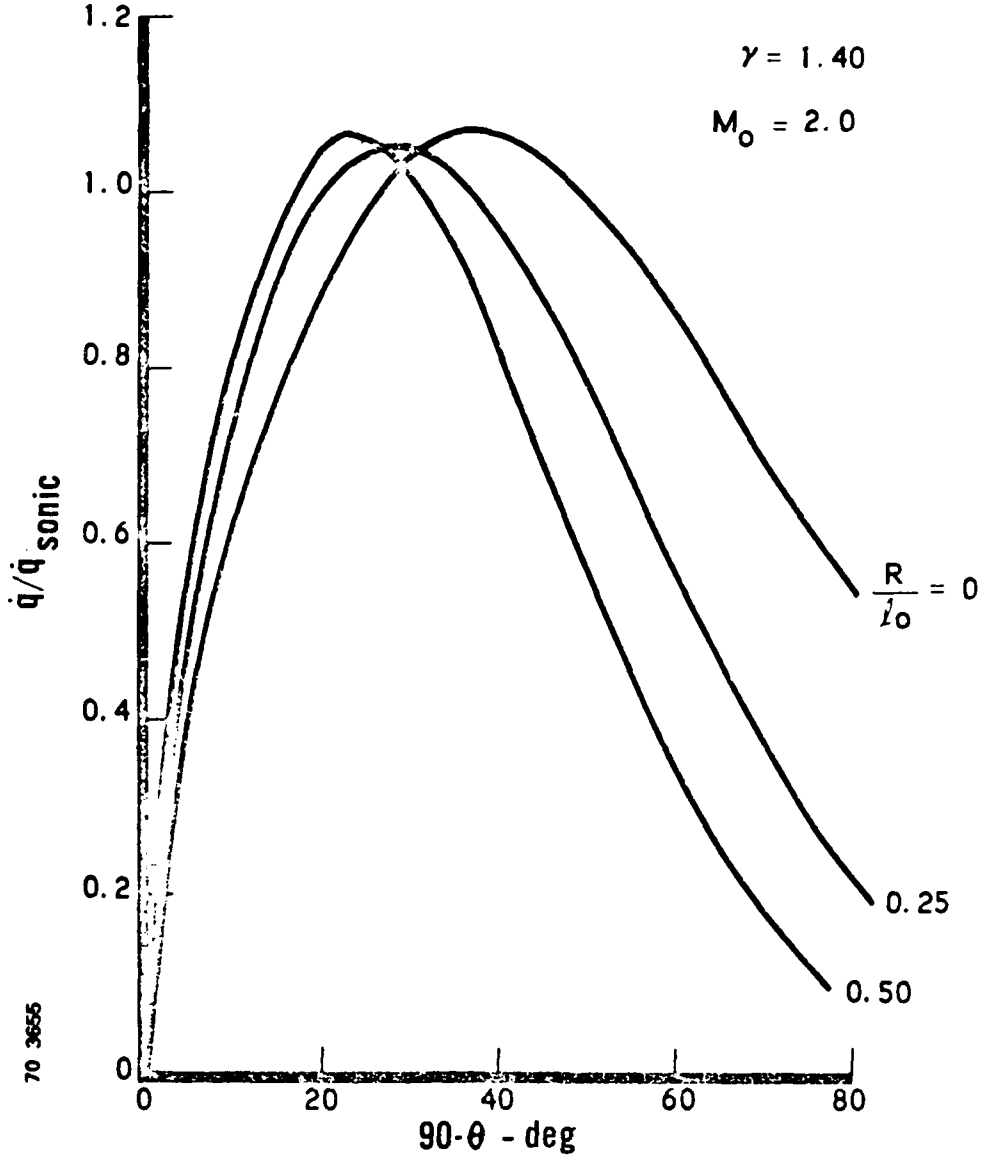

Figure 11. Turbulent Heat Transfer Distributions for a Spherical Nose in a Spherical Source Flow

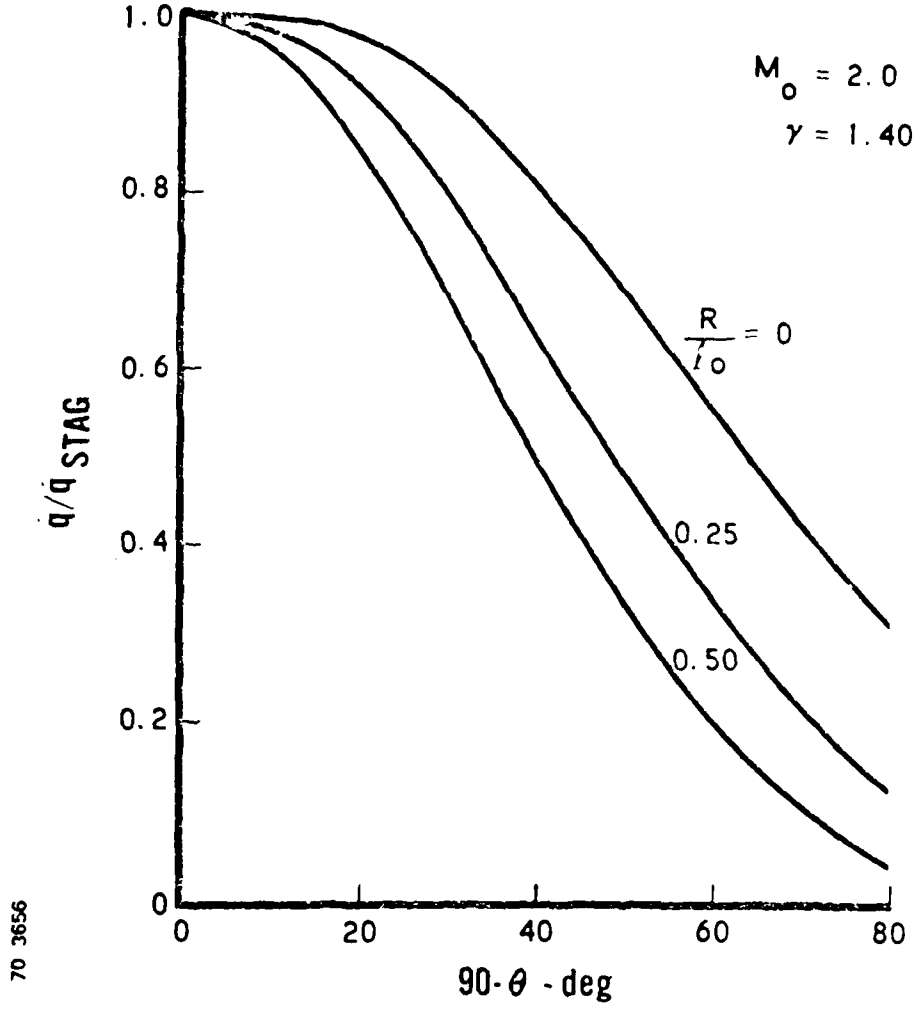

Figure 12. Laminar Heat Transfer Distributions for a Spherical Nose in a Spherical Source Flow

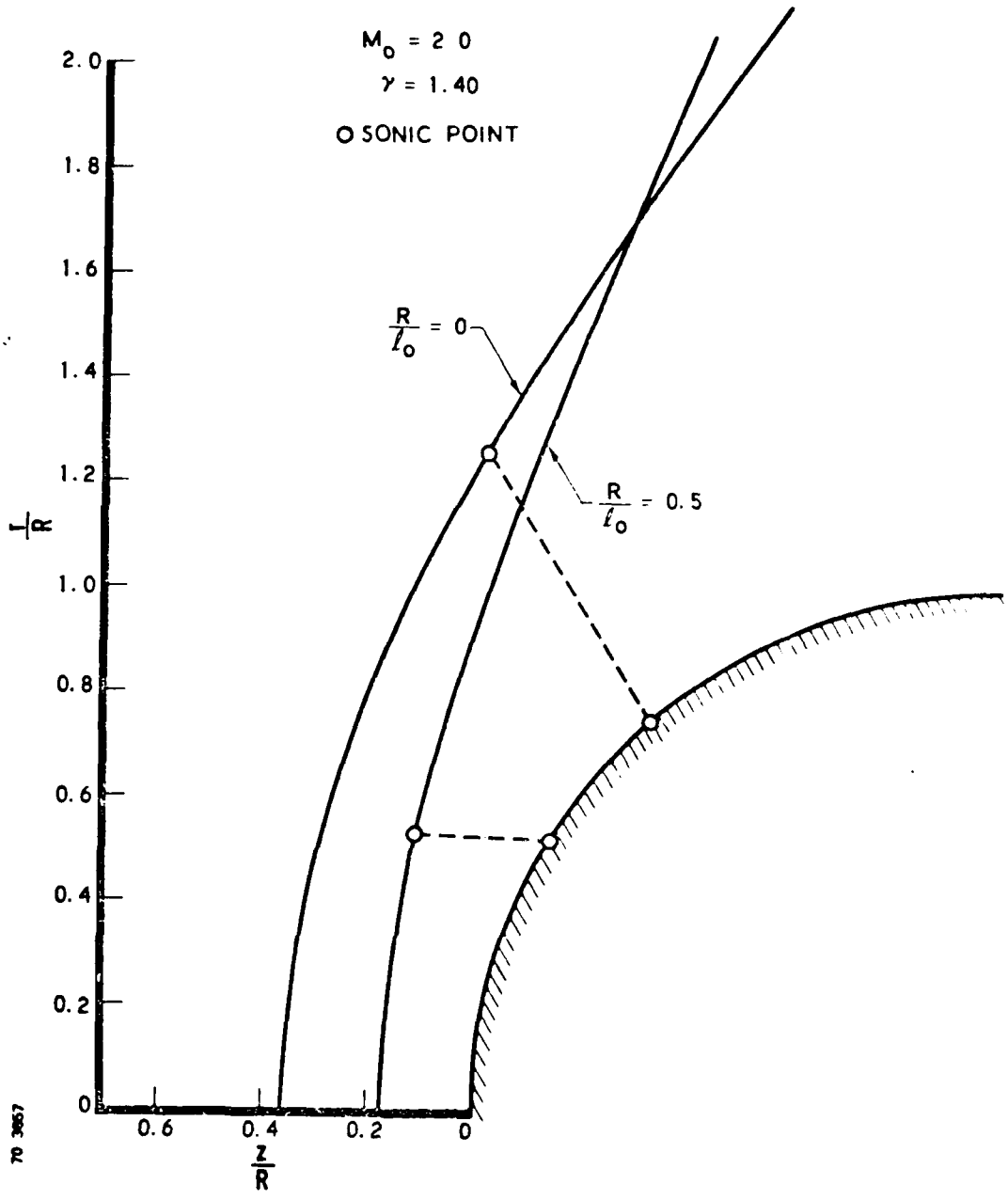

Figure 13. Shock Shapes for a Spherical Nose in a Spherical Source Flow

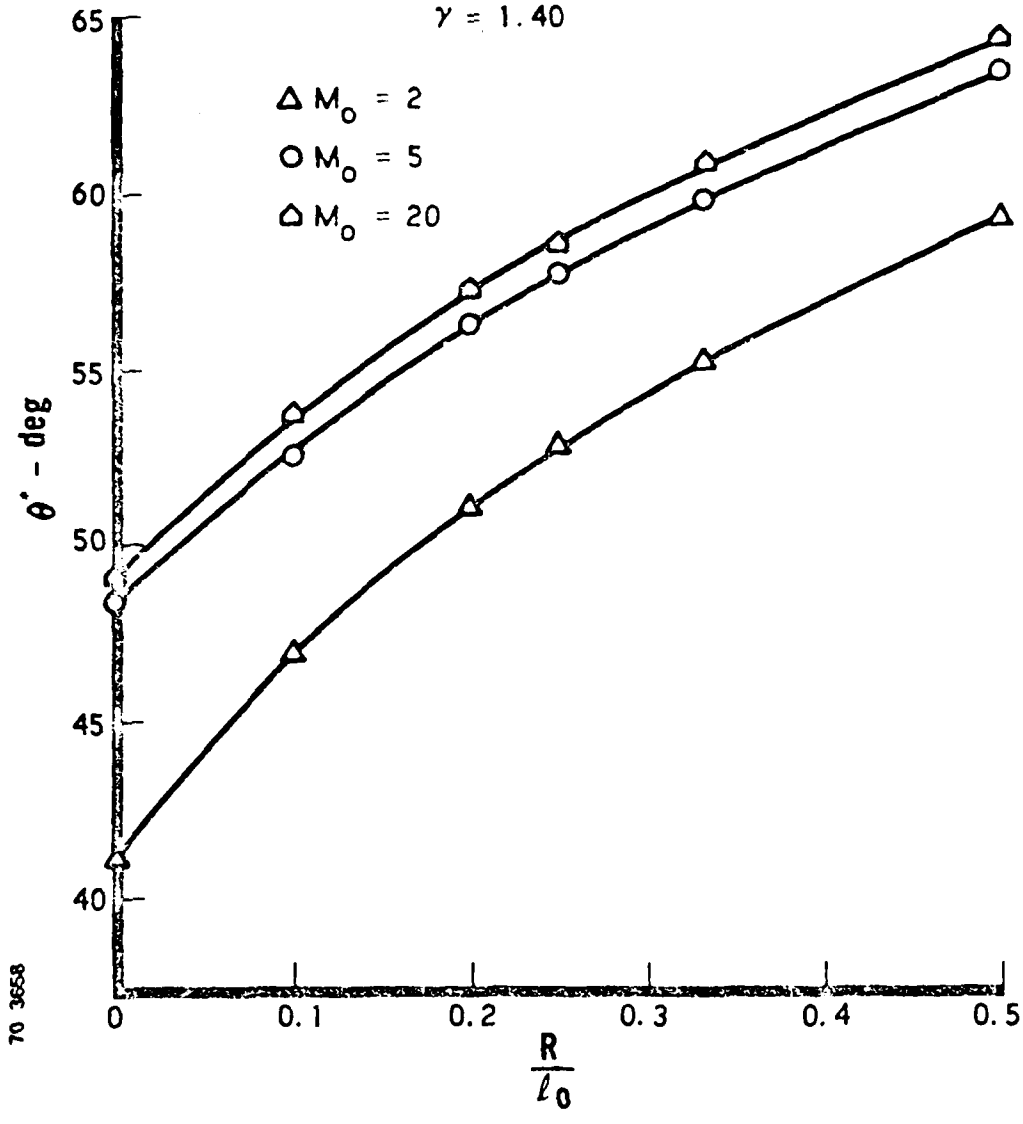

Figure 14. Sonic Point Location on a Sphere in a Spherical Source Flow

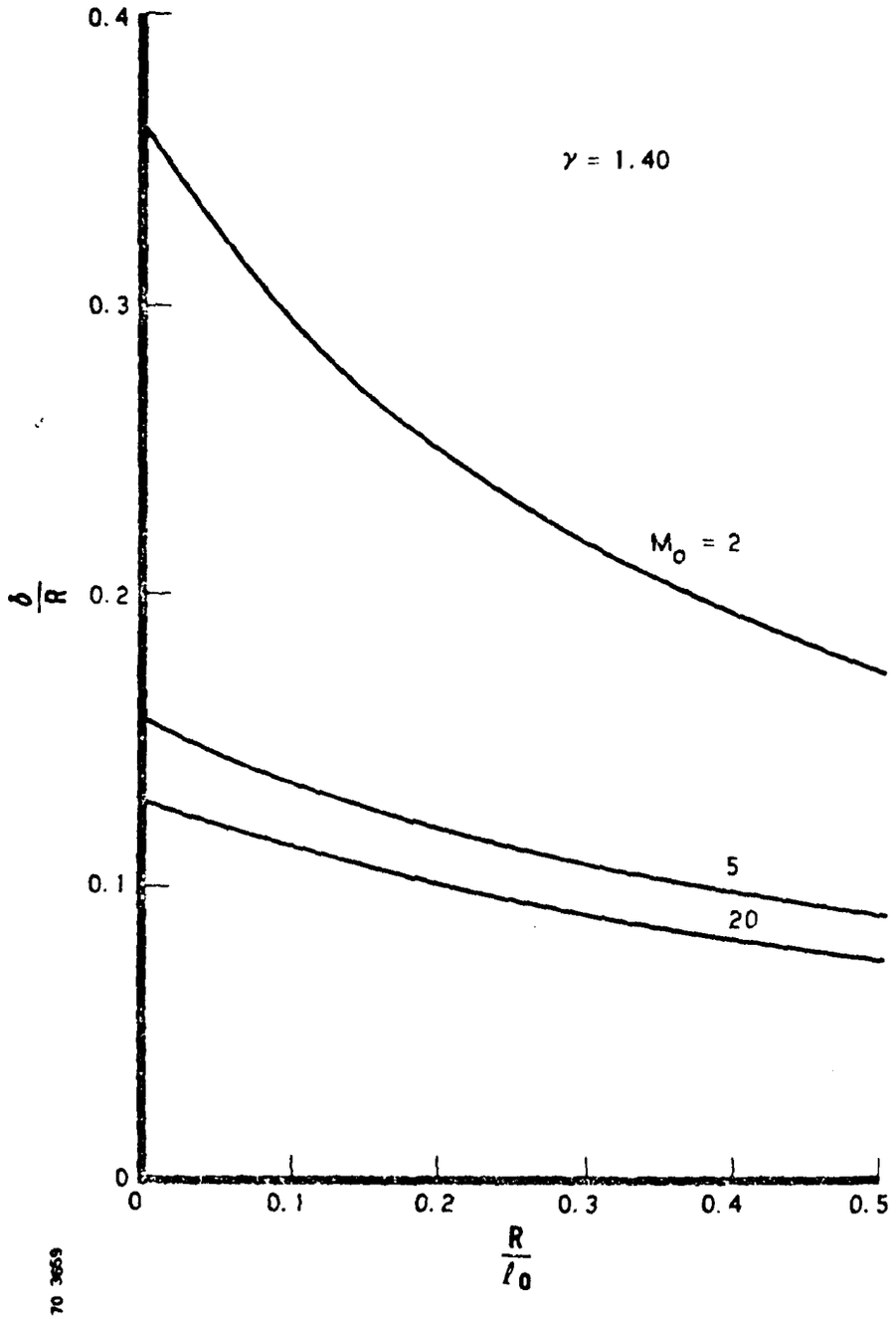

Figure 15. Shock Standoff Distance for a Sphere in a Spherical Source Flow

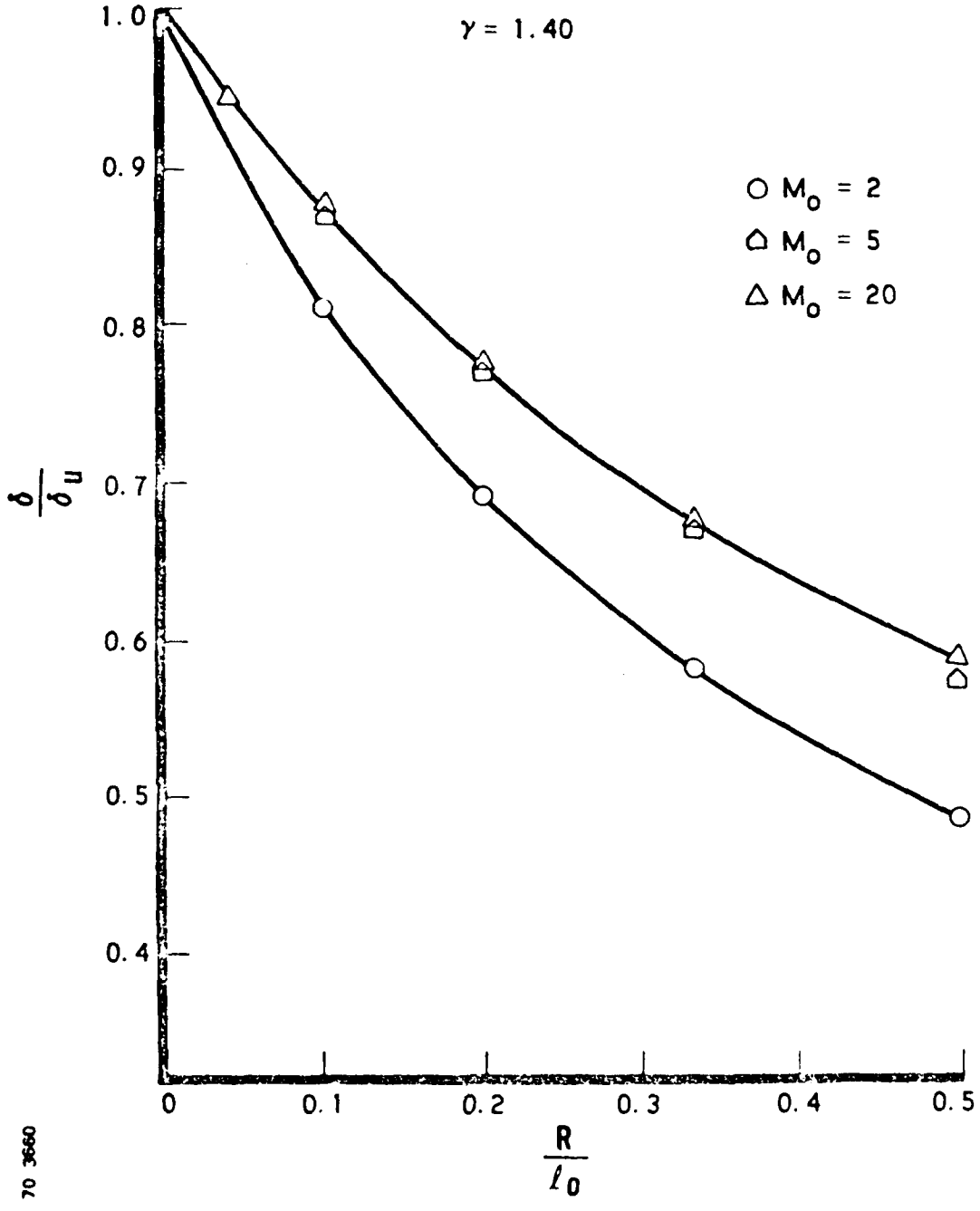

Figure 16. Effect of Mach No. on Shock Standoff Distance for a Sphere in a Spherical Source Flow

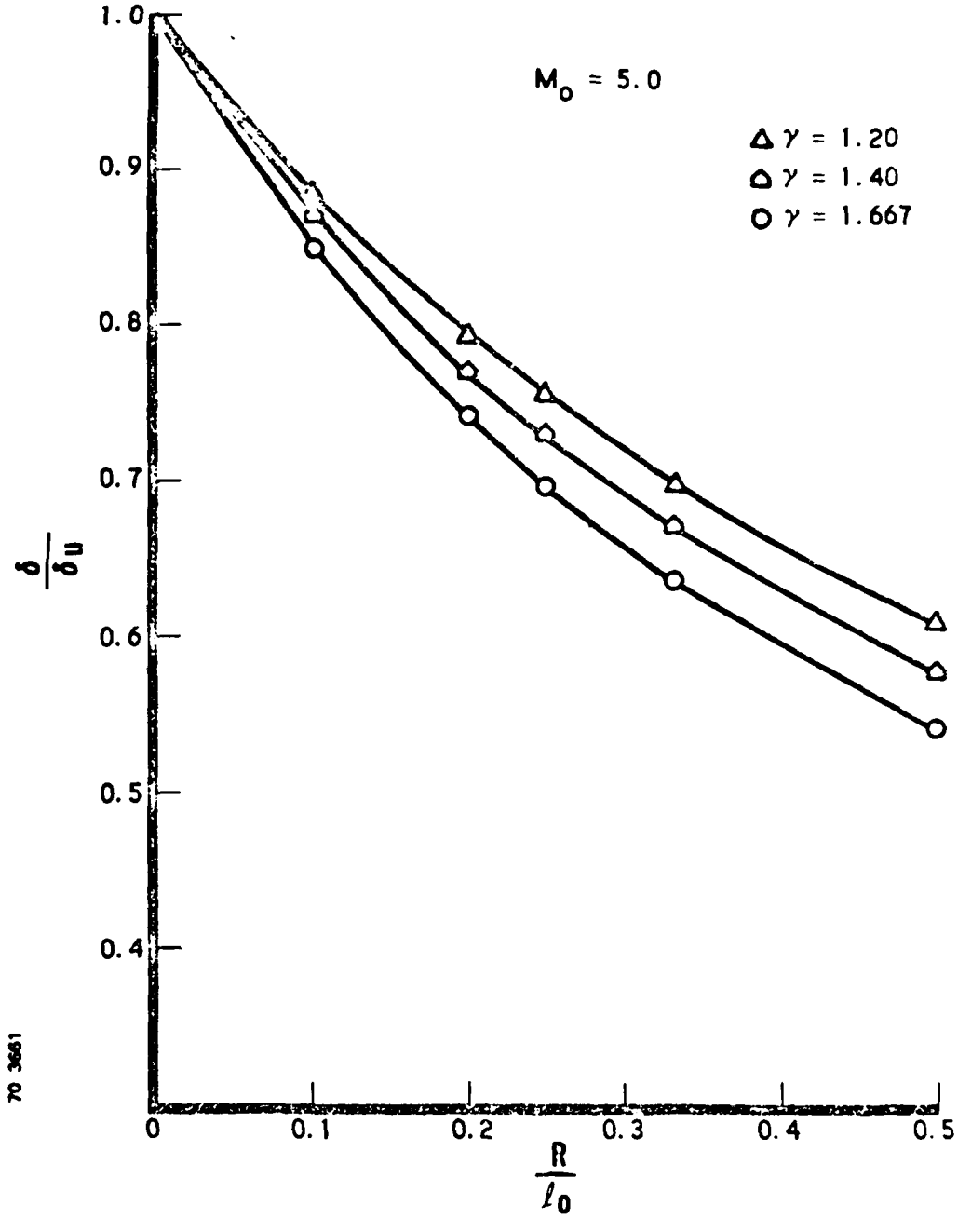

Figure 17. Shock Standoff Distance for Spherical Nose in a Spherical Source Flow

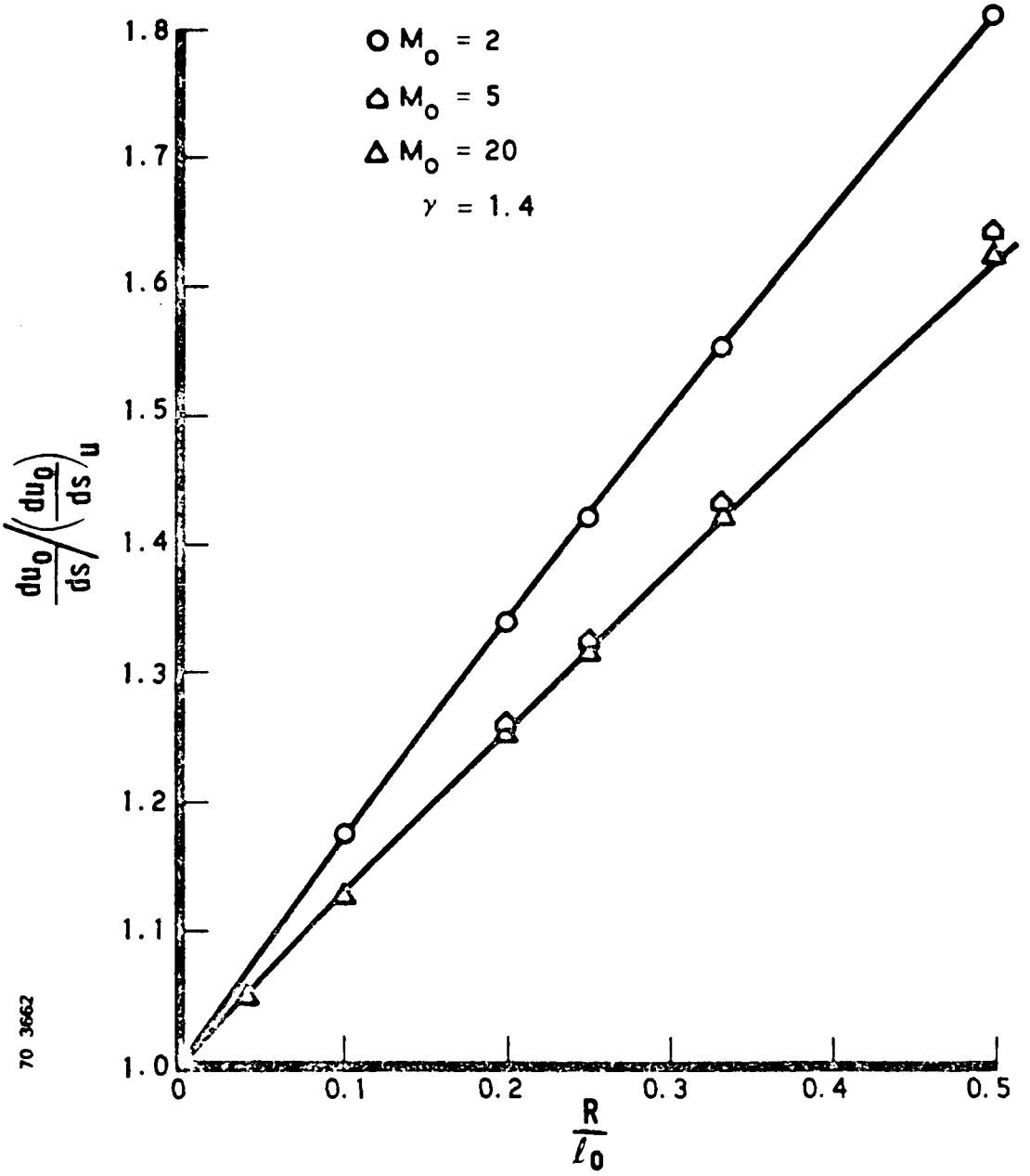

Figure 18. Effect of Mach No. Upon the Stagnation Point Velocity Gradient for a Sphere in a Spherical Source Flow

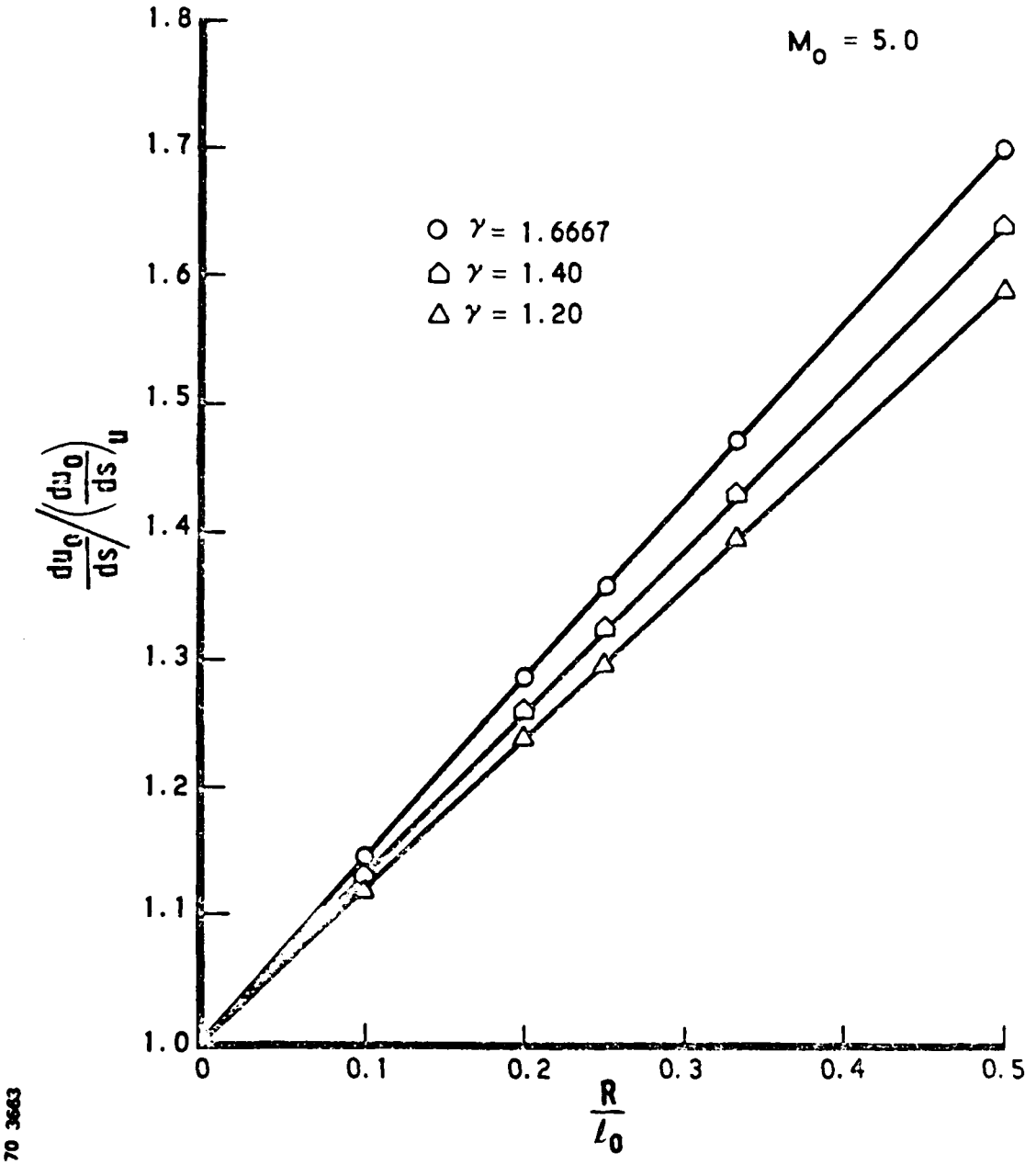

Figure 19. Effect of the Specific Heat Ratio Upon the Stagnation Point Velocity Gradient for a Sphere in a Spherical Source Flow

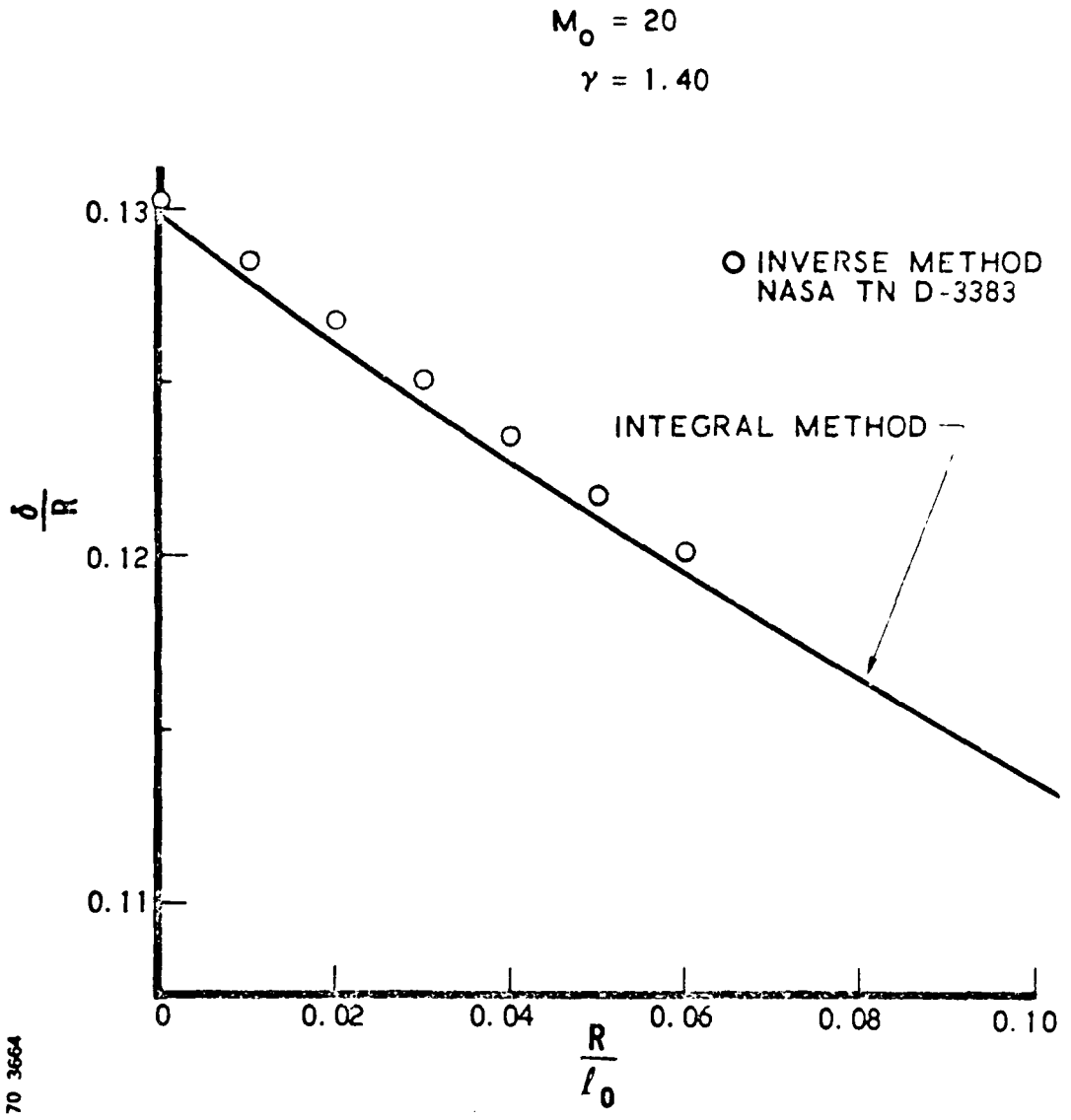

Figure 20. Comparison of Shock Detachment Distances for a Sphere in a Spherical Source Flow

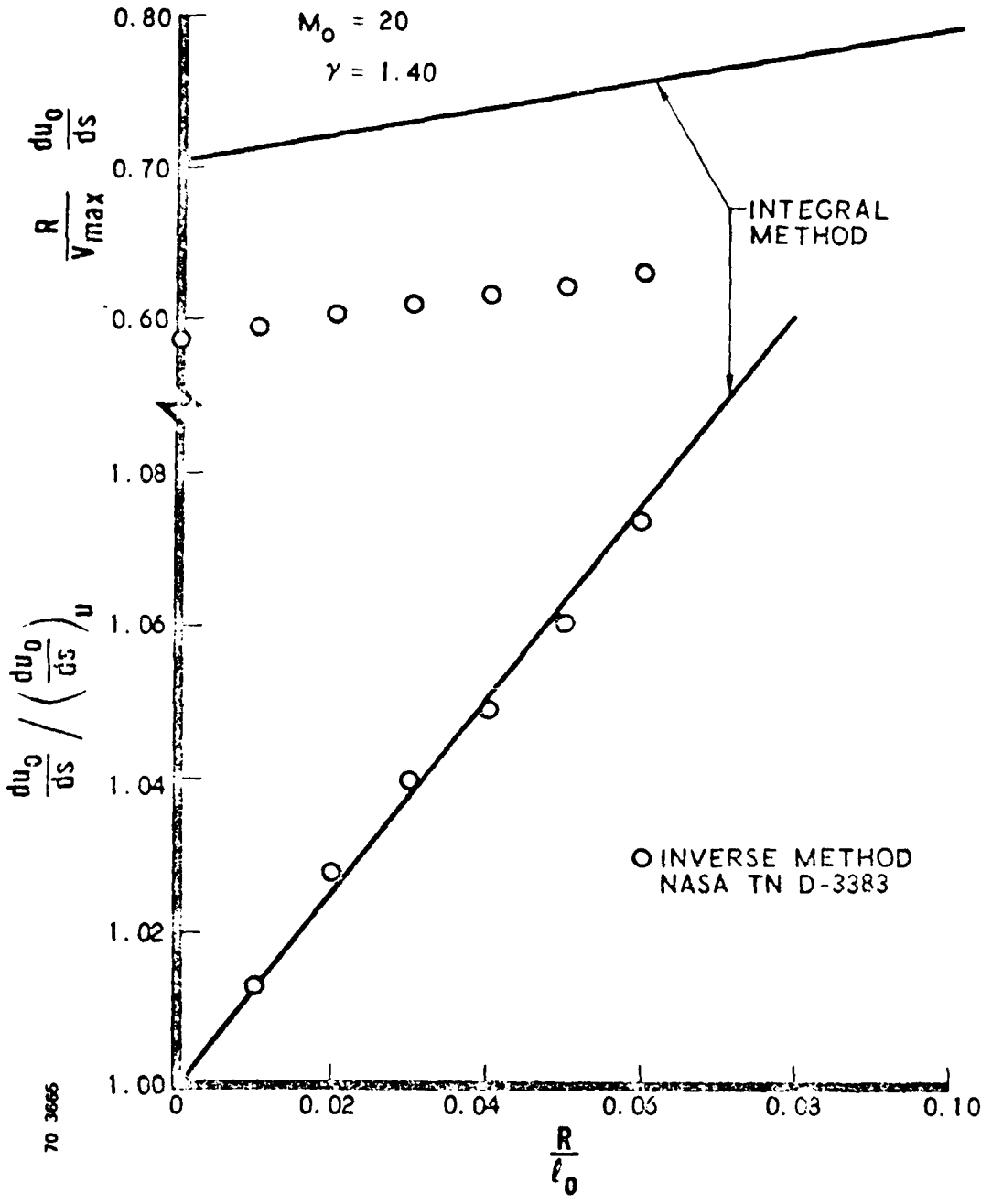

Figure 21. Comparison of Stagnation Point Velocity Gradients for a Sphere in a Spherical Source Flow

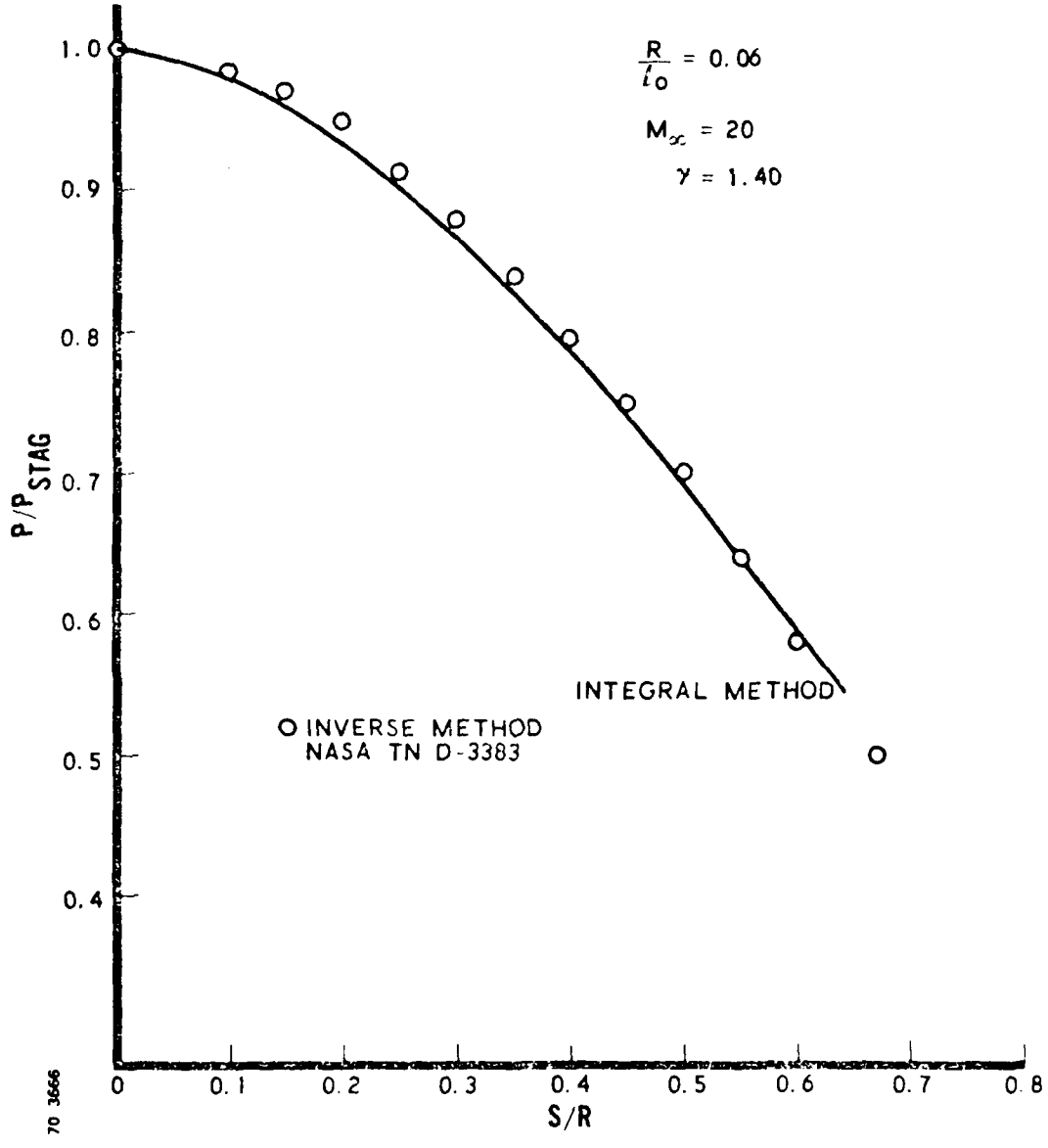

Figure 22. Comparison of Pressure Distributions for a Sphere in a Spherical Source Flow

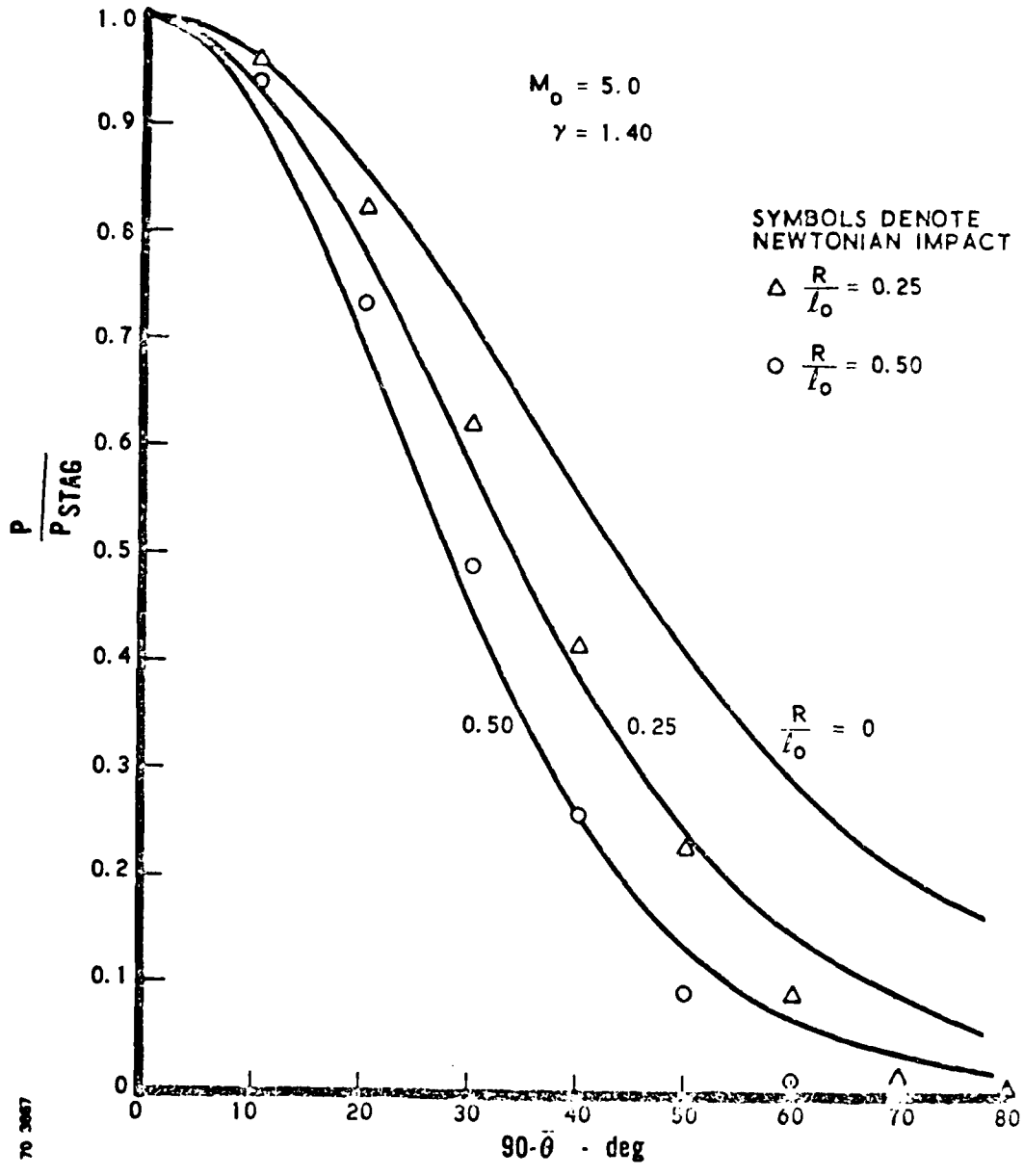

Figure 23. Comparison of Pressure Distributions on a Sphere in a Spherical Source Flow with Newtonian Impact Theory

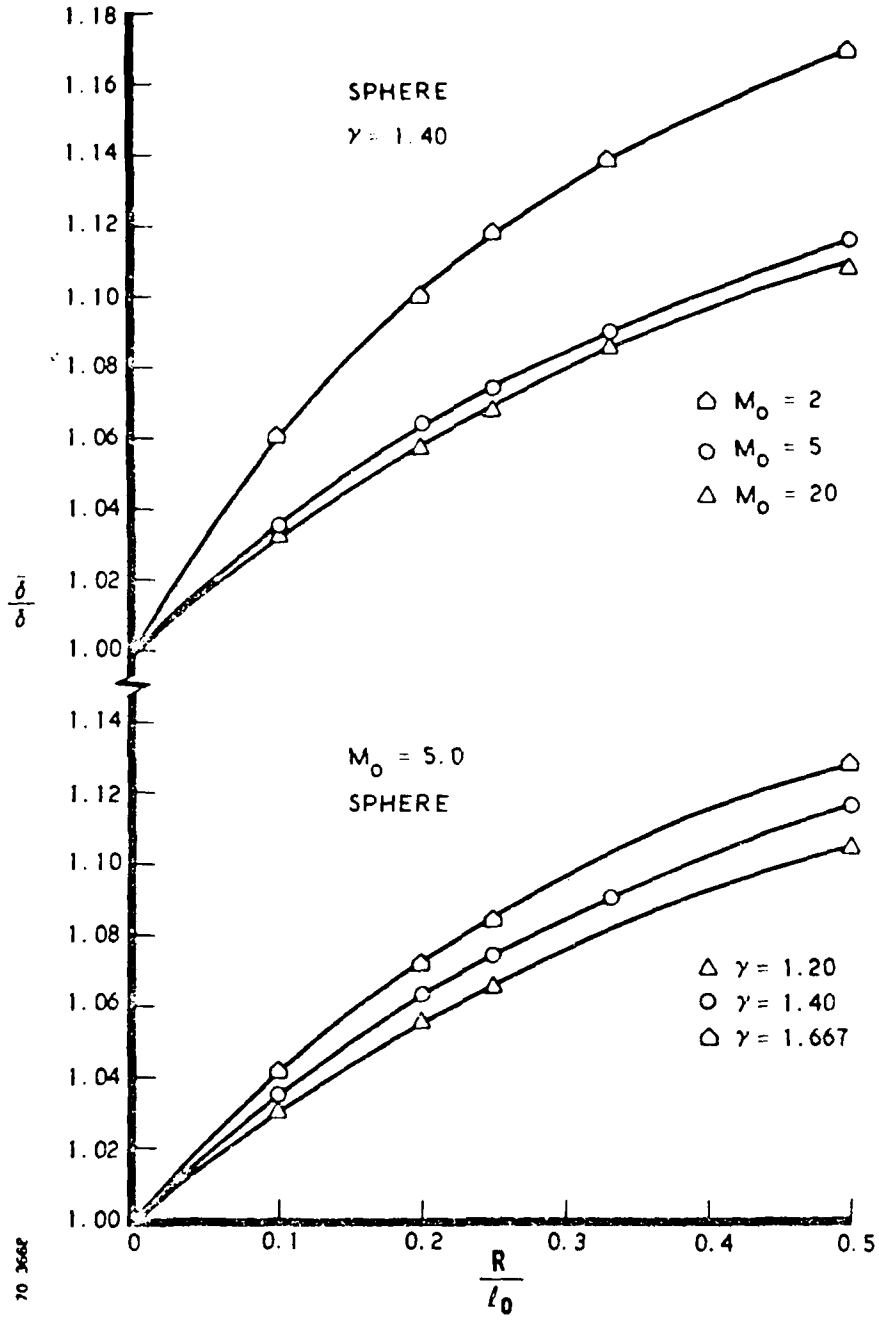

Figure 21. Sensitivity of the Shock Standoff Distance to the Free Stream Gradient Terms

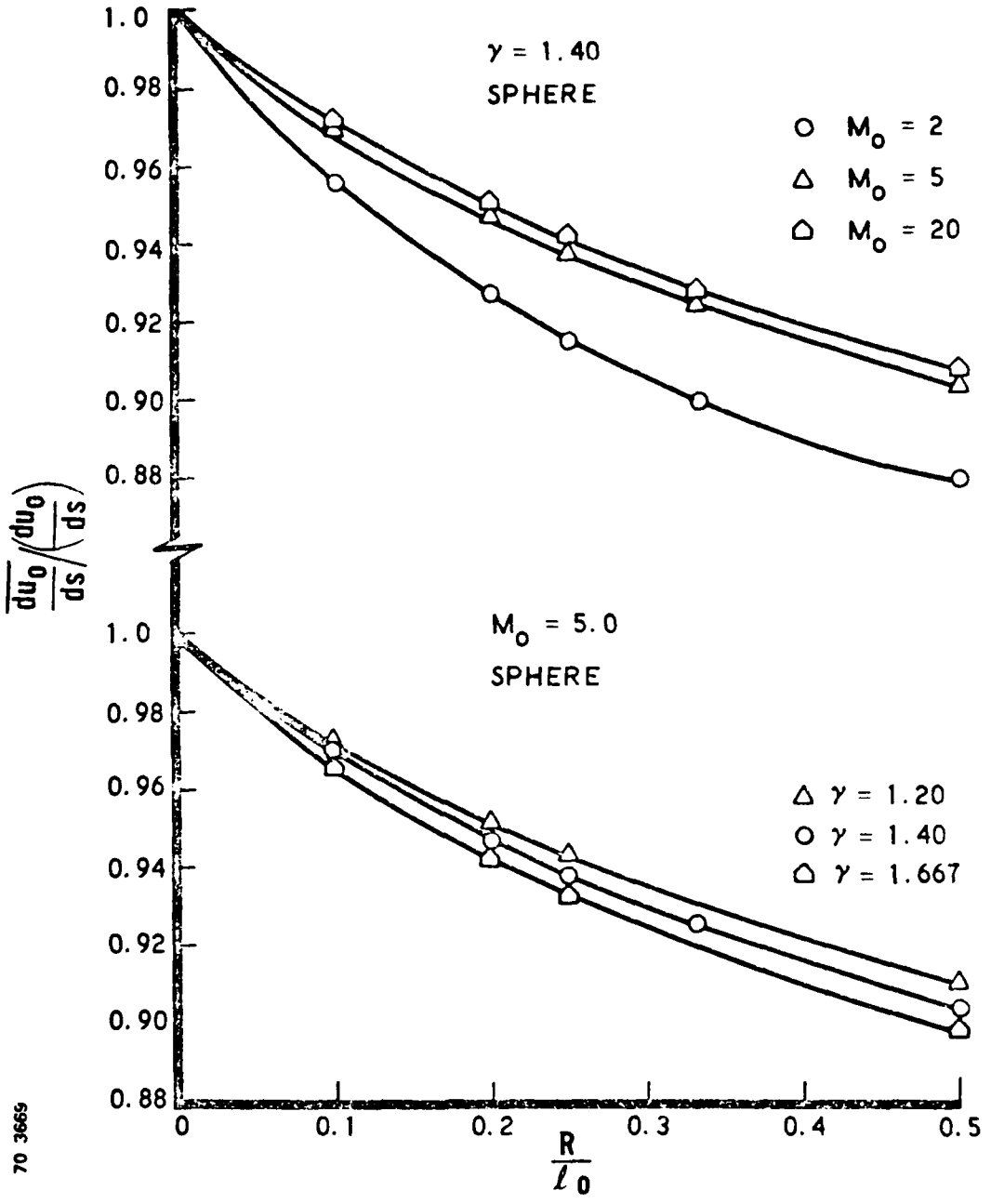

Figure 25. Sensitivity of the Stagnation Point Velocity Gradient to the Free Stream Gradient Terms

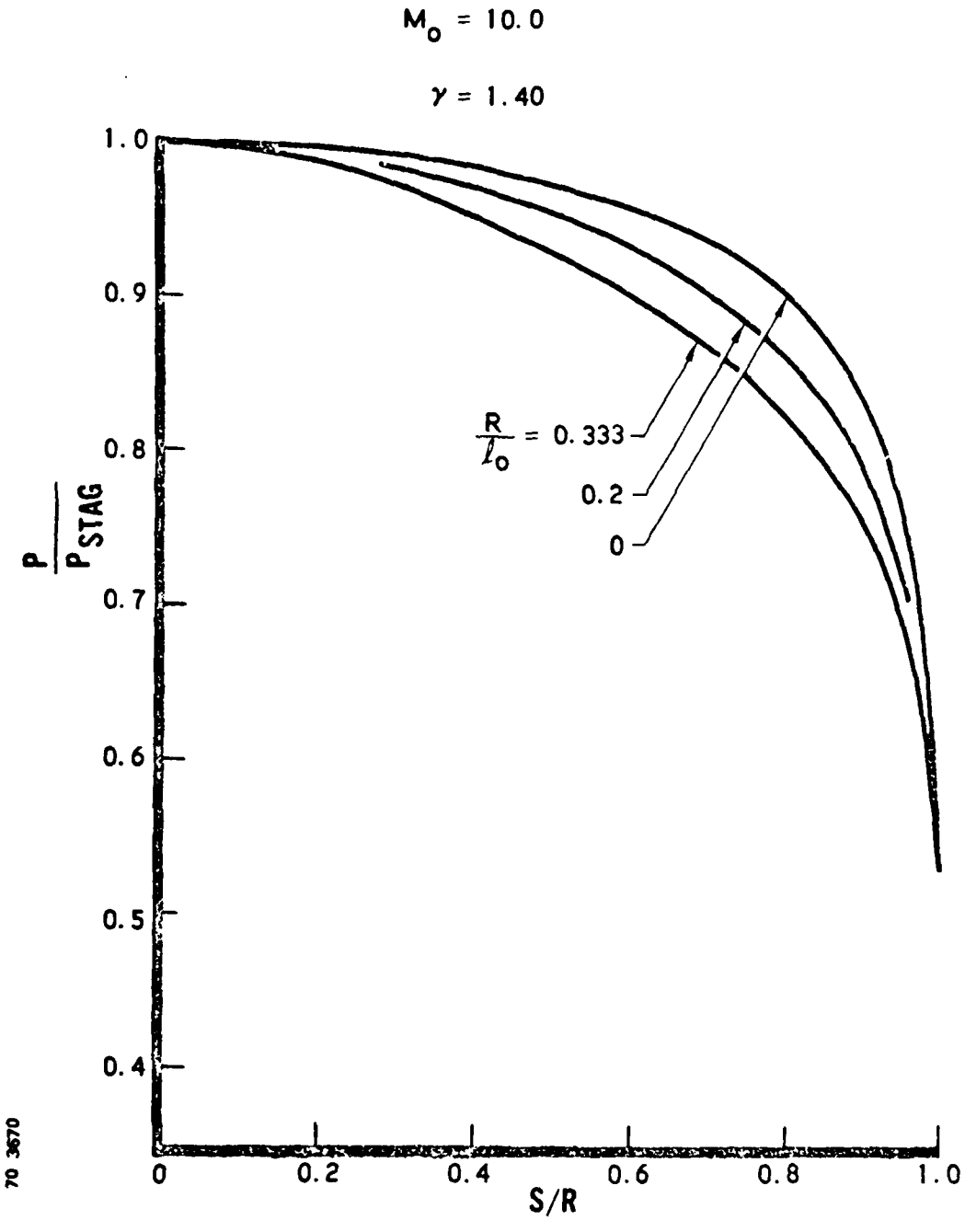

Figure 26. Pressure Distributions on a Circular Disk in a Spherical Source Flow

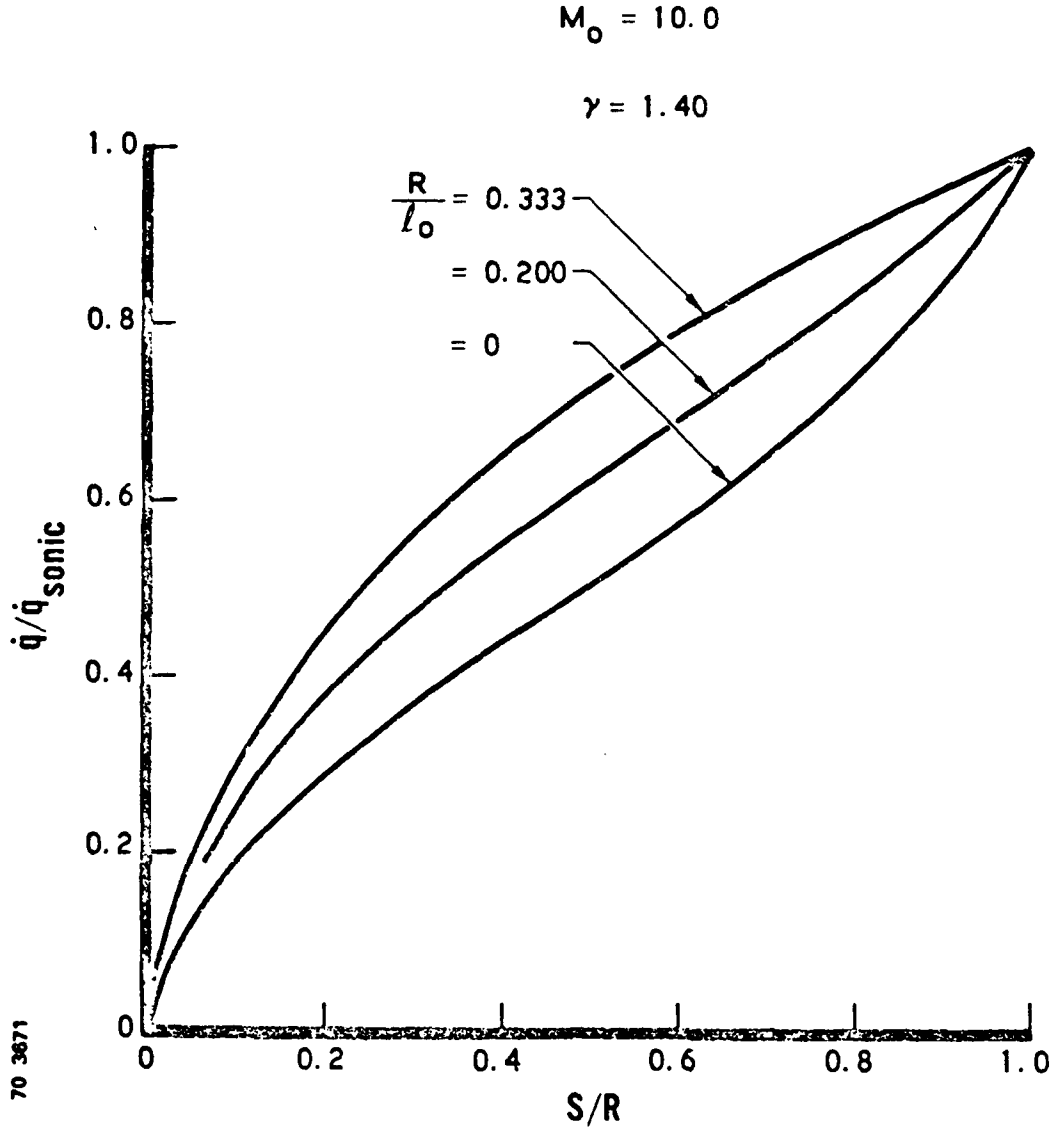

Figure 27. Turbulent Heat Transfer Distributions on a Circular Disk in a Spherical Source Flow

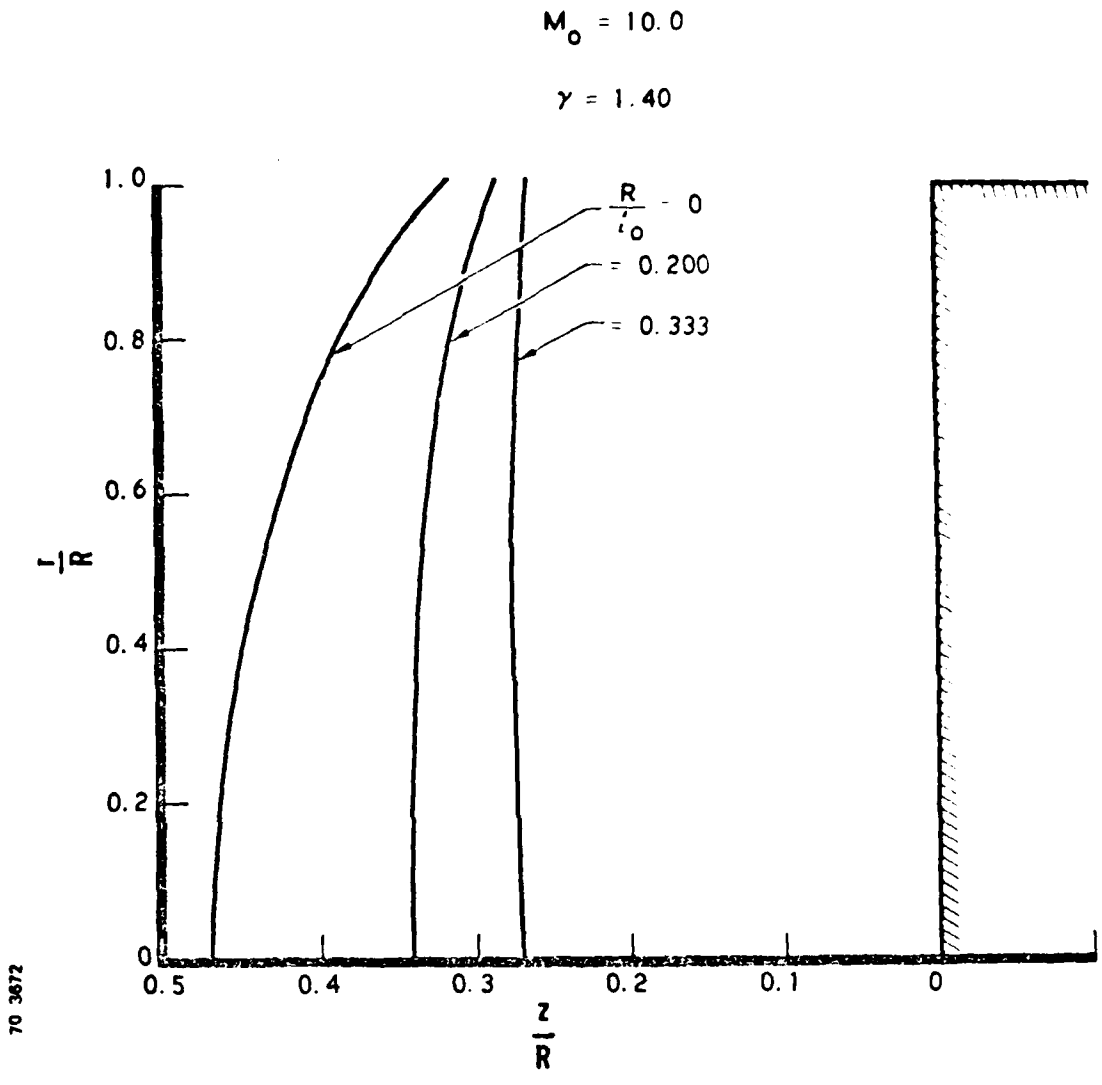

Figure 28. Shock Shapes for a Circular Disk in a Spherical Source Flow

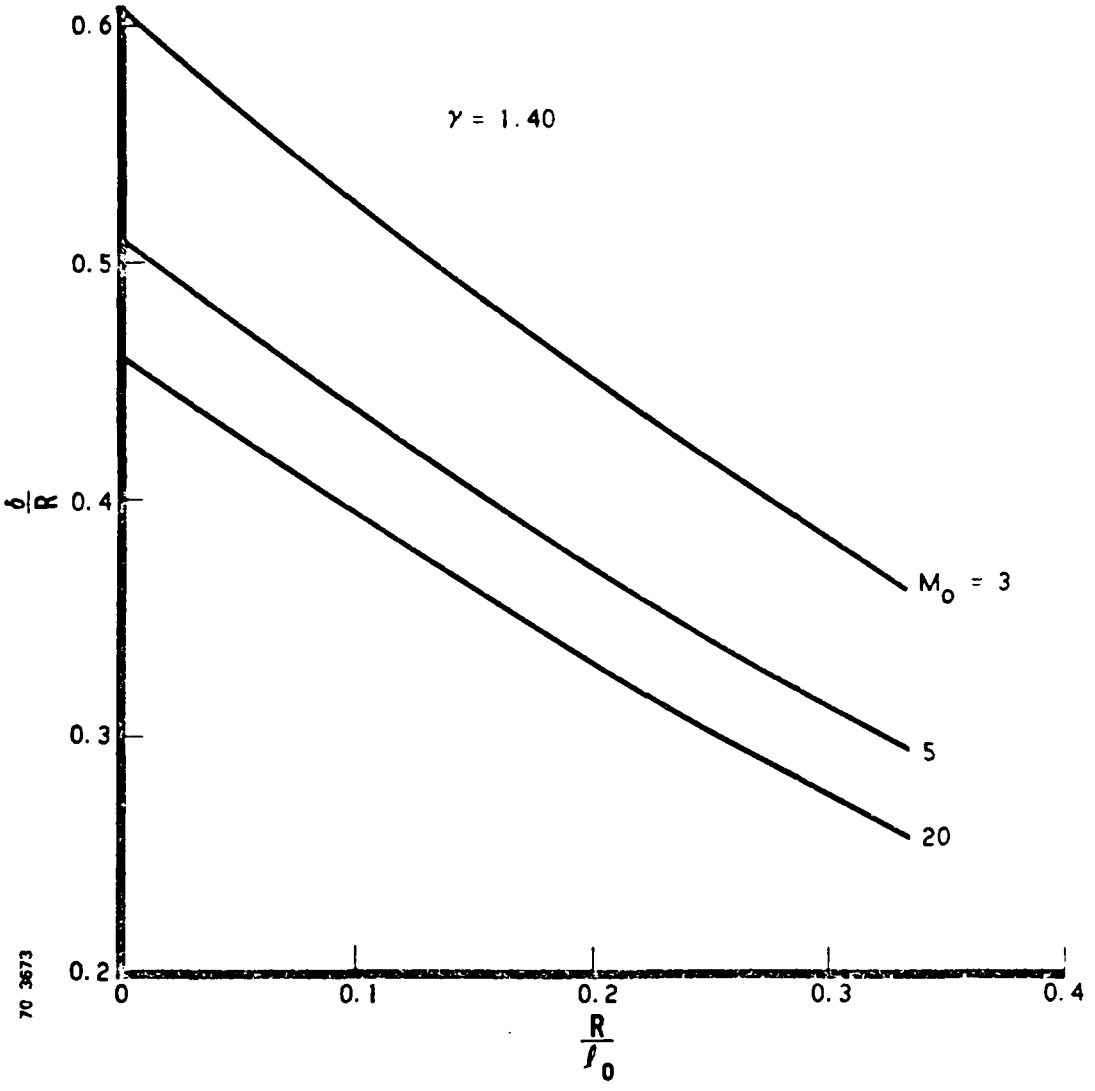

Figure 29. Shock Detachment for a Circular Disk in a Spherical Source Flow

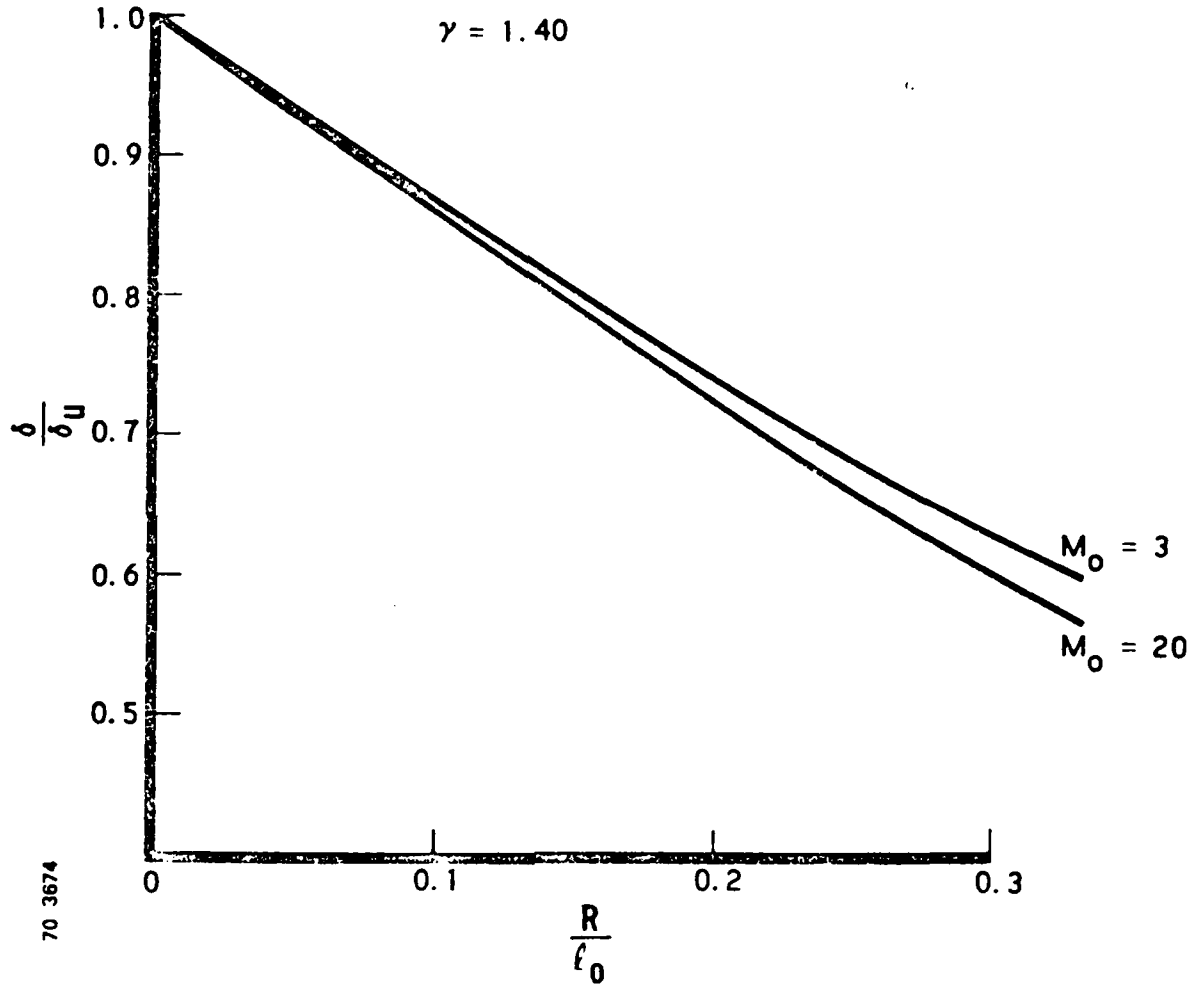

Figure 30. Mach No. Effect Upon the Shock Detachment Distance for a Circular Disk in a Spherical Source Flow

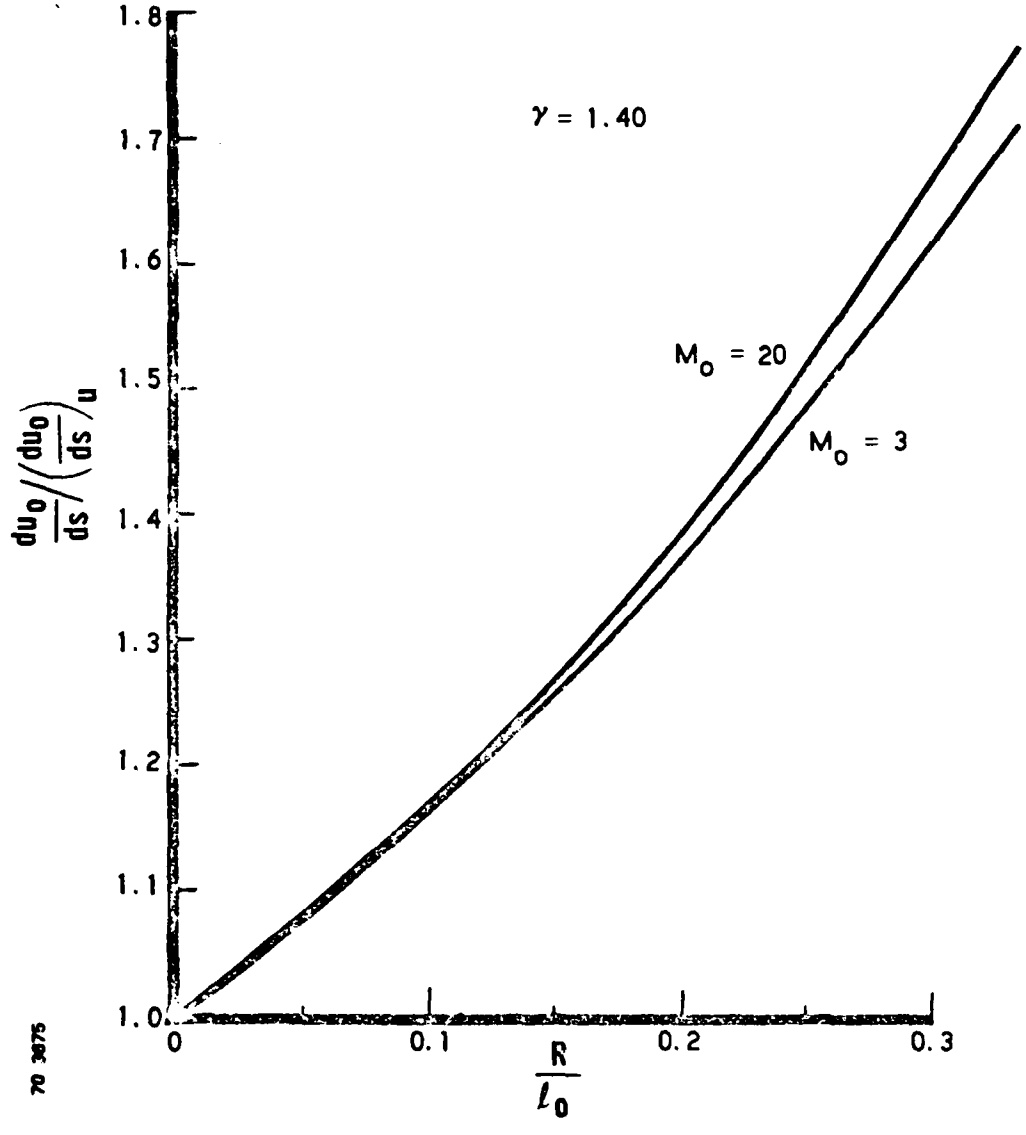

Figure 31. Mach No. Effect Upon the Stagnation Point Velocity Gradient for a Circular Disk in a Spherical Source Flow

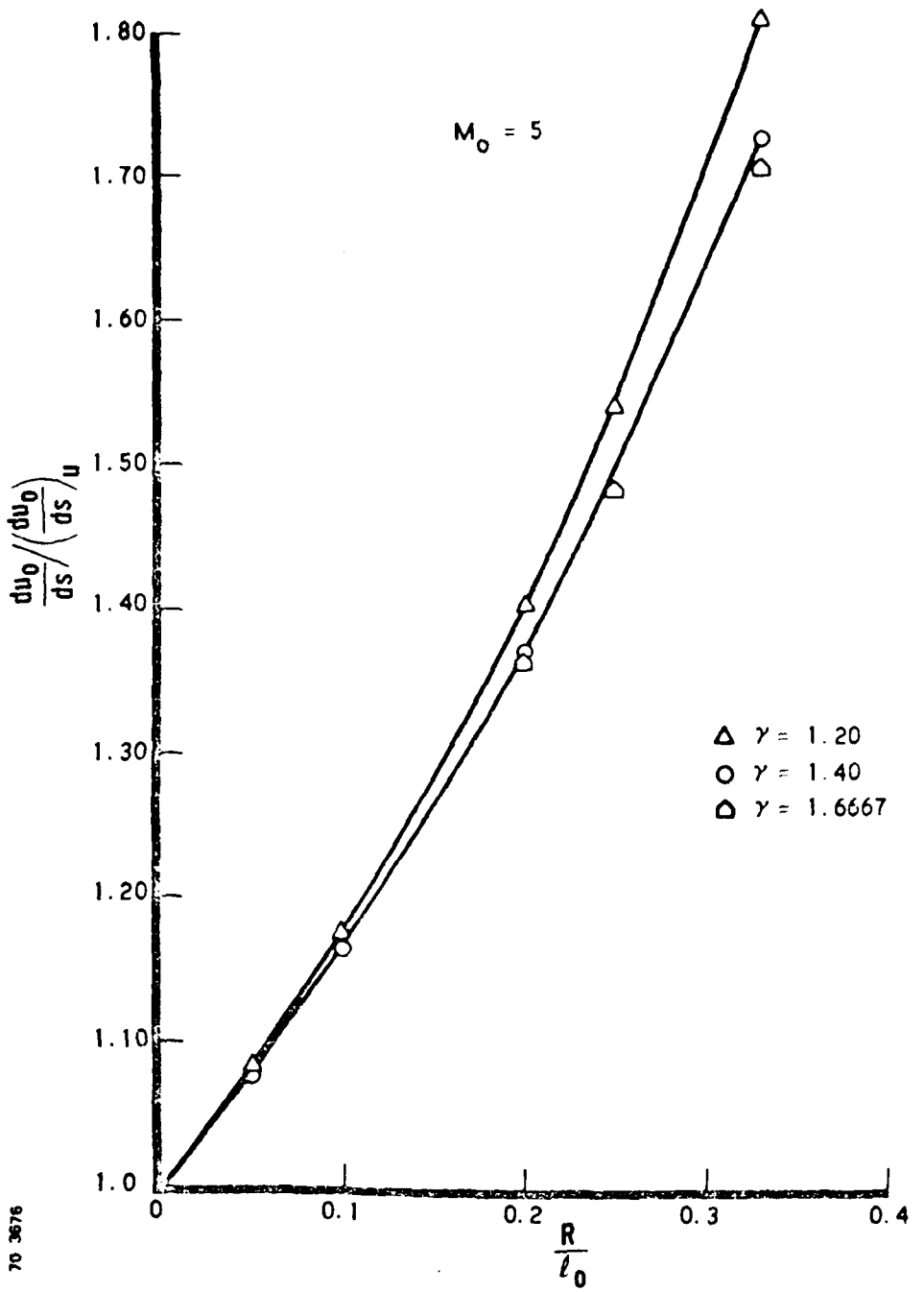

Figure 32. Effect of Specific Heat Ratio Upon Stagnation Point Velocity Gradient for a Circular Disk in a Spherical Source Flow

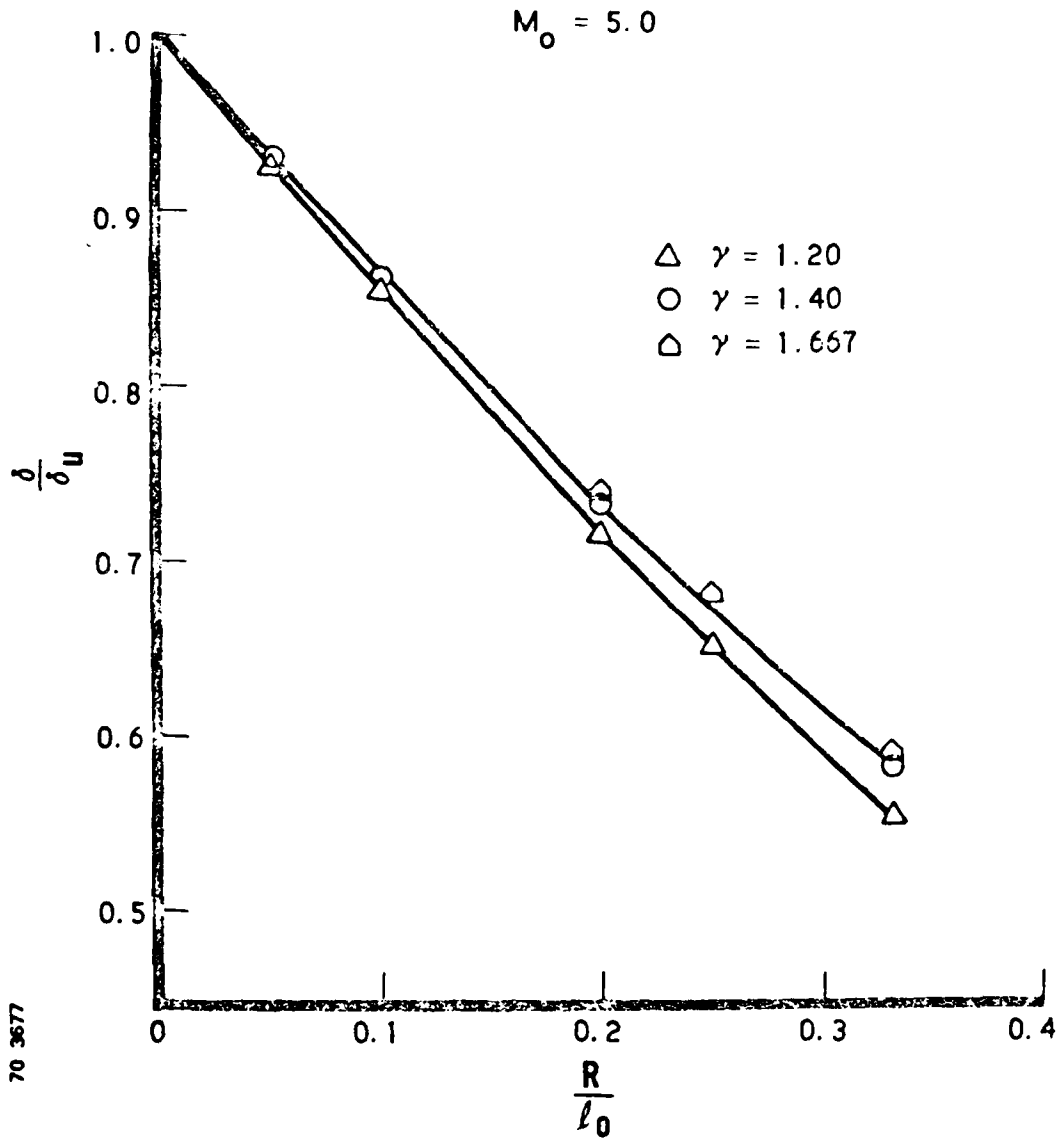

Figure 33. Effect of Specific Heat Ratio Upon Shock Standoff Distance for a Circular Disk in a Spherical Source Flow

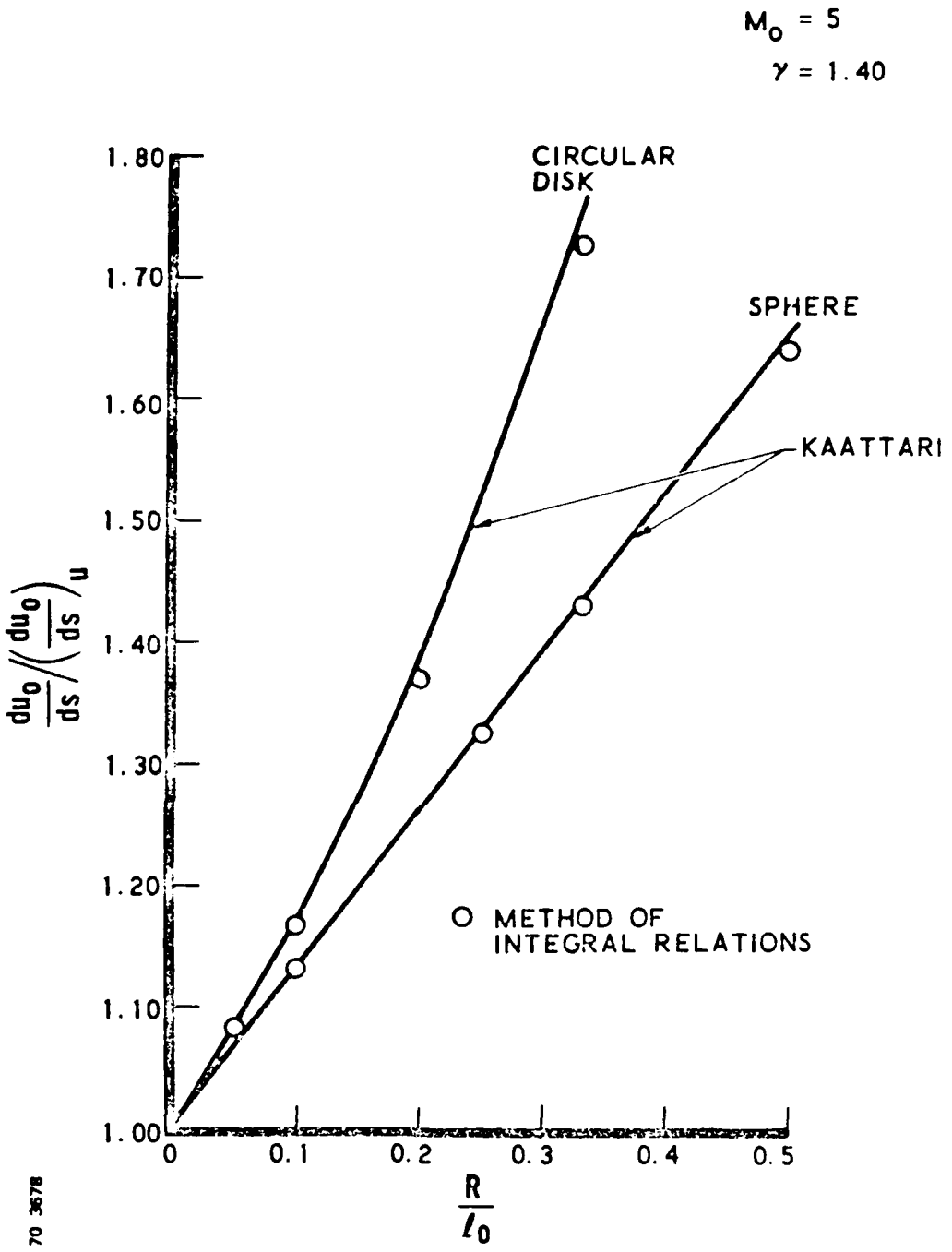

Figure 34. Comparison of Stagnation Point Velocity Gradients for a Sphere and Circular Disk in a Spherical Source Flow

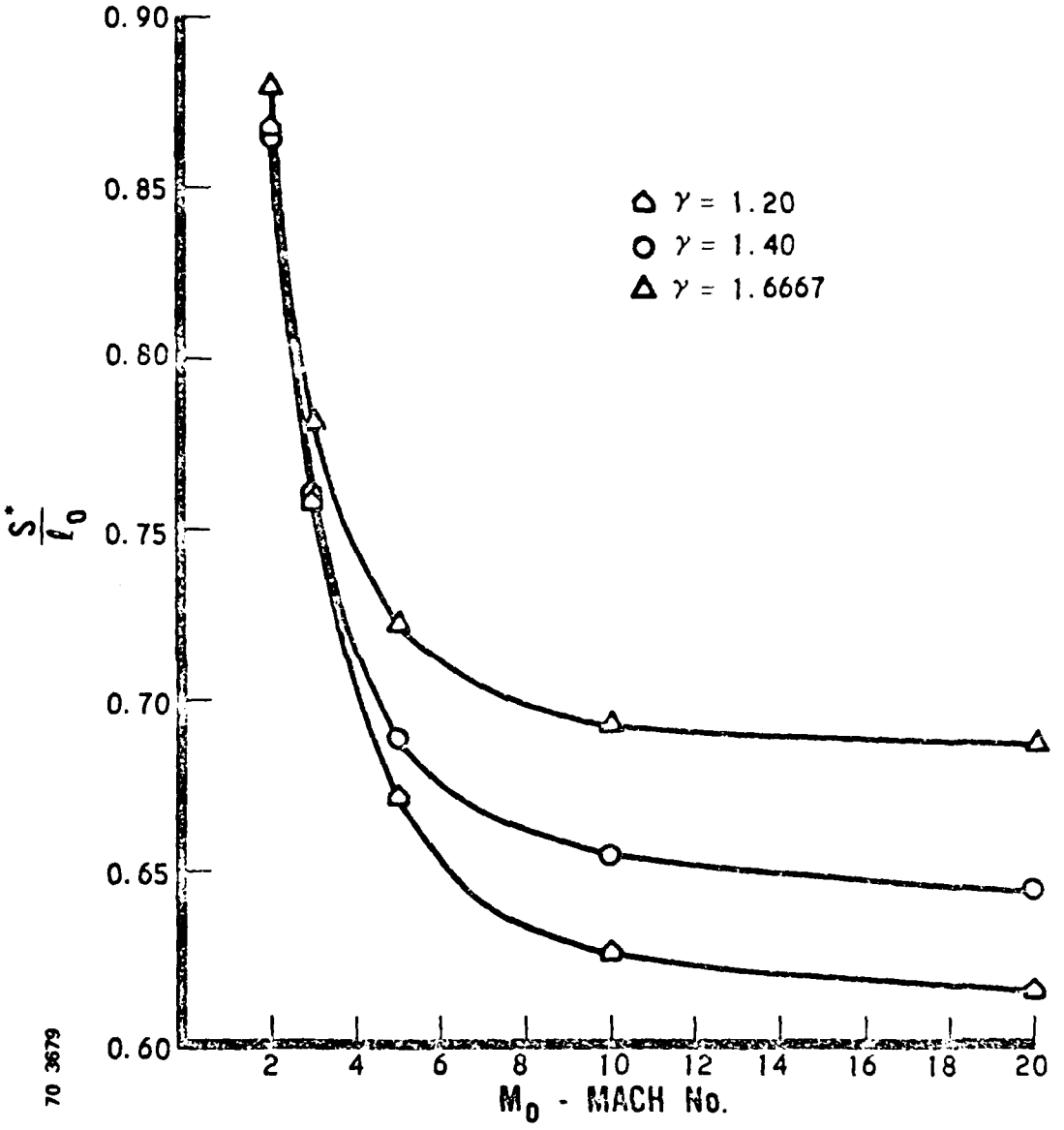

Figure 35. Sonic Point Location on an Infinite Circular Disk in a Spherical Source Flow

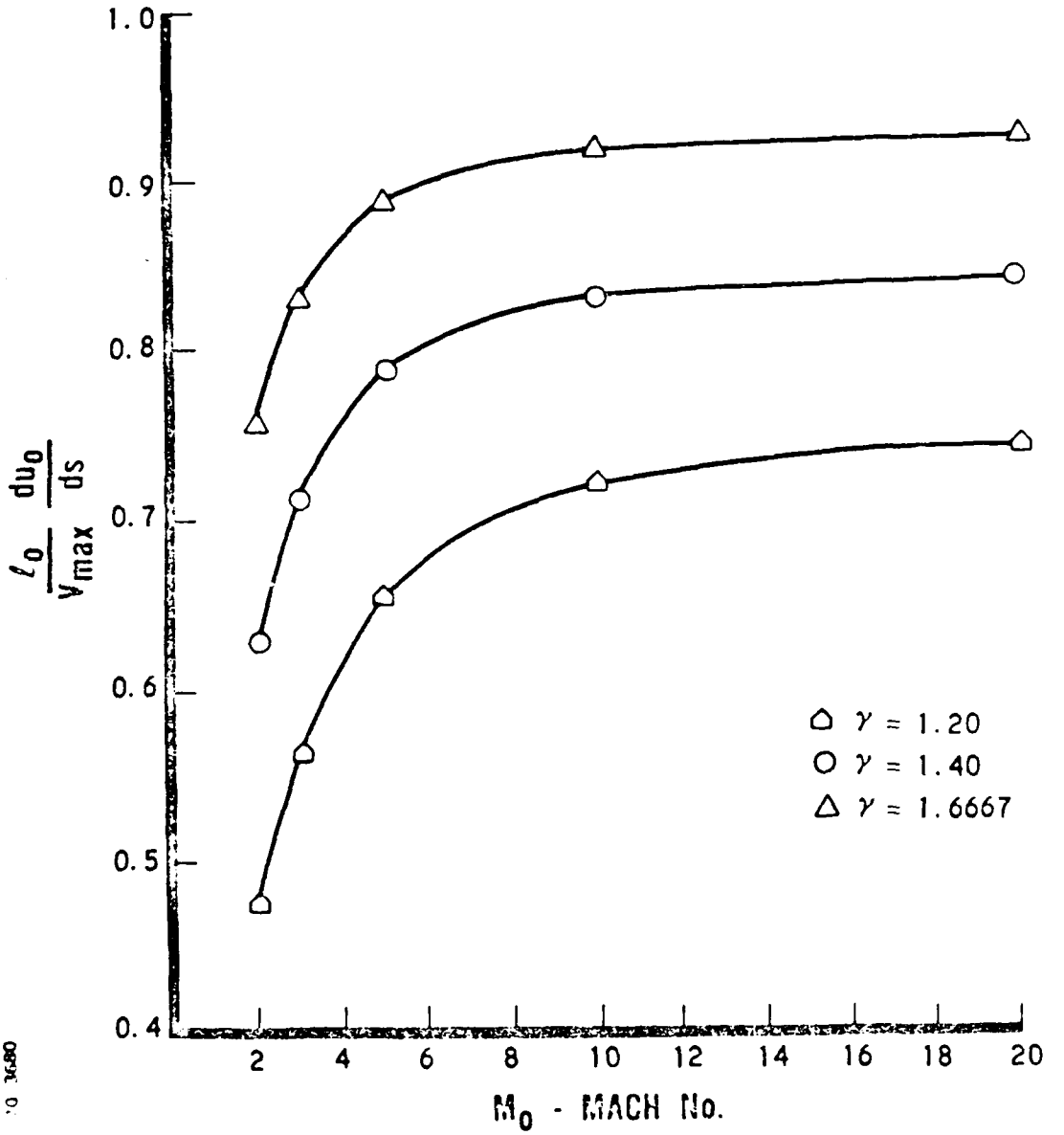

Point Velocity Gradient for an Infinite Circular Disk in a

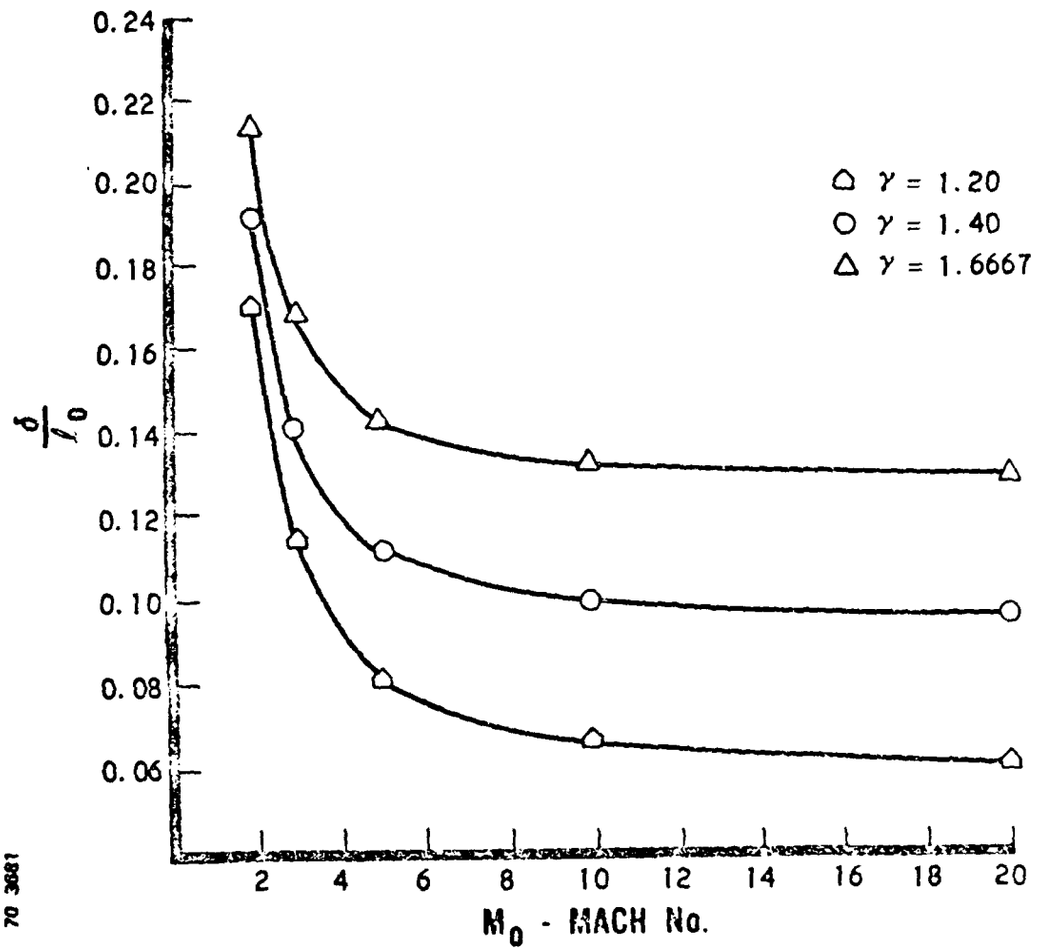

Figure 37. Shock Standoff Distance for an Infinite Circular Disk in a Spherical Source Flow

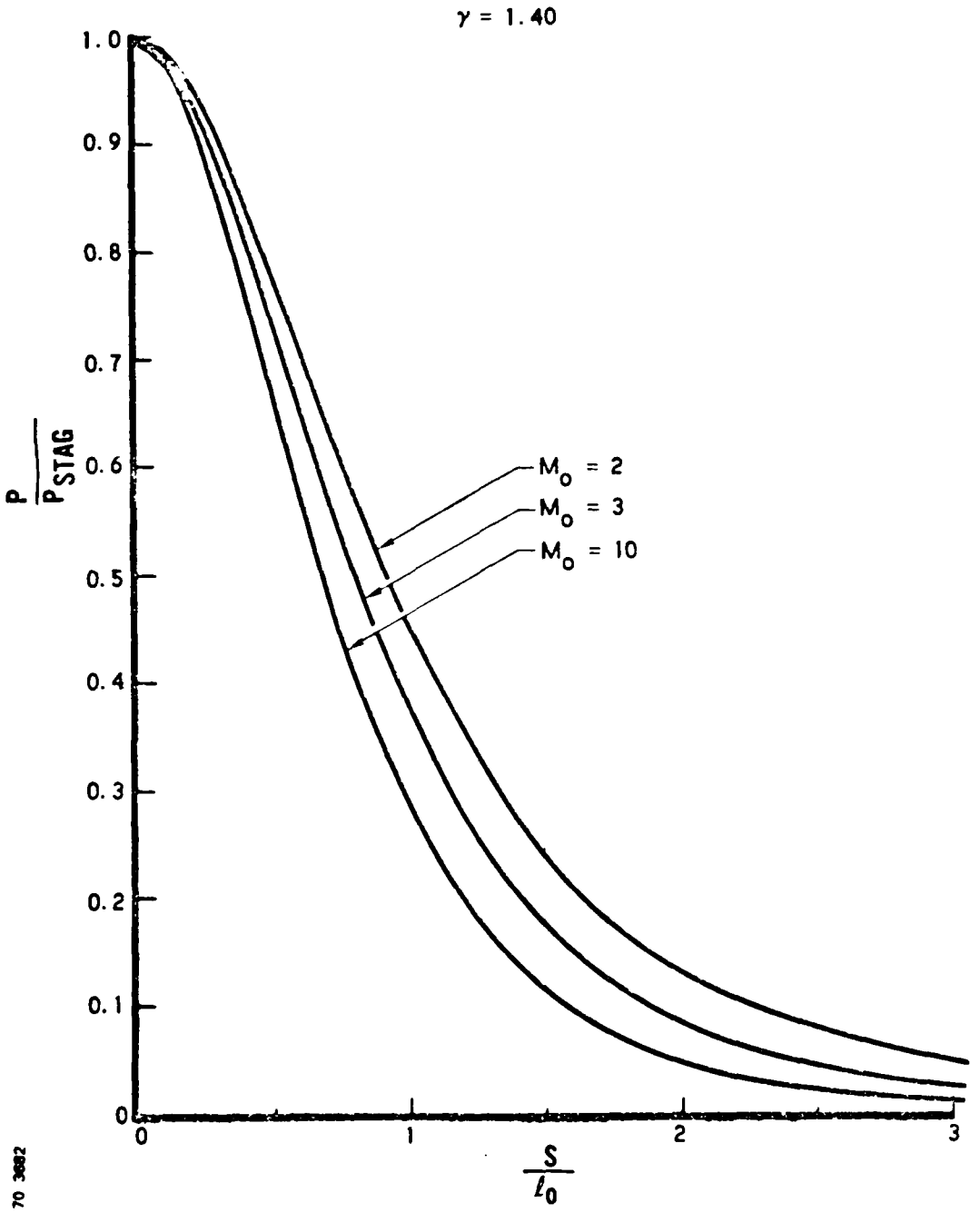

Figure 38. Pressure Distributions in an Infinite Circular Disk in a Spherical Source Flow

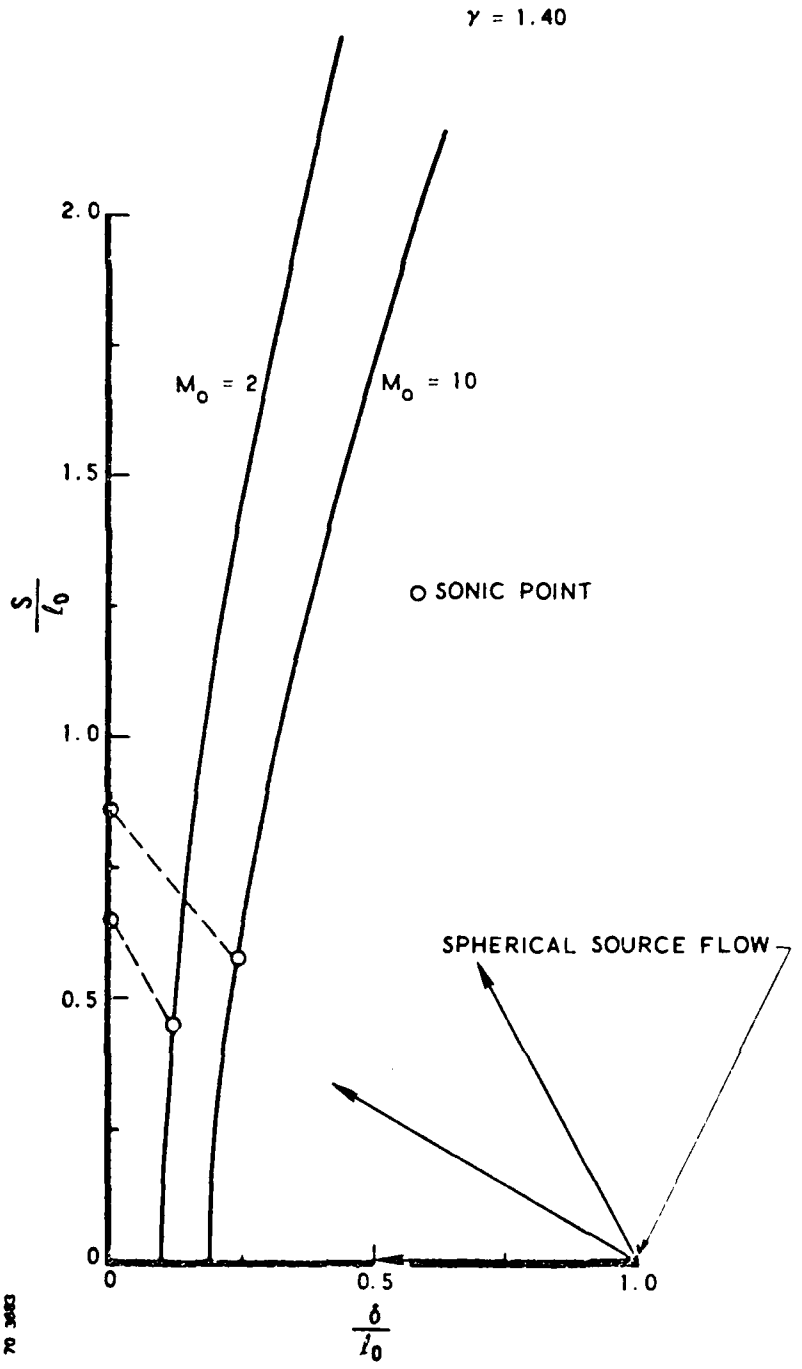

Figure 39. Shock Shape on an Infinite Circular Disk in a Spherical Source Flow

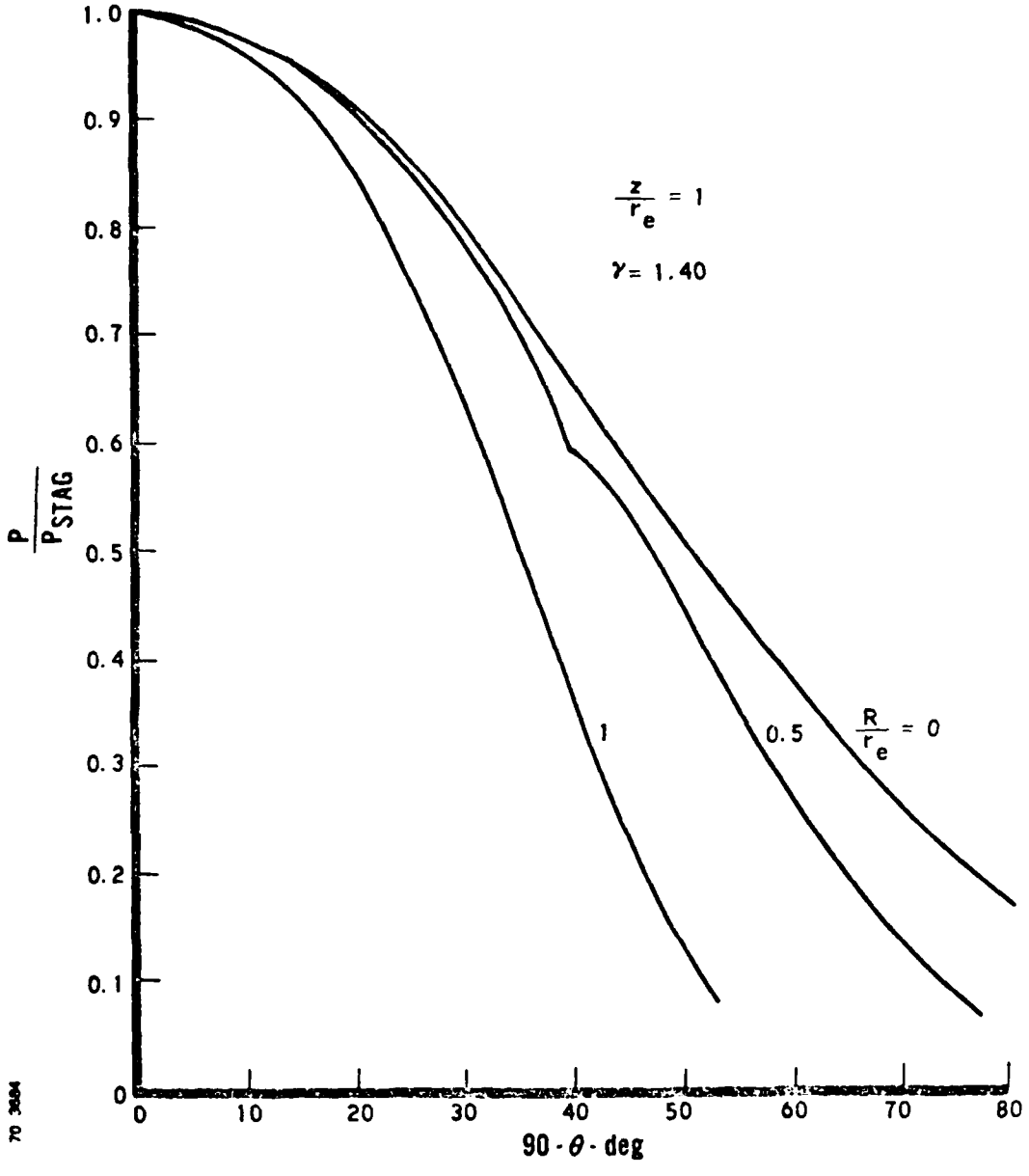

Figure 40. Pressure Distributions on a Sphere in a Mach 2 Exhaust Plume

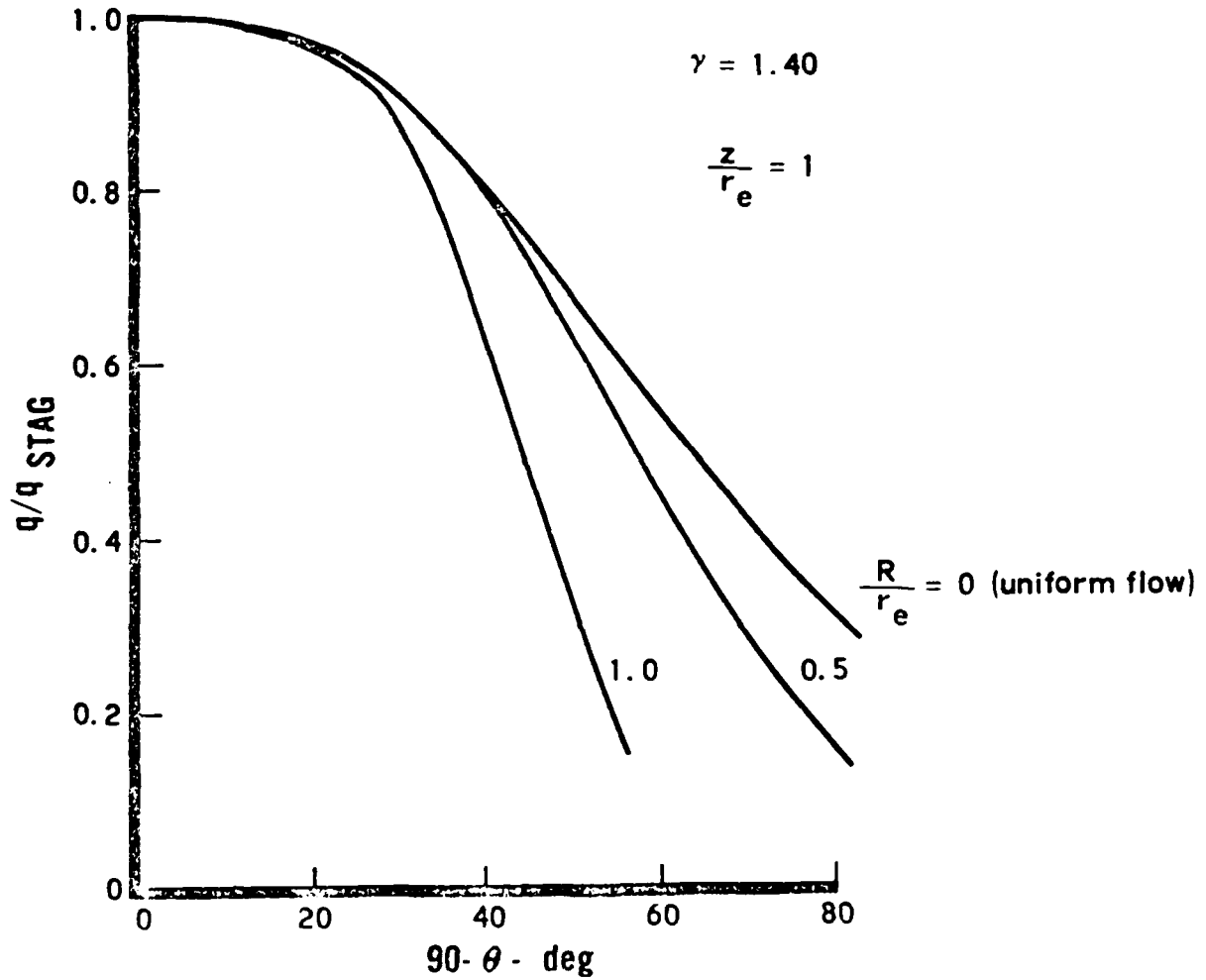

Figure 41. Laminar Heat Flux Distributions for a Sphere in a Mach 2 Exhaust Plume

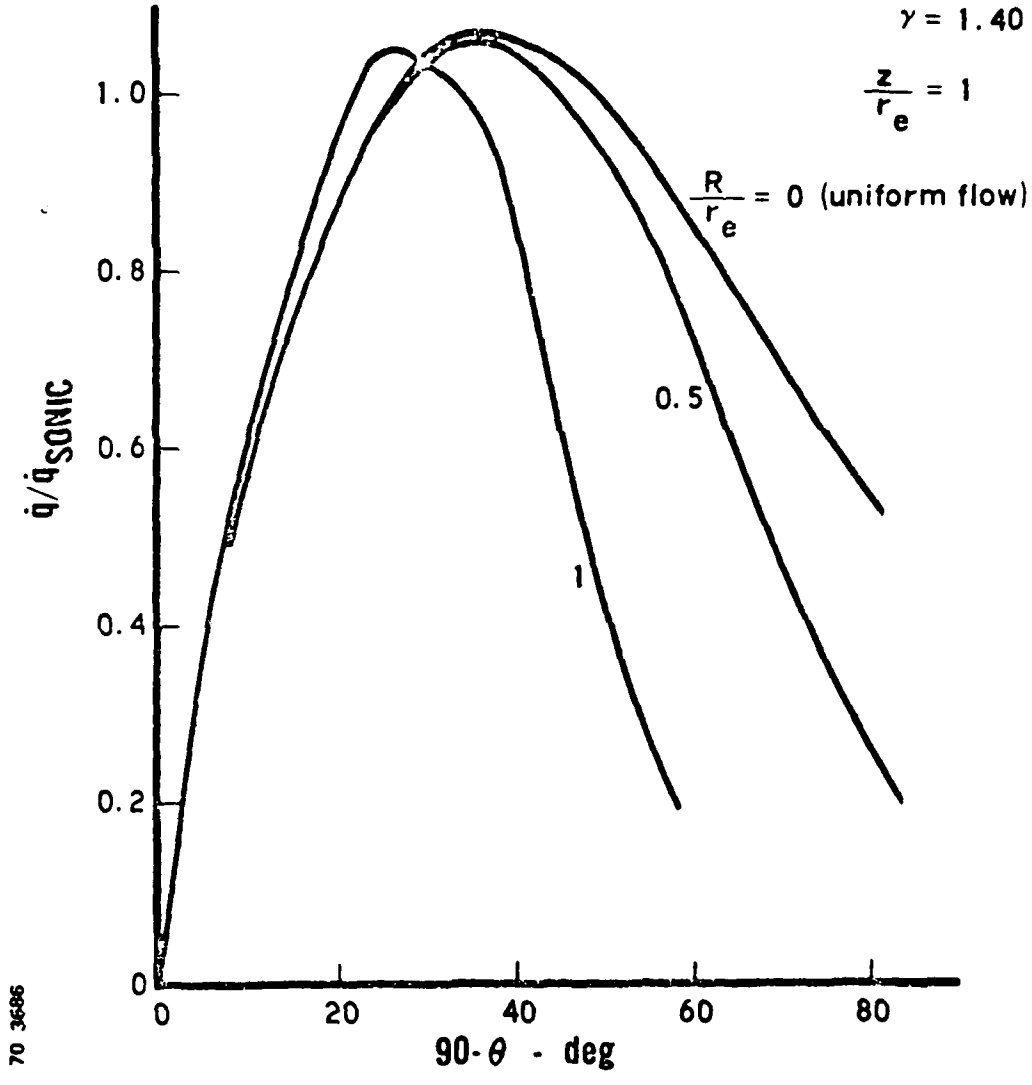

Figure 42. Turbulent Heat Transfer Distributions for a Sphere in a Mach 2 Exhaust Plume

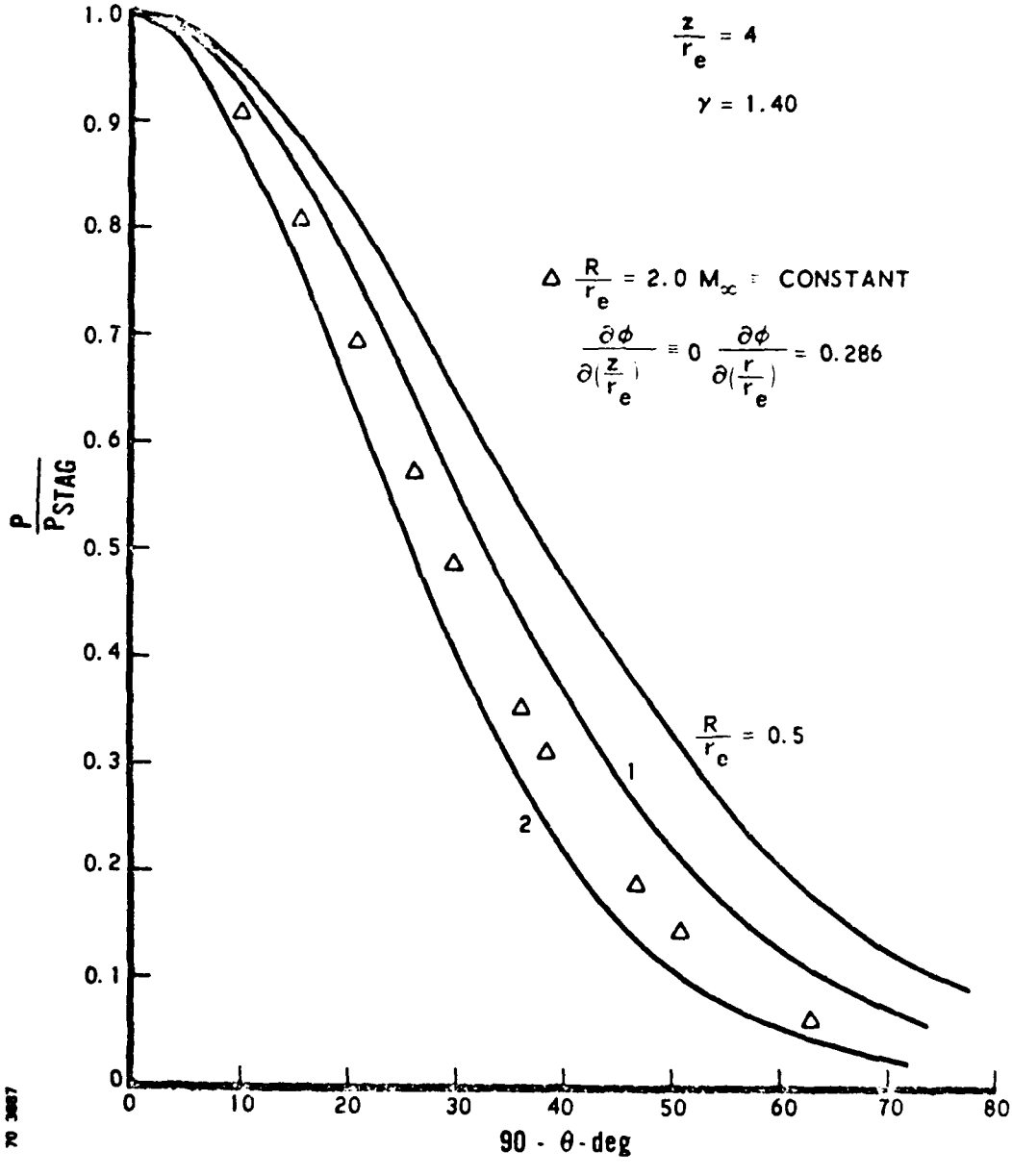

Figure 43. Pressure Distributions on a Sphere in a Mach 2 Exhaust Plume

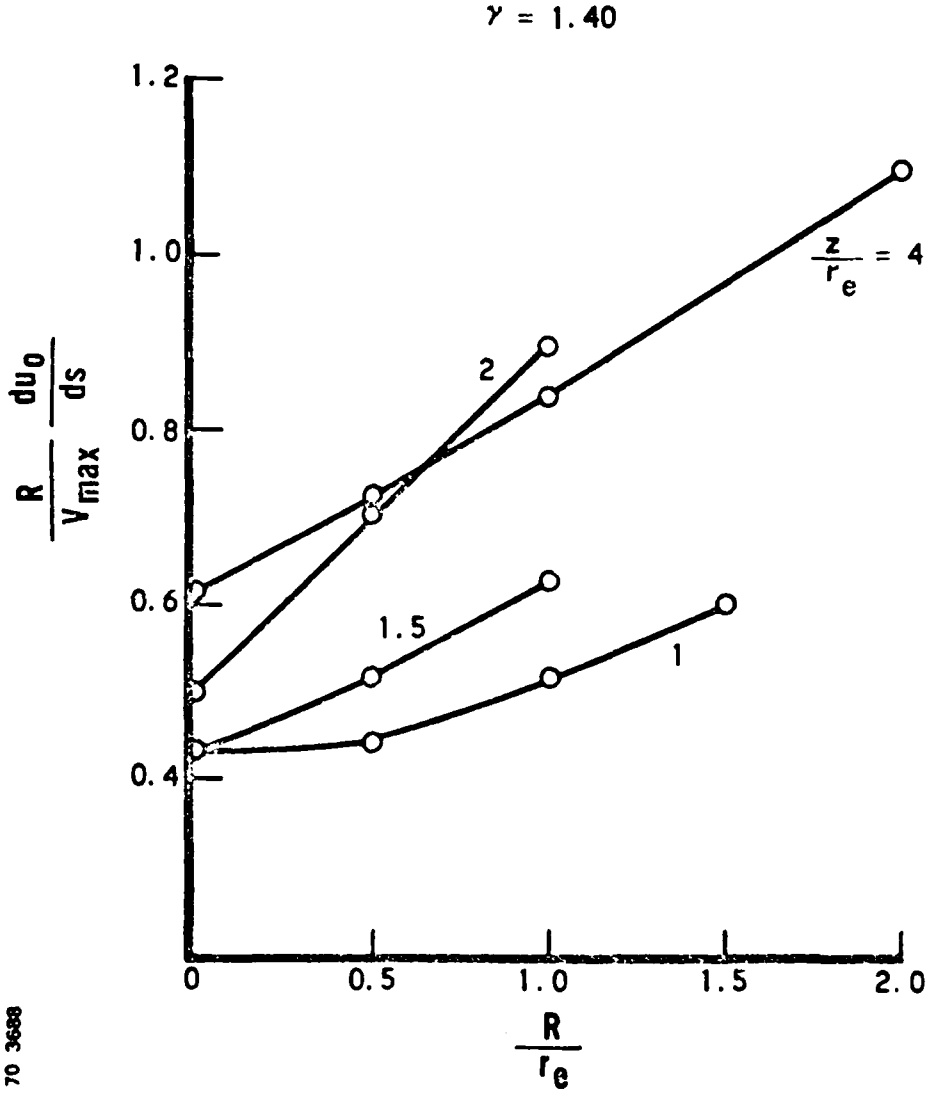

Figure 44. Stagnation Point Velocity Gradient for a Sphere in a Mach 2 Exhaust Plume

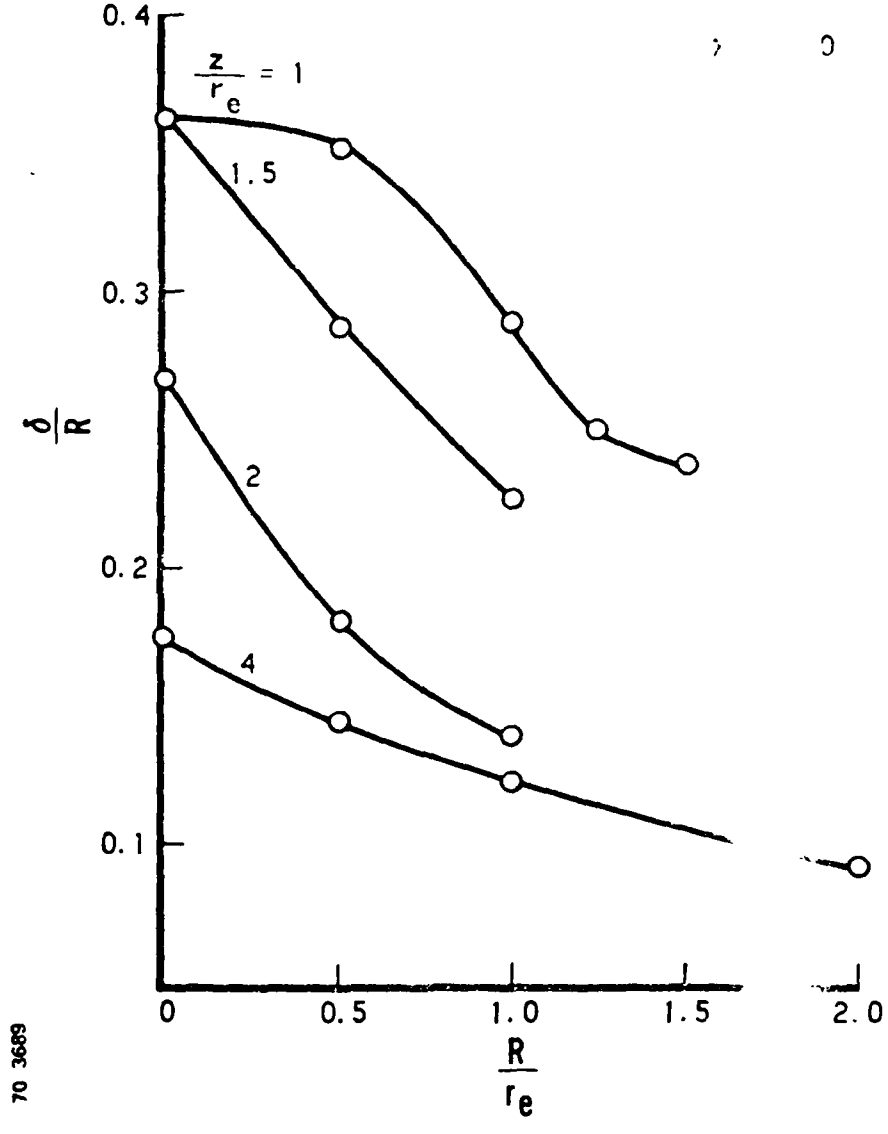

Figure 45. Shock Standoff Distance for a Sphere in a Mac[illegible]haust Plume

UNCLASSIFIED

Security Classification

DOCUMENT CONTROL DATA · R&D

(Security classification of title, body of abstract and indexing annotation must be entered when the overall report is classified)

1 ORIGINATING ACTIVITY (Corporate author) The Aerospace Corporation San Bernardino, California	2a REPORT SECURITY CLASSIFICATION Unclassified 2b GROUP ND-1111.1(-5)

3 REPORT TITLE

THE BLUNT BODY PROBLEM IN AN EXPANDING NON-UNIFORM FLOW FIELD

4 DESCRIPTIVE NOTES (Type of report and inclusive dates)

Technical Report

5 AUTHOR(S) (Last name, first name, initial)

Crowell, P. G.

6 REPORT DATE	7a TOTAL NO OF PAGES	7b NO OF REFS
70 SEP 07	92	18

8a CONTRACT OR GRANT NO	9a ORIGINATOR'S REPORT NUMBER(S)
F04701-69-C-0059 b PROJECT NO	TR-0059(S6816-76)-2
c d	9b OTHER REPORT NO(S) (Any other numbers that may be assigned this report) SAMSO TR-70-302

10 AVAILABILITY/LIMITATION NOTICES

This document has been approved for public release and sale; its distribution is unlimited.

11 SUPPLEMENTARY NOTES	12 SPONSORING MILITARY ACTIVITY
	Space and Missile Systems Organization Air Force Systems Command Norton Air Force Base, California 92409

13 ABSTRACT

The method of integral relations has been used to compute the inviscid flow over a blunt body immersed in a nonuniform, expanding flow field. Emphasis has been placed on defining the flow environment experienced by a nose tip model in the exhaust plume of an underexpanded arc jet or rocket engine. Accordingly, the integral method has been formulated for an arbitrary description of a free stream which possesses both axial and radial gradients in Mach No., flow angle, total pressure, and total enthalpy.

Computations are presented for two different descriptions of the free stream (spherical source flow and the exhaust plume from a contoured, Mach 2 nozzle) and two body shapes (sphere and circular disk). Results indicate a first order effect on all the blunt body characteristics.

The influence of the free stream derivatives of Mach No. and flow angle has been examined and found to exert only a second order effect upon the solutions, thereby allowing a considerably simplified description of the free stream. Moreover, it has been demonstrated that the influence of an expanding flow field upon a blunt body may be approximately characterized in terms of the flow angle gradient normal to the plume axis. Consequently, definition of the plume flow field is required only along its axis.

The possibility of sonic point movement off a sharp corner onto the face of a circular disk has been investigated and found to be entirely possible for a nonuniform free stream. To identify the magnitude of the free stream flow divergence required to move the sonic point off the corner, a set of solutions was obtained for an infinite circular disk in a spherical source flow.

DD FORM 1473

UNCLASSIFIED

Security Classification

14	KEY WORDS
	blunt body
	integral relations
	non uniform flow
	exhaust plumes
	arc jets
	source flow
	free jets

Abstract (Continued)

Model size constraints, for the simulation of uniform flow pressure and heating distributions, have been identified for ablation testing in exhaust plumes. Furthermore, the region of a plume flow field immediately downstream of the Mach rhombus has been identified as the worst possible test location is simulation of a uniform flow environment is desired.

Requirements have been identified for additional cold flow experiments to define the capabilities and limitations of simulating uniform flow environments in underexpanded exhaust plumes.

AEROSPACE CORPORATION

EXTERNAL DISTRIBUTION LIST

(REFERENCE: COMPANY PRACTICE 7-21-1)

REPORT TITLE

The Blunt Body Problem in an Expanding Non-Uniform Flow Field

REPORT NO.	PUBLICATION DATE	SECURITY CLASSIFICATION
TR-0059(S6816-76)-2	7Ø SEP Ø7	UNCLASSIFIED

MILITARY AND GOVERNMENT OFFICES	ASSOCIATE CONTRACTORS AND OTHERS

(NOTE: SHOW FULL MAILING ADDRESS; INCLUDE ZIP CODE, MILITARY OFFICE SYMBOL, AND "ATTENTION" LINE)

SAMSO

Capt. Don Baldwin, SMYSR, B-3 2120
Capt. George Hess, SMYSR, B-3 2120
Capt. William Mercer, SMYSE, B-3 1140
Capt. Larry Hillebrand, SMYSE, B-3 1140
Lt. Rees Padfield, SMYSE, B-3 1140

SMYSR (Reentry Vehicle Technology Under Systems Definition)

SMYSE (Environmental Technology Branch Under Systems Definitions Division in Reentry Systems)

Location: Aerospace Corporation
1111 Mill Street
San Bernardino, California
92401

OTHERS

James Carpenter
Cornell Aeronautical Laboratory
P.O. Box 235
Buffalo, New York 14200

Ed Fisher
Cornell Aeronautical Laboratory
Cornell University
P.O. Box 235
Buffalo, New York 14200

Stan Tate
Cornell Aeronautical Laboratory
Cornell University
P.O. Box 235
Buffalo, New York 14200

Pete Brandt
TRW Systems
One Space Park
Redondo Beach, California 90278

Matt Sherman
Philco Ford, SRS
Ford Road
Newport Beach, California 9266[illegible]

Paul Schneider
Lockheed Missiles & Space Co.
1111 Lockheed Way
P.O. Box 504
Sunnyvale, California 94088

AFR 310-2 DISTRIBUTION STATEMENTS X'd BELOW APPLY					IF LIST COMPRISES TWO OR MORE SHEETS, COMPLETE THIS SIGNATURE BLOCK ON LAST SHEET ONLY
1. X	2.	3.	4.	5.	

APPROVED BY _____ (FOR AEROSPACE CORPORATION) DATE 7/15/70

APPROVED BY Lawrence Hillebrand Capt. SMYSE (FOR COGNIZANT AF OFFICE) (SYMBOL) DATE 7/15/70

SHEET 1 OF 5

AEROSPACE CORPORATION

EXTERNAL DISTRIBUTION LIST

(REFERENCE: COMPANY PRACTICE 7-21-1)

REPORT TITLE

The Blunt Body Problem in an Expanding Non-Uniform Flow Field

REPORT NO.	PUBLICATION DATE	SECURITY CLASSIFICATION
TR-0059(S6816-76)-2	70 SEP 07	UNCLASSIFIED

MILITARY AND GOVERNMENT OFFICES	ASSOCIATE CONTRACTORS AND OTHERS

(NOTE: SHOW FULL MAILING ADDRESS; INCLUDE ZIP CODE, MILITARY OFFICE SYMBOL, AND "ATTENTION" LINE.)

OTHERS (cont'd.)

Dr. Merrill Minges, MAAS
AFML
Wright-Patterson AFB
Dayton, Ohio 45433

George Johnson
McDonnell Douglas Aircraft Co.
3000 Ocean Park Blvd.
Santa Monica, California 90406

Don Tune
McDonnell Douglas Aircraft Co.
3000 Ocean Park Blvd.
Santa Monica, California 90406

Bob Lowe
McDonnell Douglas Aircraft Co.
3000 Ocean Park Blvd.
Santa Monica, California 90406

Don Boekemeier
McDonnell Douglas Aircraft Co.
Lambert St. Louis Municipal Airport
P.O. Box 516
St. Louis, Missouri 63134

Don Howey
Avco Corporation
201 Lowell Street
Wilmington, Massachusetts 01887

D. F. McVey
Sandia Corporation
Albuquerque, New Mexico 87115

AFR 310-2 DISTRIBUTION STATEMENTS X'd BELOW APPLY

1. \	2.	3.	4.	5.

IF LIST COMPRISES TWO OR MORE SHEETS, COMPLETE THIS SIGNATURE BLOCK ON LAST SHEET ONLY

APPROVED BY [signature] (FOR AEROSPACE CORPORATION) DATE 7/ /70

APPROVED BY Lawrence Hillebrand Capt (FOR ORGANIZATION)

AD-A111 163 AEROSPACE CORP SAN BERNARDINO CA TECHNOLOGY DIV F/G 20/4
THE BLUNT BODY PROBLEM IN AN EXPANDING, NONUNIFORM FLOW FIELD.(U)
JUL 70 P G CROWELL F04701-69-C-0059
UNCLASSIFIED TR-0059(56816-76)-2 SAMSO-TR-70-302 NL

AEROSPACE CORPORATION

EXTERNAL DISTRIBUTION LIST

(REFERENCE: COMPANY PRACTICE 7-21-1)

REPORT TITLE

The Blunt Body Problem in an Expanding Non-Uniform Flow Field

REPORT NO	PUBLICATION DATE	SECURITY CLASSIFICATION
TR-0059(S6816-76)-2	7Ø SEP Ø7	UNCLASSIFIED

MILITARY AND GOVERNMENT OFFICES	ASSOCIATE CONTRACTORS AND OTHERS

(NOTE: SHOW FULL MAILING ADDRESS; INCLUDE ZIP CODE, MILITARY OFFICE SYMBOL, AND "ATTENTION" LINE.)

OTHERS (cont'd.)

Mike Abbot
Aerotherm Corporation
485 Clyde Avenue
Mt. View, California 94[illegible]

Roald Rindall
Aerotherm Corporation
485 Clyde Avenue
Mt. View, California 94[illegible]

Jerry C. South
NASA
Langley Research Center
Langley Station
Hampton, Virginia 23365

Mamoru Inouye
NASA
Ames Research Center
Moffett Field
Mt. View, California 94[illegible]

Joe Doyle
AFFDL
Wright-Patterson AFB
Dayton, Ohio 45433

Irv Sacks
Avco Corporation
201 Lowell Street
Wilmington, Massachusetts 01887

AFR 310-2 DISTRIBUTION STATEMENTS X'd BELOW APPLY				
1. X	2.	3.	4.	5.

IF LIST COMPRISES TWO OR MORE SHEETS, COMPLETE THIS SIGNATURE BLOCK ON LAST SHEET ONLY

APPROVED BY _____ (FOR AEROSPACE CORPORATION) DATE 7/15/70

APPROVED BY _____ (FOR CONTRACT AF OFFICE) SAN JOSE DATE 7/15/70

AEROSPACE CORPORATION

EXTERNAL DISTRIBUTION LIST

(REFERENCE: COMPANY PRACTICE 7-21-1)

REPORT TITLE

The Blunt Body Problem in an Expanding Non-Uniform Flow Field

REPORT NO.	PUBLICATION DATE	SECURITY CLASSIFICATION
TR-0059(S6816-76)-2	7Ø SEP Ø7	UNCLASSIFIED

MILITARY AND GOVERNMENT OFFICES	ASSOCIATE CONTRACTORS AND OTHERS

(NOTE: SHOW FULL MAILING ADDRESS; INCLUDE ZIP CODE, MILITARY OFFICE SYMBOL, AND "ATTENTION" LINE.)

OTHERS (cont'd)

Professor Toshi Kubota
Firestone Flight Sciences Lab.
California Institute of Technology
1201 East California Boulevard
Pasadena, California 91109

Professor Paul M. Chung
Professor of Fluid Mechanics
College of Engineering
Department of Energy Engineering
University of Illinois
P.O. Box 4348
Chicago, Illinois 60680

Dr. Harold R. Jacobs
Department of Mechanical Engineering
College of Engineering
University of Utah
Salt Lake City, Utah 84112

AFR 310-2 DISTRIBUTION STATEMENTS X'd BELOW APPLY

1. X	2.	3.	4.	5.

IF LIST COMPRISES TWO OR MORE SHEETS, COMPLETE THIS SIGNATURE BLOCK ON LAST SHEET ONLY

APPROVED BY _____ (FOR AEROSPACE CORPORATION) DATE 7/15/76

APPROVED BY _____ (FOR COGNIZANT AF OFFICE) (COMMD.) DATE 7/16/76

SHEET 1 OF 1

AEROSPACE CORPORATION

EXTERNAL DISTRIBUTION LIST

(REFERENCE: COMPANY PRACTICE 7-21-1)

REPORT TITLE

The Blunt Body Problem in an Expanding Non-Uniform Flow Field

REPORT NO.	PUBLICATION DATE	SECURITY CLASSIFICATION
TR-0059(S6S16-76)-2	7Ø SEP Ø7	UNCLASSIFIED

MILITARY AND GOVERNMENT OFFICES	ASSOCIATE CONTRACTORS AND OTHERS

(NOTE: SHOW FULL MAILING ADDRESS; INCLUDE ZIP CODE, MILITARY OFFICE SYMBOL, AND "ATTENTION" LINE.)

OTHERS (cont'd)

Dick Bartle
Avco Corporation
201 Lowell Street
Wilmington, Massachusetts 01887

Vic DiCristina
Avco Corporation
201 Lowell Street
Wilmington, Massachusetts 01887

Matt Brunner
General Electric Corp.
3198 Chestnut Street
Philadelphia, Pennsylvania 19104

Phil Cline
General Electric Corp.
3198 Chestnut Street
Philadelphia, Pennsylvania 19104

Darius Brandt
General Electric Corporation
3198 Chestnut Street
Philadelphia, Pennsylvania 19104

Mickey Blackledge
Lockheed Missiles & Space Co.
Huntsville, Alabama 35804

AFR 310-2 DISTRIBUTION STATEMENTS X'd BELOW APPLY

1. X	2.	3.	4.	5.

IF LIST COMPRISES TWO OR MORE SHEETS, COMPLETE THIS SIGNATURE BLOCK ON LAST SHEET ONLY

APPROVED BY _____ (FOR AEROSPACE CORPORATION) DATE 7/15/70

APPROVED BY _____ (FOR GOVERNMENT OFFICE) SMYSE (SYMBOL) DATE 7/15/70

SHEET ____

AEROSPACE CORPORATION

INTERNAL DISTRIBUTION LIST

(REFERENCE: COMPANY PRACTICE 7-21-1)

REPORT TITLE

The Blunt Body Problem in an Expanding Non-Uniform Flow Field

REPORT NO.	PUBLICATION DATE	SECURITY CLASSIFICATION
TR-0059(S6816-76)-2	70 SEP 07	UNCLASSIFIED

(NOTE: FOR OFF-SITE PERSONNEL, SHOW LOCATION SYMBOL, e.g. JOHN Q. PUBLIC/VAFB)

R. Baker
P. Crowell (5)
S. Breshears
J. Crenshaw
J. Fedele
F. Fernandez
A. Galloway
J. Gebhard
R. Gilbert
L. Glatt
E. G. Hertler
H. Lee
P. Legendre
S. Lubard
J. Murdock
D. Nowlan
R. Ross
M. Steiger
R. Strickler
B. L. Taylor
K. Victoria
W. Welsh
H. White
S. L. Zeiberg
J. D. Stewart (ESO)
C. Pel (ESO)

Aerospace Libraries
San Bernardino (1)
SBC/SBTCR (1)
General Offices (2)

Project File (P. Crowell)
B1, 2610

APPROVED BY [signature] DATE 7/15/70

SHEET ___ OF ___

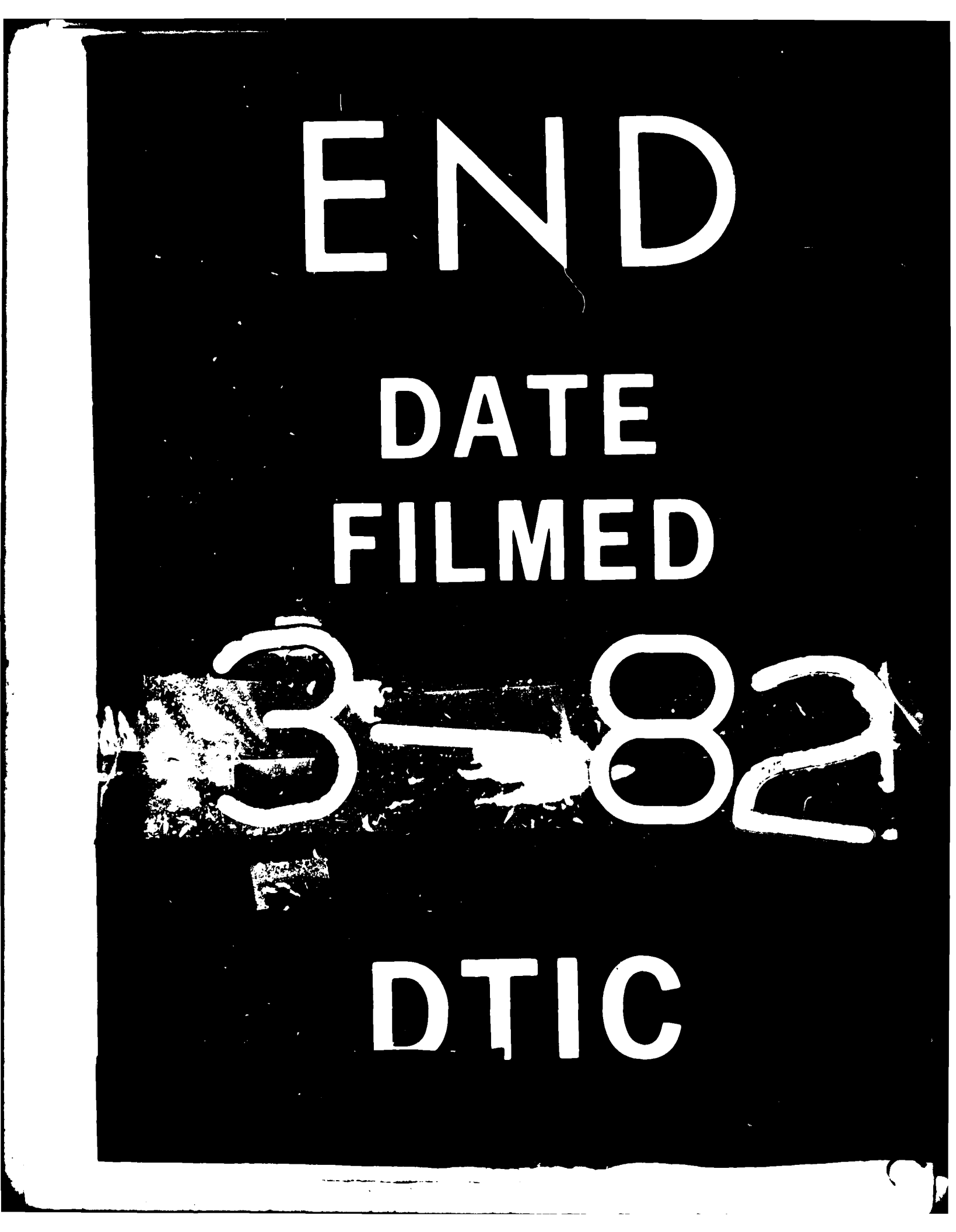
END
DATE
FILMED
3-82
DTIC